

INSTRUMENTATION FOR RAINFALL SAMPLING

by

© HECTOR HARO, M. Ing. E.

A Thesis

Submitted to the School of Graduate Studies

in Partial Fulfilment of the Requirements

for the Degree

Doctor of Philosophy

McMaster University

May 1984

INSTRUMENTATION FOR RAINFALL SAMPLING

DOCTOR OF PHILOSOPHY (1983)
(Electrical Engineering)

McMASTER UNIVERSITY
Hamilton, Ontario

TITLE: Instrumentation for Rainfall Sampling

AUTHOR: Hector Haro, Ing. M. E. (National University
of Mexico)
M. Ing. E. (National University
of Mexico)

SUPERVISOR: Dr. R. Kitai, Department of Electrical and
Computer Engineering

NUMBER OF PAGES: xiv, 222

ABSTRACT

An instrumentation package for sensing rainfall amount and intensity with fine time and space resolution is described. The package comprises a drop counter precipitation sensor, a microcomputer-based data acquisition system, and an intelligent data decoder. The accuracy of the precipitation sensor and the parameters that affect it are discussed. The reliability is reviewed and typical rainfall data are included. A comparison is made between the performance and accuracy of the new precipitation sensor and conventional tipping bucket raingauges. The merits and demerits of the new system are discussed.

ACKNOWLEDGEMENTS

I would like to express my sincere gratitude to Dr. R, Kitai and Dr. W. James for their helpful advice, criticism, and encouragement throughout the course of this work.

Thanks are also due to Mike Frendo and David Capson for their encouragement and useful suggestions and to Kim Capson for reading the manuscript.

To the Computational Hydraulics Group at McMaster University are also due my thanks for their helpful comments.

Finally, I am grateful to my wife Leticia and son Hector for their cooperation and constant encouragement for the completion of this work.

TABLE OF CONTENTS

	Page
ABSTRACT	iii
ACKNOWLEDGEMENTS	iv
LIST OF FIGURES	viii
LIST OF TABLES	xii
LIST OF SYMBOLS	xiii
CHAPTER 1 INTRODUCTION	1
PART ONE: BACKGROUND REVIEW	
CHAPTER 2 SCOPE OF THE THESIS	7
2.1 Precipitation	7
2.2 Hydrological problem	11
2.3 Mathematical models for stormwater management	16

CHAPTER	3	MEASUREMENT OF PRECIPITATION	21
	3.1	Remote measurement of precipitation	24
	3.2	Point precipitation measurement	26
CHAPTER	4	DROP FORMATION PROCESSES	36
	4.1	Review of drop formation theory	37
	4.2	Summary	57
PART TWO: INSTRUMENTATION SYSTEM DEVELOPMENT			
CHAPTER	5	DROP COUNTER PRECIPITATION SENSOR	60
	5.1	Sensor description	61
	5.2	Summary of tests performed	71
	5.2.1	Test procedure	72
	5.2.2	Tests to determine sensor design	76
	5.2.3	Tests to determine sensor performance	82
	5.2.4	Tests to determine sensor sensitivity	99
	5.3	Field calibration tests	104
CHAPTER	6	DATA ACQUISITION SYSTEM	108
	6.1	Circuit description	109
	6.2	Data acquisition system versions	122
	6.2.1	Low-Power version	122
	6.2.2	Precipitation collector version	125

6.2.3 Tipping bucket raingauge version 130

CHAPTER	7	DATA DECODER	132
	7.1	Circuit description	132

CHAPTER	8	DATA PROCESSING	151
	8.1	Data Collected	151
	8.2	Data presentation	154

PART THREE: CONCLUSIONS

CHAPTER	9	CONCLUSIONS	164
---------	---	-------------	-----

REFERENCES			169
------------	--	--	-----

BIBLIOGRAPHY			186
--------------	--	--	-----

APPENDIX	A	PRECIPITATION SENSOR TESTS	188
----------	---	----------------------------	-----

APPENDIX	B	DATA ACQUISITION SYSTEM PROGRAM	197
----------	---	---------------------------------	-----

APPENDIX	C	DATA DECODER PROGRAM	211
----------	---	----------------------	-----

LIST OF FIGURES

Figure		Page
3.1	Tipping bucket raingauge diagram	30
4.1	Jet length as a function of flow rate (From Brodkey, [3])	39
4.2	Drop weight correction curve (From Harkins and Brown, [9])	46
4.3	Drop formation in the case of a solution of glycerol and alcohol using a tip having a diameter of 1.448 cm (From Edgerton, [10])	48
4.4	Flow-Area plot suggested by Ohnesorge (Z-Number is a function of the type of liquid and tube dimensions) (From Marshall, [18])	55
4.5	Jet breakup at various flow rates (From Christiansen and Hixon, [20])	56
5.1	Drop counter precipitation sensor	62
5.2	Narrow chamber drop generator plug	64
5.3	Wide chamber drop generator plug	67
5.4	Wide chamber drop generator plug and optoelectronic sensor	70

5.5	Voltage signal generated by optoelectronic sensor	71
5.6	Testing apparatus	73
5.7	Rainfall intensity test results corresponding to 100 drops in 10 seconds	78
5.8	Nozzle inside diameter test results	80
5.9	Nozzle length test results	81
5.10	Precipitation sensor calibration test data sheets	85
5.11	Precipitation sensor standard performance	88
5.12	Histogram of test results	90
5.13	Precipitation sensor performance without fine mesh screen (see text)	100
5.14	Effect of fine mesh screen breather aperture on sensor performance	102
5.15	Effect of water temperature on sensor performance	105
6.1	DAS block diagram	110
6.2	DAS circuit diagram. Capacitors are in microfarads and resistors in kilohms	111
6.3	Typical signal generated by the presence of a drop	112
6.4	Data memory map	116
6.5	Plot of tape speed against time	120
6.6	DAS-LP circuit modification diagram	123
6.7	DAS-LP control signals timing diagram	124

6.8	DAS-MOE circuit modification diagram	128
6.9	DAS-MOE data signals timing diagram	129
7.1	DD block diagram	133
7.2	Filter block diagram	135
7.3	Filter circuit diagram. Capacitors are in nanofarads and resistors in kilohms	137
7.4	PLL block diagram	139
7.5	PLL and voltage comparator circuit diagram. Capacitors are in nanofarads and resistors in kilohms	144
7.6	Microcomputer and line driver circuit diagram	146
7.7	Tape information and word structure timing diagram	147
8.1	One complete block of information and its interpretation. The first number represents the acquisition time and the second the amount of rain. Starting time: October 5, 18:30 hrs. One drop is equivalent to 0.0046 mm of rain	153
8.2	Sample run of FASTPLOT	156
8.3	"Average" time distribution model	159
8.4	Hyetograph using 10 minute time-step: (a) tipping bucket raingauge, (b) drop counter precipitation sensor	161
8.5	Hyetograph using 5 minute time-step: (a) tipping bucket raingauge,	

	(b) drop counter precipitation sensor	162
8.6	Hyetograph using 1 minute time-step:	
	(a) tipping bucket raingauge,	
	(b) drop counter precipitation sensor	163
9.1	Envisaged real-time microcomputer-control system	168

LIST OF TABLES

Table		Page
5.1	Simulated rainfall intensity test results corresponding to 100 drops in 10 seconds (Number of drops at 5 second intervals)	77
5.2	Wetting test results (Conical-shaped fine mesh screen)	83
5.3	Summary of characterization test results	87
5.4	Summary of maximum rainfall intensity test results	93
6.1	Data acquisition system technical data	121

LIST OF SYMBOLS AND ABBREVIATIONS

- A = Precipitation sensor collection area (1 E-02) [m²]
- A_n = Nozzle area [m²]
- D_f = Diameter of the drop which would form at the nozzle velocity U_j if a jet did not form [m]
- D_n = Nozzle inside diameter [m]
- g = Acceleration of gravity, 9.8 [m/s²]
- M = Drop mass [Kg]
- Q = Volume flow rate of dispersed phase [m³/s]
- r = Nozzle radius [m]
- T = Temperature [°C]
- U_j = Nozzle velocity at which jet first forms [m/s]
- U_n = Average nozzle velocity [m/s]
- V = Drop volume [m³]
- V_f = Drop volume after break off from the nozzle [m³]
- W = Drop weight [Kg·m/s²]
- γ = Surface tension [N/m]
- Δρ = Difference between densities of dispersed and continuous phase [Kg/m³]
- μ = Viscosity of continuous phase [Kg/m·s]
- ρ = Density of dispersed phase [Kg/m³]
- ρ' = Density of continuous phase [Kg/m³]
- σ = Water specific weight [N/m³]

- fh = PLL frequency lock range (Hz)
- fo = VCO free running frequency (Hz)
- H(s) = PLL closed-loop transfer function
- Kd = PLL phase detector gain factor (V/radians)
- Ko = VCO gain factor (radians-sec/V)
- tb = One bit time transmitting at 300 bps (3.333 ms)
- Vc(t) = PLL control signal (V)
- Ve(t) = Phase detector output signal (V)
- Vi(t) = PLL input signal (V)
- Vo(t) = VCO output signal (V)

PART ONE: BACKGROUND REVIEW

CHAPTER 1

INTRODUCTION

The first quantitative hydrometeorological measurement made was for rainfall; rainfall records date back to the fourth Century B.C. and their use indicates knowledge of rainfall amounts, crop requirements and forecasting techniques. Since the inception of the raingauge, both the principles and the purpose have remained unchanged: collect precipitation over a known area to measure the amount of water falling and express this amount in units of depth. It is assumed that this depth of water collected is representative of the depth of rain falling in the surrounding area.

Many existing raingauge networks are capable of monitoring the amount of rainfall, but unless the network is dense and the data processed by a computer system, the spatial and temporal distribution of rainfall cannot be determined accurately and rapidly.

Appropriate knowledge of the precipitation phenomenon is essential for efficient management of our water resources. Water resource management has been complicated by

several factors such as the continuous growth of urban areas, rigorous water quality regulations and the need for control of urban flooding, and economic use of hydroelectric potential. As a result, the hydrometeorologist needs better instrumentation to collect, store, communicate and process rainfall information.

Rainfall is not only different from one event to another; it also varies continuously throughout a storm. Intensity varies from the beginning to the end of a rain-storm and from point to point in the area covered by the storm. Consequently, it is essential to provide amount, time of onset and cessation, and time and space distribution of rainfall.

The Secretary General-elect of the World Meteorological Organization (WMO), Dr. Godwin P. Obasi, recently commented [1] about the need for better meteorological observation networks and improvements in collecting and using those observations. Dr. Obasi pointed out the need for improving the network of data collection stations all over the globe. He observed that more conventional stations are often less costly and easier to maintain than satellites.

It is customary for hydrologists to design their field network in a way which minimizes capital and maintenance costs. Costs for individual instruments in present use are significant, being of the order of \$1000.00 for a complete monitoring station. Operating costs are high,

since conventional data collection and processing require a high labor content. As a result, the data collected tends to be insufficient.

Typically civil engineers use a methodology for hydrology that is based on simplified assumptions, such as uniform spatial distribution of rain over large catchment areas. Dynamic tracking of storms, storm models based on the kinematics of a cell within the rainstorm, and similar improvements, have had to await the advent of better spatial and temporal sampling of rainfall. It has been shown [2] that these observations and models of storms lead to considerable improvements in estimates of runoff and pollutant washoff, a matter of great importance in municipal engineering and flood management.

This thesis describes an innovative precipitation instrumentation package for monitoring rainfall intensity with fine time and space resolution. The package consists of a drop counter precipitation sensor, a microcomputer-based data acquisition system, and an intelligent data decoder.

The operation of the package is as follows: the precipitation sensor collects rainfall in a funnel which channels it through a stainless steel tube. The rain water leaves the tube in the form of drops, the drops being of almost constant size. The falling drops close an electrical circuit, enabling them to be counted. Given the drop volume

and the number of drops counted during a certain time interval, rainfall amount and intensity can be calculated.

The data acquisition system senses the drops and counts them over a programmable time interval, writing the counts temporarily in the microcomputer memory. The acquisition system also processes the data and stores it on standard audio cassette tapes.

The cassettes are removed and transported to the central site where they are interpreted by the data decoder. The time interval between cassette removals can be many months. The data decoder retrieves the information stored on tape, then verifies and communicates the rainfall time series to a central computer where the data is processed further. The rainfall data collected by the system is used to calculate total amounts and intensities of rainfall, as well as the time of onset and cessation of rainfall events.

The content of this thesis has been divided into three parts. Part one presents the definition of the problem and a review of rainfall monitoring gauges and drop formation theory.

The discussion of the problem is presented in Chapter 2. The problem is presented from three different points of view: the need for hydrologists to better understand the precipitation phenomenon, the nature of precipitation, and the use of computer programs to process the data collected to produce the information desired.

Chapter 3 describes the types and characteristics of different rainfall monitoring systems, with emphasis on point precipitation measurement gauges. An early history of raingauges is included.

Drop formation theory, which is relevant to the operation of the drop counter precipitation sensor, is introduced in Chapter 4.

Part two presents the development of the elements included in the precipitation instrumentation package. Details of the precipitation sensor configuration and operation are presented in Chapter 5. Experimental results obtained with the sensor and the effects on its performance resulting from variations in design and operation parameters such as nozzle diameter and length and rain water temperature are included.

Chapters 6 and 7 deal with the hardware and software design of the electronic instrumentation included in the package. Chapter 6 describes the microcomputer-based data acquisition system and the versions that have been developed to satisfy specific data collection requirements. Chapter 7 details the design of the data decoder. Listings of the microcomputer program for the data acquisition system and data decoder are included in Appendices B and C respectively.

Data processing is the subject of Chapter 8. A sample of the data collected and the processes involved in obtaining of the hyetographs is shown. Part three (Chapter 9)

discusses the overall performance of the precipitation package and leads to some conclusions together with suggestions for further improvements.

The research and development described by this thesis have been widely disseminated through journals and conferences. A paper [3] describing the operation of the system was published in the IEEE Transactions on Instrumentation and Measurement. Up to now, the work has been presented at four conferences [4-7], two of them by invitation. In these conferences, the possible improvements in stormwater management modelling as a result of automated, low-cost and high resolution rainfall monitoring systems were emphasized. As a consequence, enquiries from a variety of specialists have been received, several concerning the possibility of acquiring a complete instrumentation package with various remote monitoring systems, while others asked for samples of the system for evaluation purposes.

At the present time, four rainfall monitoring networks have been set up as a result of joint projects with different universities and government organizations; two in Toronto, one in Ottawa and one in Halifax. Systems for evaluation have been sent to Calgary, Kentucky, Norway and Mexico. Due to the increasing use of the system, operation and maintenance user's manuals for each of the three components of the precipitation package have been produced [8-11].

L

CHAPTER 2
SCOPE OF THE THESIS

Water is an indispensable and potentially damaging resource; its effective management is an important duty of our society. Effective planning and management will result only if the hydrologist is able to understand the continuous process by which water is stored or transported.

Hydraulic structures such as dams, bridges, channels, and outfalls are used to control flow. Reliable mathematical models are necessary to evaluate and predict the performance of hydraulic structures under expected or known conditions.

2.1. PRECIPITATION

Water is one of the most important elements on earth, covering nearly three fourths of its surface. It has played a decisive role in human history. The existence of cities, for example, has depended on the availability of this resource.

Water is continuously moving through a cycle - the hydrological cycle [12] which encompasses the process of motion, loss, and recharge of the earth's waters. It should be recognized that the hydrological cycle has neither begin-

ning nor end. Water evaporates from the land, oceans, and other water surfaces to become part of the atmosphere. The moisture evaporated is lifted, carried, and temporarily stored in the atmosphere until, under the proper conditions, the vapour condenses to form clouds and finally precipitates and returns to the earth.

The precipitation which falls upon land is dispersed in several ways: the greater part is temporarily retained in the soil as soil moisture, and ultimately given off by plants and returned to the atmosphere by evaporation; a portion of the water finds its way over the surface soil to stream channels (surface runoff); while other water penetrates farther into the ground to become part of the groundwater supply. Under the influence of gravity, both surface streamflow and groundwater percolate to deeper zones and may eventually be used by plants or discharged into the oceans. Finally, the water is evaporated into the atmosphere to complete the cycle.

The primary source of our fresh water supplies is precipitation and its recorded data are the basis of many investigations and decisions relating to supplies, floods, drought, irrigation, and regulating structures. The increasing demand for water in the face of a relatively constant supply necessitates an efficient supply of this data.

Precipitation can be defined as particles of solids or liquids that fall from the atmosphere and reach the

ground. Some kind of moisture is always present in the atmosphere, even on cloudless days or in the most arid conditions. For water precipitation to occur, cooling and condensation of the water vapour must first take place to form clouds. The cooling needed for significant amounts of precipitation is achieved by lifting the air, and this is accomplished by convective or convergence systems resulting from unequal radiative heating of the earth's surface and atmosphere or by orographic barriers. The cloud droplets and ice crystals formed by the condensation must then grow by some means until they are large enough to fall.

Precipitation is often labeled according to the factor mainly responsible for lifting the air to effect the large scale cooling required for significant amounts of precipitation. Some of the precipitation types are cyclonic, warm-front, cold-front, convective, and orographic. There are various forms of precipitation, but the most important are drizzle, rain, glaze, frost, snow, snow pellets, hail, and ice pellets. The total amount of precipitation in a stated period is expressed as the depth to which it would cover a horizontal projection of the Earth's surface if there were no losses by evaporation, runoff, or infiltration [13].

Rain consists of liquid water drops mostly larger than 0.5 mm. in diameter. Rainfall usually refers to amounts of liquid precipitation and is classified in North Am-

erica in three intensities [12]:

1. Light. For rates of fall up to 2.5 mm./hr. inclusive.
2. Moderate. From 2.5 to 7.6 mm./hr.
3. Heavy. Over 7.6 mm./hr.

Rainfall is classified as excessive when amounts R in millimeters, for durations T from 5 to 180 minutes, equals or exceeds those given by

$$R = 5 + T/4$$

Precipitation varies geographically, temporally, and seasonally. It is also highly variable in space and time [14 15] and therefore, difficult to measure accurately. The amount, intensity and areal distribution of precipitation in the form of rain and snow are essential factors in hydrology.

The requirements for collected precipitation data depend, to a high degree on the purposes for which the data is collected. In hydrological design it is very often necessary to examine critically how precipitation measurements were made, and how accurately they represent the true volumes of water involved. There are two main objectives in precipitation gauging. The first is to ensure that the gauge collects the same amount of rain that would have reached the ground had the gauge not been there, i.e., to obtain a representative sample at each gauge site. The second is to estimate accurately the amount and distribution of

precipitation over a given area (watershed) by means of the data collected by the gauges at a number of locations.

2.2 HYDROLOGICAL PROBLEM

"Hydrology treats of the waters of the earth, their occurrence, circulation, and distribution, their chemical and physical properties, and their relation with the environment, including their relation to living things. The domain of hydrology embraces the full life history of water on the Earth" [16]. Hydrology is used in engineering mainly in connection with the design and operation of hydraulic structures. "Civil engineers in hydraulics and hydrology are concerned with the planning, design, construction, and operation procedures connected with the conservation, control, and utilization of water to satisfy the social, aesthetic, economic, and physical needs of people" [17]. Civil engineers are interested in more than just obtaining a qualitative understanding of the hydrological cycle and measuring the quantities of water in transit in this cycle. They must deal quantitatively with the interrelations between the various factors to accurately predict the influence of man-made works on these relationships.

Linsley [12] notes two basic steps in hydrological studies: data collection and methods of data analysis. It is difficult to treat hydrological processes by rigorous deductive reasoning due to the complex features of the natural

processes involved. It is necessary to start with observed facts, and through their analysis, to establish the systematic patterns that govern these events. As a result, without adequate historical data for the particular problem, the hydrologist is in a difficult position.

Typical hydrological problems involve making estimates of extremes not observed in a small data sample, hydrological characteristics at locations where no data has been collected (such locations are more numerous than sites with data), and the effects of man's action on the hydrological characteristics of an area.

The planning, organization, implementation, and maintenance of rainfall data and its integration into comprehensive databases, constitute the central point of hydrological information system design [18]. To properly integrate a database, attention should be paid to the starting point - data entry. Computer compatible systems providing rainfall time series are essential if large quantities of data are to be stored. Once a data base has been properly integrated, its content can be efficiently processed in several ways. Rainfall databases are the starting point for most hydrological studies. For example, rainfall data is needed by the models used to evaluate the quantity and quality of stormwater runoff and combined sewer overflows. These in turn are necessary for finding strategies for minimizing pollutant loadings to receiving waters [19-21].

Conventional rainfall data is typically averaged over long time periods and as such, do not reflect fluctuations in rain intensity which are critical in urban pollutant washoff. Since rainfall data is averaged, the results obtained on pollutant washoff are also averaged. This type of data provides poor estimates of peak concentrations which often represent shock loads for the aquatic life [22]. Although shock loads may not be sustained for a sufficiently long time to kill the aquatic life, they may impair it. There is insufficient information on the combined effects of time and heavy metals on aquatic life due to urban shock loads to draw definite conclusions. However, rainfall information at short time intervals is essential for accurately simulating observed pollutant washoff from urban areas.

One of the most important infra-structures to be considered in the development of cities is the stormwater collection, transport, and treatment system. The design of this infra-structure should be based, among other things, on land use, soil type, meteorological zone, and types of pollutants expected to be washed off by the runoff. This analysis does not stop once the drainage system has been built. The information is essential for developing new criteria for future developments in the area.

Combined sewer overflows and stormwater discharges are typical problems of stormwater management. Stormwater flows through combined sewers to a sewage treatment plant

(STP). A plant will have limited capacity for wastewater treatment. During high rainfall events the amount of flow to the STP is controlled by means of diversion structures. The purpose of these structures is to divert flow in excess of the STP capacity to the receiving waters. The water diverted is untreated and carries large pollutant loads thus contaminating the receiving waters. One way to reduce the pollutant loads to the receiving waters is by means of a more efficient control of the diversion structures.

Real-time control of an urban drainage system requires a synchronized data collection network with control devices operating automatically [23]. The operation of these devices is dependent on some decision criterion, typically the depth of flow and the amount of rain at a control location. A real-time control system must integrate the available data with a predictor model for the decision variable.

Thunderstorms cause the most frequent and severe urban flooding. This is largely due to high rainfall intensities and volumes over a short period of time; usually less than one hour. Thunderstorms exhibit single and multi-cellular structures, each cell being circular or oval in horizontal cross-section. As the cell develops, it varies in intensity and spatial distribution. Several programs have been developed to analyze storm cell movement and distribution. STOVEL (STorm VELocity) [24,25] is a program de-

veloped to analyze point rainfall records using hyetographs as basic input. It determines a storm velocity vector consisting of direction and speed which is necessary for analysis of cell motion, and cell growth and decay mechanisms. From the Cartesian co-ordinates of at least three raingauges and the relative time-of-peak at each site, STOVEL calculates the direction and speed of a storm cell. Once the rainfall data has been pre-processed by STOVEL, other programs called THOR4DPT and THOR4D are implemented using STOVEL output data directly. THOR4DPT models a kinematic storm cell and computes synthetic rainfall at a rain gauge station. The user then compares the computed and observed hyetographs focusing on characteristics such as total precipitation, peak rainfall intensity, shape, and duration. Program THOR4D simulates rainfall in each separate subcatchment. This is achieved by developing a spatial and time-averaged hyetograph assumed to be the average rainfall falling on the subcatchment. In this manner, every discretized subcatchment will have a distinct hyetograph associated with it. Spatially averaged hyetographs integrated over the computational time step are used as input to hydrological simulation models.

Typically, engineering hydrologists use a simplistic approach to determine the spatial and temporal distribution of rain over significantly large catchment areas. This methodology is based on assumptions such as uniform spatial

distribution. The use of such a methodology is mainly due to the relatively high cost of the instruments in present use. Also, the maintenance costs are high, since conventional data collection systems require a high labour content. In the recent past, it has been customary for hydro-meteorologists to design their field networks in a way which minimizes system cost (capital and maintenance).

Advanced storm analysis, such as dynamic tracking of storms, storm models based on kinematics of cells within the rainstorm, and similar improvements have had to await the advent of better spatial and temporal sampling of rainfall. It has been demonstrated [26] that these storm models lead to considerable improvements in daily, monthly, and annual estimates of runoff and pollutant washoff, a matter of great importance in municipal engineering and flood management.

2.3 MATHEMATICAL MODELS FOR STORMWATER MANAGEMENT

Hydrological design methodology is changing rapidly as a result of the reduced cost of high speed digital computers. Mathematical approaches, such as synthesis and simulation are practical engineering procedures to investigate the design and operation of hydraulic structures to varying degrees of complexity.

Synthesis is used in Hydrology to estimate the value of missing data from historical records. This procedure relies on the statistical properties of the existing data.

Simulation is the mathematical description of the real world system that imitates its behavior. Simulation may be used to review historical events or predict the response of the physical system to a specific action.

A large number of computer models have been developed for simulating the various phases of the hydrological cycle [27,28]. Some of the models used in estimating quantity and quality of storm water runoff from urban drainage areas and other small watersheds are the Storm Water Management Model (SWMM), the Storage, Treatment, Overflow, Runoff Model (STORM), and the University of Cincinnati Urban Runoff Model (UCUR).

A very widely accepted and applied stormwater simulation model is SWMM [29]. This model is designed to simulate real storm events on the basis of rainfall inputs (hyetographs) and system characterization (catchment, conveyance, storage/treatment, and receiving waters) to predict outcomes in the form of quantity and quality values. This program is divided into five main subroutine blocks. Each block has a specific function, and the results of each block are stored to be used as part of the input to other blocks. The function of the blocks is as follows:

1. EXECUTIVE BLOCK: this block is the first and last to be used, and performs all the necessary interfacing between the other blocks.

2. **RUNOFF BLOCK:** in this block, the drainage area is characterized by features such as size, degree of imperviousness and slope. The rainfall is assumed evenly distributed over the catchment and routed through gutters and pipes to inlets after the infiltration and surface storage have been satisfied. This block also provides time-dependent pollutional graphs.
3. **TRANSPORT BLOCK** calculates the system infiltration and the water quality of the flows in the system. It also determines the quality and quantity of dry weather flow.
4. **STORAGE/TREATMENT BLOCK** simulates the changes in the hydrographs and pollutographs of the sewage as it passes through an optional wastewater treatment facility.
5. **RECEIVING WATER BLOCK** models the water quality effect of the effluent from the modelled sewer system on the receiving waters.

FASTSWMM [30] is a computer program package that makes it possible to run parts of the SWMM program from a terminal in a pseudo-conversational mode.

The fundamental first step in organizing a simula-

tion model involves a detailed characterization of all of the components of the system and the collection of appropriate data.

If the potential value of the models is to be realized, the mathematical functions employed and the data collected must represent the real world as closely as possible. Linsley states that "While it may seem desirable to subdivide the watershed into many subareas so that the variable characteristics of soil, topography, and vegetation may be correctly represented, little real advantage may result if the precipitation on all subareas must be estimated from a single rain gage."

The use of appropriate rainfall data acquisition instrumentation and a properly constituted network, regarding the number of gauges and their location, may greatly improve the development of these simulation models[15,28].

The uses for which precipitation data are intended should determine network density and raingauge characteristics; a relatively sparse network of stations would suffice for determining monthly or annual averages over large catchment areas, while a very dense network of gauges with very high time and quantitative resolution is required to determine the spatial and temporal distribution of storm event rainfall.

Most rainfall intensity monitoring is at present based on tipping bucket raingauges (TBRG) and chart record-

ers. TBRG's and recorders are large, cumbersome, and expensive. The equipment incorporates systematic and random errors due to timing limitations and manual data processing. Missing data occur due to mechanical failures. Time and quantity resolution of the system is low (usually 5 to 10 minutes and 0.2 millimeters per hour respectively). The data collected from a raingauge network based on TBRG's and chart recorders have been inadequate for stormwater modeling. Consequently, the main purpose of this study is to produce an automated, low-cost, high-resolution, reliable, and intelligent system for rainfall intensity data measurement, acquisition and presentation.

CHAPTER 3

MEASUREMENT OF PRECIPITATION

A large variety of instruments and techniques have been developed for gathering information on the various phases of precipitation. Instruments for measuring amount and intensity of precipitation are the most important. Other instruments include devices for measuring raindrop size distribution, the time of onset and cessation of precipitation (pluvioscope), and devices designed to determine the direction from which the rain is coming (vectopluviometers) [31].

The most widely used instrument for measuring amounts and intensities of precipitation is the rain gauge. The rain gauge, which has been called hyetometer, ombrometer and pluviometer, is the oldest meteorological instrument giving quantitative results. In theory, it is probably the simplest of the meteorological instruments, yet a great deal of research and experiment has been done to make it an accurate instrument.

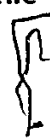
From its inception, a rain gauge has been simply an open receptacle exposed to the sky. After rain, the depth of water in the receptacle was measured with a measuring stick. In the 17th century it was found that the reading of

the gauge could be made easier and more accurate by leading the rainwater from a relatively large surface into a receptacle of smaller area. This observation started further studies related to the dimensions and shape of the instrument.

The early history of the raingauge [31-33] shows that it was invented independently in India, Palestine and China. The first measurement dates back to the fourth century B.C. and is attributed to the minister of Chandragupta, founder of the Maurya Dynasty of India. The earliest reference to a raingauge was made by Kautilya in his book "Arthashastra" (the science of politics and administration), which was probably written in the fourth century B.C. [34, 35]

The raingauge used was simply a bowl with a diameter of about 45 centimeters (the approximate distance from the elbow to the fingertips). Rainfall was measured by the Indians for two reasons; as an important aid in determining the annual crop to be sown, and because lands were taxed according to the amount of rainfall they received every year. There is no indication that the Indians of this period had thought of expressing the rainfall as depth of water.

The next mention of rainfall measurement appears in a Palestinian book of religious writings called "Mishnah". The book records the Jewish activities from the second century B.C. to the second century A.D. [36]. Like the Indian practice, rainfall was measured in Palestine primarily be-



cause of its importance to agriculture. Biswas observes that there seems to be no connection between the Indian practice and the Palestinian development. Both were independent and isolated practices and did not continue for a long time.

In China, the flooding of rivers and canals has always been a serious problem, and hence, it is not surprising to find that raingauges were used as early as 1247 A.D. [37]. Biswas observes that "The book "Shu Shu Chiu Chang" (a mathematical treatise in nine sections) by Chhin Chiu-Shao has a series of problems concerning the shape of raingauges, called thien Chih Tshe yü. The raingauges he described were conical- or barrel-shaped vessels. There was one installed at every provincial and district capital." Chiu-Shao also discussed a method of determining the amount of rainfall over a given area from the observations of point precipitation.

The first attempt to build a recording raingauge seems to have been made in England by Sir Christopher Wren in 1662 [33]. There is no evidence to indicate that the raingauge was used for obtaining regular observations of rainfall. He described two types of recording raingauges. One of them was a vessel which empties itself when a certain amount of water had flowed into it. This was the first version of the Tipping Bucket raingauge which is now widely used. The principle of operation of the Tipping Bucket was

known before Wren's time by the Arabs, in the dark ages, but there is no evidence to indicate that any Tipping Bucket raingauge was built before the time of Sir Christopher Wren.

Presently, three different types of instruments are used to estimate the amount and intensity of precipitation: raingauge (in-site gauging), radar, and satellite (remote gauging). Each has its own characteristics and is suitable for specific applications.

3.1 REMOTE MEASUREMENT OF PRECIPITATION

Radar has been used extensively as a research and observation instrument by meteorologist since the late 1940s. The real-time application of radar was limited to the determination of the direction, range, motion, and qualitative estimates of precipitation. The advent and use of high speed digital computers has been essential in the development of radar and satellite systems for the measurement of rainfall. The computers, for example, translate the digital radar data into the rainfall estimates by integrating the radar signal. They also calculate the motion and space distribution of a storm.

A radar transmits pulses of electromagnetic energy [38,39]. The radiated wave is partially reflected by water droplets and ice crystals and returns to the radar. The amount of energy returned depends on such factors as drop size distribution, number of particles per unit volume, physical

state, shape of the individual elements, etc. The time interval between emission of the pulse and appearance of the echo is a measure of the distance of the target from the radar.

Radar is being used with increasing frequency in the solution of hydrological problems. The information obtained can be used to delineate the area and relative intensity of storm activity over large areas (usually within 200 km. depending on radar characteristics) and is therefore a very useful hydrometeorological instrument.

Because of factors that affect returned power, the accuracy of radar measurements of precipitation varies with duration, area, storm type, and distance. Numerous comparisons [40,41] suggest that radar measurements of rainfall are within one half to twice the gauge measurements within a 110 km. range, with larger deviations for longer distances. Since measurements by ordinary gauge networks may be appreciably in error as a result of inadequate sampling, and since radar can detect and estimate precipitation between sampling gauges, conjunctive use of radar and gauge network should yield more accurate measurements than can be obtained from either alone.

Meteorological satellites yield information on precipitation over large areas where gauge networks or radar are inadequate or nonexistent, such as over oceans. The leading problem in satellite information is that satellites

cannot measure rainfall directly, and the solution requires evaluation of a rainfall coefficient on the basis of the amount and type of clouds, the probability of rainfall, and likely rainfall intensity associated with each cloud type. A major problem is that satellite photographs often do not show precipitation-producing clouds because of overlaying cloud layers. Satellite-borne microwave radiometers, which can be used to calculate the liquid-water content of clouds, may provide the ultimate answer to precipitation measurements from space [39].

3.2 POINT PRECIPITATION MEASUREMENT

Point precipitation is measured by gauges at specific locations. The resulting data permit the estimation of the amount and intensity of precipitation in the vicinity of the gauge. Point precipitation data are widely used to estimate areal variability of precipitation.

The instrument used to measure point precipitation is the rainfall gauge. Rainfall gauges in their simplest form are containers, most of them hollow cylinders which are open at one end. They consist basically of three components: collector, funnel, and receiver. The rim of the collector has a sharp edge which is bevelled on the outside and falls away vertically on the inside to optimize the collection. Funnels have been added to aid in collecting and they are shaped to prevent splash loss. The collected

rain is channeled into the receiver where it is stored. The receiver has a narrow neck and is protected from radiation so as to minimize evaporation loss. The amount of rain collected is determined by measuring the water contained in the receiver.

Any open receptacle with vertical sides may be used as a raingauge, but for purposes of optimizing rainfall collection and making measurements of different gauges comparable, some standards have been set. Standards for field instrumentation have typically been established by meteorologists at the national level. Huff [42] and Jones [43] have shown that the amount of rain collected depends on the size, shape, and exposure of the raingauge.

Because of the large variation in intensity of rainfall, it is very difficult to measure the whole range adequately with only one type of raingauge. Accordingly, a large variety of instruments have been developed. The two most important types are 1) rainfall gauges that sense the amount of rain that falls in a given period of time, and 2) rainfall intensity gauges or ~~rate-of-rainfall~~ gauges, which measure the intensity of rainfall at any instant.

Rainfall gauges are used primarily to determine the times of onset and cessation of rain, and the amounts which have fallen in each part of the period covered, e.g., the amounts in each hour of a daily record. In addition, the intensity of rainfall can be found approximately by measur-

ing the slope of the trace of the record from a recording rain gauge. Intensity is a measure of the quantity of rain falling in a given time, e.g., mm of rain per hour.

Rain gauges can be further divided into two main classes; non-recording and recording.

The non-recording gauges, usually called standard rain gauges, storage gauges or simply totalizers, are hollow cylinders and comprise the usual three basic components: collector, funnel, and receiver. Totalizers are used to measure amounts of seasonal precipitation in remote sites where frequent servicing is impractical. The gauge receiver has a large capacity, usually 1500 to 2500 mm. The readings are obtained either with a ruler, scaled container or by weighing. The Canadian gauge [44] has a 90.6 mm. (3.57 in.) diameter orifice, and when mounted has its orifice at 305 mm. (1 ft.) above the ground level. Its capacity is 114 mm. (4.5 in.), a value which has been found to be small for some applications.

Recording gauges have been designed to provide a record on a chart, punched cards or magnetic tape showing the incidence of precipitation as a function of time. The most common types of recording rain gauges are the weighing type, the float type and the tipping bucket. Because of their bulk and exposure, recording gauges tend to catch less precipitation than standard gauges.

In the weighing type, the weight of the receiving

container plus the rain which has fallen is recorded. This type of gauge normally has no provision for emptying itself; hence the scale value is limited and with large periods of rain some records may be lost. These gauges are designed to prevent excessive evaporation losses. Some difficulties are caused by oscillation of the balance in strong winds. These types of gauges are recommended for accurate snowfall measurements.

In the float type gauge, rain is led into a float chamber containing a light, hollow float. As the water level rises the vertical movement of the float is recorded. By adjusting the dimensions of the instrument any desired scale can be obtained. To provide a record over a long period of time the float chamber has to be very large. In this case a compressed scale on the chart is required or some means has to be provided for emptying the chamber.

The tipping bucket rain gauge, which is the most widely used, is based on a very simple principle of operation. A short description of the gauge given by the World Meteorological Organization [45] follows: "The rain is led from a conventional collector to a light metal container, or bucket, divided in two compartments. This container is so balanced that when one compartment holds a predetermined weight of water the container tilts allowing the compartment to empty and the rain to fall into the other compartment. This tilting process is repeated each time the predetermined

sample has been collected. The tilting of the bucket is counted electrically and recorded on a moving chart". Figure 3.1 shows a tipping bucket rain gauge. The Canadian tipping bucket rain gauge [46,47] has a 254 mm. (10 in.) collection diameter and tilts at every 0.25 mm. (0.01 in.) of rain.

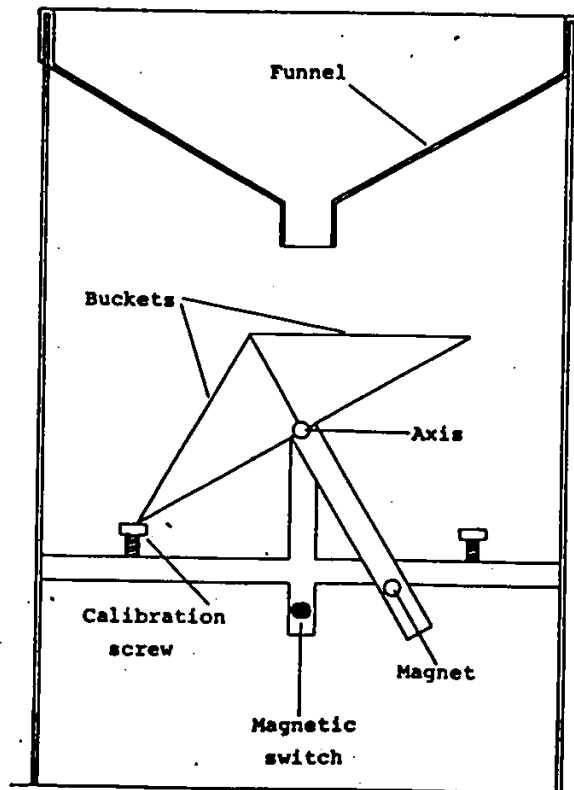


Figure 3.1 Tipping bucket rain gauge diagram

The output signal of the tipping bucket is usually recorded on strip chart recorders. Commonly used models of this type of gauge require chart changes on a daily or sev-

eral days basis. A typical instrument has a 24 hour chart with a 0.5 mm. of rain by 10 minutes grid.

Two advantages of this type of raingauge are as follows:-

1. The output it produces can be transmitted over long distances,
2. The comparability of measurements that can be made because of its wide use.

Its disadvantages are:-

1. The instrument is not very suitable for use in very light rain because of the discontinuous nature of the record. The times of onset and cessation of rain cannot be accurately determined.
2. Evaporation losses of the water in the buckets in hot weather may be a relatively large percentage of light rainfalls.
3. The gauge must be serviced regularly to ensure good performance.
4. The balance mechanism tends to deteriorate because of use, time, and humidity [48].

5. In rainfall of 125 to 150 mm./hr. the bucket tips every 6 to 7 seconds. About 0.3 seconds is required to complete the tip, during which some water is still pouring into the already filled compartment. This may cause the recorded rate to be as much as 5 percent too low [49].

While in principle the instantaneous rate of rainfall can be measured from the slope of the record of a recording raingauge, in practice the rate of fall varies so widely that it is not feasible to do this for heavy rains and at the same time provide a legible record of light rain.

In order to provide accurate readings of the instantaneous rainfall rate, it is necessary that the measurement device respond faster than any variations in the parameter being measured. However, since very little data is available to indicate the rate at which rainfall could vary, the instruments are designed to respond as rapidly as is practical.

In spite of the fact that rate-of-rainfall rain-gauges are not widely used, several prototypes have been constructed for special purpose studies. The most common are:

1. Capacitor type [50,51]: The collected water is channeled to flow between two rod-shaped electrodes of a capacitor which constitutes one arm of an RC

bridge. The capacitance increases with the rain rate. The AC voltage across the bridge is processed to give a DC output which is nearly proportional to the rainfall rate.

2. Turbine type [52]: The vertical motion of the collected water is arrested before it leaves the nozzle of the funnel so that the drops leave the nozzle with no kinetic energy. The potential energy delivered as the water falls is coupled to the water turbine, and the angular speed of the turbine is linearly related to the flow rate of the water.
3. Drop-generator type [53-55]: The principle of the instrument is very simple. The amount or intensity of rainfall is measured by converting the rain water into drops of almost equal size which are counted by an electronic device.

Middleton in his book "Invention of the Meteorological Instrument" [31], observes that the first drop counter type rate-of-rainfall gauge was described by W. J. E. Binne in 1892. He used a very small funnel with a piece of cambric with the idea of producing uniform size drops. The drops fall one by one onto a plate and make a momentary electric contact. Each drop produced was supposed to correspond to 0.01 inches of rain. Some time later W.

Gallenkamp used a larger funnel and more frequent drops. The apparatus used was a sort of tipping bucket that tipped at individual drops.

Sprung in 1907 built a Gallenkamp drop counter and found that he could do it without moving parts by letting the drops fall into the space between two electrodes. Middleton pointed out that Sprung did not make any observation about the constancy of drop size at different rainfall rates. It is rather surprising that the idea has not been more widely investigated.

In general and for all types of raingauges, precipitation measurements are subject to various errors, called local errors [56,57]. Most of these errors are small, but have a general tendency to yield measurements that are too low. These errors include splash in and out of the gauge, evaporation losses, losses in wetting of the surface, and inaccuracies due to improper levelling of the instrument. These errors are an order of magnitude smaller than the major error caused by the effect of wind about the gauge. The stronger the wind, the greater the effect for a given shape and size.

Wind interacts with features of the gauge's surroundings and particularly with the gauge itself. The vertical acceleration of air forced upward over a gauge imparts an upward acceleration to precipitation about to enter the gauge and results in a deficient catch. The deficiency is

greater for small raindrops than for large and is thus greater for light rain than for heavy.

There are ways to reduce the effects of wind [44, 56, 58]. Since wind increases with height above ground, it is advantageous to keep the gauge orifice as low as possible. Pit gauges essentially reduce the orifice level to that of ground level; however, they are seldom practical for watershed use. An alternative way to overcome the wind is through the use of shields. Two basic types of shields are in general use; rigid (Nipher) and flexible (Alter, Shasta). The latter has been adopted as a standard in North America.

The location of the rain gauge is very important for accurate measurement of precipitation [59]. According to Kurtyka [60], a poorly exposed rain gauge will underestimate the total precipitation by 5 to 80 percent. A major consideration in gauge location is vandalism, and rain gauges are often fixed to roofs for this reason.

CHAPTER 4

DROP FORMATION PROCESSES

The theory of liquid drop formation and subsequent dispersion from a simple nozzle into an immiscible fluid is essential to the drop counter precipitation sensor. A number of workers have studied the formation of drops from a nozzle. These studies have been performed mainly to measure the surface tension of a liquid and to improve the spray-drying process. A chronological review of the most outstanding work is presented here.

The physical variables governing drop formation are assumed to be nozzle design, including shape and size; density and viscosity of both dispersed and continuous phases; surface tension; and velocity of the dispersed phase through the nozzle. The ultimate effect of changing these variables is a change in the average size and uniformity of drops.

This chapter considers the low flow velocity region prior to jet formation, where uniform drops are formed at the nozzle tip, and the region just above the jetting point where a jet of liquid issues from the nozzle. Under normal conditions, the precipitation sensor operates in these regions.

4.1 REVIEW OF DROP FORMATION THEORY

A drop is a self-contained body separated from the surrounding medium by a recognizable interface and whose dispersed phase is in the liquid state [61]. Drops assume spherical shapes if either surface tension forces or continuous phase viscous forces are considerably larger than inertial effects.

The process of drop formation at very low flow rates has been widely investigated because it is the foundation of the drop-weight method for the measurement of surface tension. The drop-weight method consists in weighing drops falling from the end of a vertical tube.

Surface tension of a liquid is defined as the tension trying to minimize the surface area. It is the tension that must be broken to create new particles. In general, the surface tension decreases with increasing temperature, and varies with the presence of impurities. The accurate determination of surface tension is of great importance in investigations on theories of surface structure, the structure of liquids, and in various fields of technical chemistry.

Drops attached to a surface with a gravitational force acting to pull them away are called "pendant drops". Drops resting on a surface are termed "sessile drops". Small size drops are usually called "droplets". Drops are usually formed by forcing the liquid through small orifices.

A wide variety of atomizers, spray nozzles and sprinklers have been devised to generate drops. The characteristic features of these devices are the capacity, measured in liters per second, and the quality, which depends on the median size and spread in drop size.

If a liquid is forced through a horizontal orifice into an immiscible continuous phase, drops will form at the orifice or at the end of a disintegrating cylindrical jet. Keith and Hixson [62] describe the formation of drops, as a function of the flow rate, as follows:

"At low flow (rates), drops form individually at the nozzle tip and grow in size until the buoyance force overcomes the interfacial tension and the drop is released. At increased flow rate, a point is reached where a very short continuous neck of liquid exists between the nozzle tip and the point of drop detachment; this velocity will be called the jetting point. Further increases rapidly lengthen the jet, which appears as a smooth column of liquid with occasional transient lumps (Rayleigh jet). Finally, the jet takes on a ruffled appearance at its outer end and the drops formed are less uniform than in the earlier stages; this occurs at or near the maximum length of the jet and is called the critical velocity. Increasing the flow further decreases the jet length and increases drop nonuniformity until the jet breakup point retreats to the nozzle tip and a nonuniform spray of rather small drops results; this last

point will be called the disruptive velocity (point of atomization)." Figure 4.1 is a plot of jet length versus flow rate, as described above.

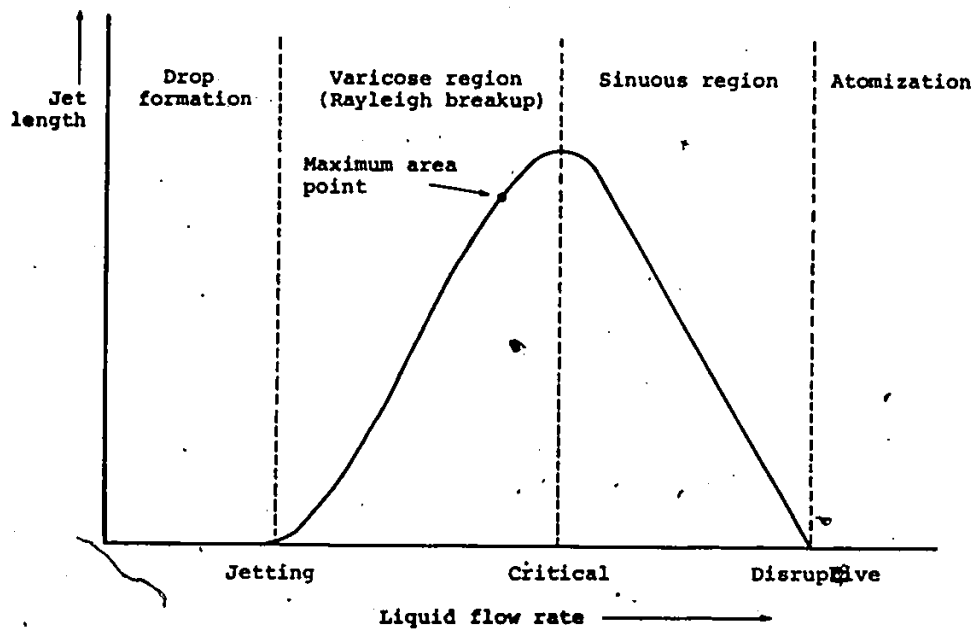


Figure 4.1 Jet length as a function of flow rate

(From Brodkey, [63])

The buoyant force is defined as the resultant force exerted on a body by a static fluid in which it is submerged or floating. The buoyant force always acts vertically upward.

The actual mechanism of drop formation is complex. Hauser [64] describes the phenomenon of drop formation from a nozzle as follows: "The drop grows longer and larger on the end of the tip. Instability sets in and a neck forms

between the part of the drop remaining on the tip and the part that eventually falls off. This neck grows longer and narrower until the drop finally separates. At this point the drop is slightly ellipsoidal with the long axis vertical. The neck of liquid connecting the two parts of the drop narrows down to a point at the point of separation. The main drop then separates and, owing to the slight tension caused by attachment to the stem, it flattens out somewhat immediately after separation takes place. The main oscillation is marred slightly by secondary oscillations set up at the same time, so that the drop assumes somewhat irregular shapes, though the main effect is a single oscillation about its form of equilibrium, a sphere." The continuous phase is considered stagnant except for motion caused by flow of the dispersed phase.

A drop may break up due to resonance, velocity gradients, turbulent flow fields, and electrical forces.

Various attempts have been made to formulate the theoretical equations that make possible the calculation of surface tension from the volume of a pendant drop. Unfortunately, most of these formulations were based on false assumptions.

Hauser notes that Tate was the first to investigate the existing relationship between the diameter of a circular nozzle of radius r and the weight of the drop. His experiments led him to the conclusion that "Other things being the

same, the weight of a drop of liquid is proportional to the diameter of the tube in which it is formed," without himself actually going so far as to state that the weight of a drop falling from a tip is equal to the product of the circumference of the tip and the surface tension, or:

$$W = Mg = 2\pi r\gamma \quad (4.1)$$

where

W = Drop weight [Kg·m/s²]

M = Drop mass [Kg]

g = Acceleration of gravity [m/s²]

r = Nozzle radius [m]

γ = Surface tension [N/m]

This conclusion assumes that sufficient time must be allowed for the formation of the drop. In Tate's experiments the period was never less than 40 seconds [66]. Hauser does not indicate if the radius considered by Tate was the internal or external radius.

Tate's conclusion would be true only when the pendant drop is supported entirely by the surface tension and when all of the pendant drop falls, but this is far from the truth. Tate's law fails to recognize the fact that the weight of the drop is also a function of its shape.

Guthrie [65] carried out experiments on drop formation from a solid sphere and summarized the results of his

observations in 7 laws. Three are of interest here: drop-size depends on.

"the rate of dropping. Generally, the quicker the succession of the drops, the greater is the drop."

(Law 1).

"the chemical nature of the dropping liquid, and little or nothing upon its density." (Law 3).

"temperature; generally, the higher the temperature the smaller the drop." (Law 6).

Rayleigh [66] considered that "The magnitude of the drop delivered from a tube, even when the formation up to the phase of instability is infinitely slow, cannot be calculated a priori." But, he observed that although a complete solution of the dynamical problem is impracticable, interesting information may be obtained from the principle of dynamical similarity.

To investigate how far Tate's law can be relied upon, Rayleigh performed various experiments giving special attention to the effects of tube thickness on the drop size. He found that for low flow rates and up to an external diameter of one centimeter, the size of the bore is of little consequence. For larger diameters, the weight of the drop in thick wall tubes is sensibly less than in tubes with thin walls.

Rayleigh considered that the results obtained by Tate were erroneous and discovered that the weight of a drop

of any liquid of which the density and the surface tension are known can be calculated as follows:

$$W = 3.8 \gamma a \quad (4.2)$$

where

a = Dimension of the tube (external radius in the case of water delivered from a glass tube) [m].

Note that 3.8 replaces the coefficient 2π used by Tate. Rayleigh found that this formula is applicable only if the viscosity may be neglected and the ratio of the internal radius to a is near unity and constant.

It is possible to observe that at zero velocity through the nozzle not all of the drop will fall, but a portion of it will remain at the nozzle. Harkins and Humphery [67] refer to researches of Lohnstein who estimated the portion of the drop that remains in the nozzle after the drop breaks off. By doing this, he was able to reduce the problem, which would otherwise be of kinetic form, to a problem in statics. The magnitude of the falling drop is the difference between the magnitude of the hanging drop just before it falls and the remainder left in the tip after the fall. The volume predicted is a function of the radius of the tip, the square root of the capillary constant, and the surface tension

$$W = 2\pi r \gamma f(r/a) \quad (4.3)$$

where

a = Square root of the capillary constant (m)

$f(r/a)$ = A function of r/a

A procedure for determining the surface tension of a liquid is the capillary rise method. This method is based on the height (h) to which the liquid inside a narrow tube of radius r will rise. The product hr is called the capillary constant which for a given liquid, using different tube diameters, is constant.

Lohnstein determined $f(r/a)$ for different values of r/a , and his calculations of these corrections, from a theoretical standpoint, make it possible to use the drop-weight method for the determination of surface tension. Lohnstein's values are only accurate to 4%.

Morgan [68] carried out experimental investigation of Tate's law and concluded that under certain definite conditions "The surface tension of any liquid at any temperature is equal to its falling drop weight from any one tip at the same temperature, times a constant, the value of which is found once for all for that tip, and is equal to the ratio of the surface tension of some standard liquid to the drop weight of that liquid, both at some one, like, temperature."

Harkins and Humphery, using Tate's law as a point of

departure, extended Lohnstein's investigation to such an extent as to make the data a basis for a method of calculating accurate values of surface tension. They observed that variations in density over a wide range and in viscosity over a moderate range, did not affect the drop formation.

Harkins and Brown [69] derived an expression for calculating the drop volume at negligibly small flow rates by equating the buoyancy and interfacial tension forces and correcting the volume for the fraction of the liquid which remains attached to the nozzle after the drop breaks off. The new equation, similar to that of Lohnstein, is

$$W = 2\pi r\gamma F(r/V^{1/3}) \quad (4.4)$$

where $F(r/V^{1/3})$ is the Harkins and Brown correction factor which is a function of the shape of the drop. The shape depends on the ratio of some linear dimension of the tip (such as r) and a linear dimension of the drop (such as the cube root of the volume of the drop which actually falls).

This equation is more easily applied than Lohnstein's equation since all of the factors are obtained by direct experiment or by reference to a table of values, while a in Lohnstein's equation cannot be obtained from the direct results of the drop weight measurements, but must be calculated by methods of approximation. They developed an empirical correction curve to determine the volume of the

drop which actually falls if the volume of the Tate's (ideal) drop and the radius of the tip are known. Figure 4.2 shows this correction curve. They also pointed out the necessity of using a very accurately formed tip, one that is truly flat and circular and with truly sharp edges. They observed that the departure from the circular shape of the tip and the lack of sharpness are a major source of error. The error becomes more important as the tip decreases in radius.

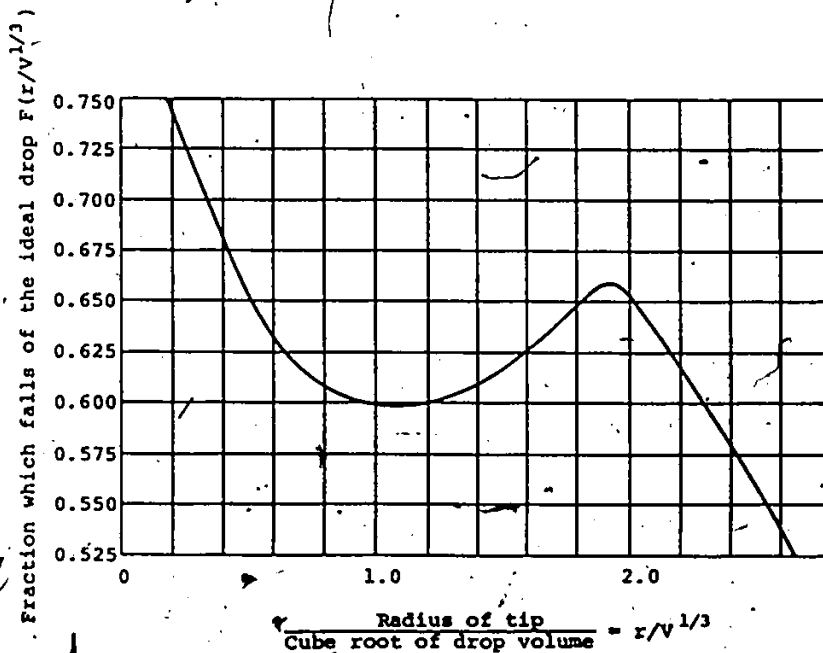


Figure 4.2 Drop weight correction curve

(From Harkins and Brown, [69])

Harkins and Brown conclude that the weight of a drop

varies rapidly with its time of detachment and that the period of drop formation should be 5 minutes or more. They found a variation of the weight of the drop of 0.26% for formation times over the range of 80 seconds to greater than 11 minutes. They pointed out that "When the rate of formation is faster than a drop in 3 minutes, on ordinary sized tips, some of the liquid streaming from the tube seems to force its way into the falling drop during the time of detachment, and consequently, a drop formed rapidly is heavier than one formed slowly."

Using a high-speed motion picture camera, Hauser and co-workers investigated the formation of drops. They observed that "While the correlation was not absolutely perfect, it can be generally said that the drops in all cases observed decrease in size with increase in the time of drop formation, being largest when the drop is formed fastest". They noted that secondary drops are produced by the segmentation of the stem that connects the two parts of the original drop at the time of drop break off, as shown in Figure 4.3. For non-viscous liquids, they observed that stem length decreases with an increase in the time of drop formation. It was found that the volume of water of the secondary drops is, on average, 3.12 percent of the main-drop volume. They concluded that the volume of the secondary drops increases with a decrease in surface tension and does not seem to be influenced by the viscosity of the liquid.

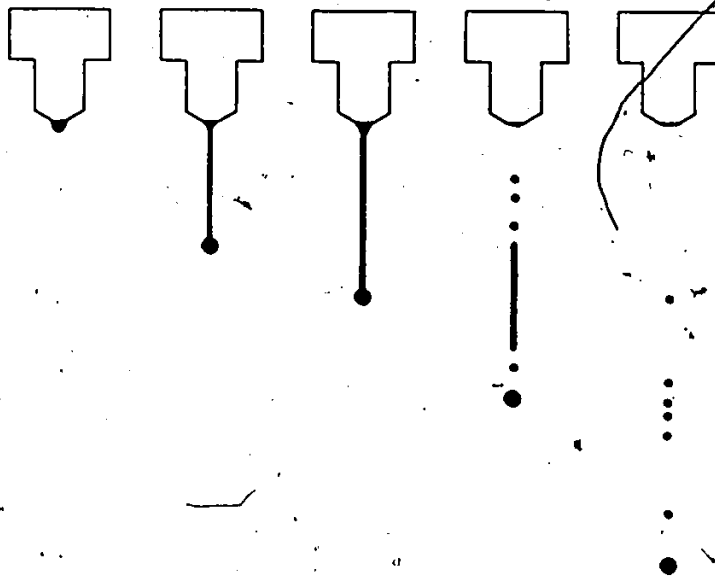


Figure 4.3 Drop formation in the case of a solution of glycerol and alcohol using a tip having a diameter of 1.448 cm. (From Edgerton, [70])

Edgerton [70] carried out experiments with different tip diameters. He observed that "for tips whose diameter is smaller than 0.5 cm, the pendant drop has a diameter greater than the diameter of the tip. On larger tips, the pendant drop has a smaller diameter than the tip on which it is formed". He concluded that viscosity and surface activity have a large effect on the mechanism of drop formation, and that the number of droplets created by drop breakup depends on the tip size and the nature of the liquid. Drops formed on the smallest tips (up to approximately 3.43 mm of exter-

nal diameter) detached without the formation of any secondary drops.

The process of drop formation depends to a high degree on the type of liquid involved. In general, liquids can be divided into: wetting liquids, such as water with glass, and non-wetting liquids, such as mercury with glass. For the case of wetting liquids, Andreas [71] observed that during drop formation drops may hang from the outer wall, from the outer rim, from the flat end, from the inner rim, or even from the inner wall of the tube. Regarding the characteristics of the nozzle, he points out that "It is desirable that the end of the tip be made from tubing having a circular cross section, and that the end be cut off perpendicular to the vertical axis. However, microscopic perfection is not essential, since the liquid surface tends to bridge over any minor irregularities."

Working with liquid-liquid systems, which under certain circumstances are similar to liquid-air systems, and very low flow rates, Hayworth and Treybal [72] observed that drop size is uniform and reproducible for a given velocity, and increases with increased velocity reaching its upper limit at very near the jetting velocity. Drop size also increases by increasing nozzle diameter, surface tension, viscosity of the continuous phase and decreased difference in density between the two phases. Using the Harkins and Brown volume correction factor, they developed a semi-theoretical

equation which permits prediction of drop size up to 30 cm per second velocity through the nozzle.

Izard and co-workers [73] working with liquid-liquid systems observed two different patterns of drop formation. "One results when the discontinuous phase preferentially wets the nozzle, and the other when it does not. In the latter case the drops are formed somewhat below the sharp edge of the top of the nozzle, whereas in the former case the dispersed phase liquid wets the nozzle to the sharp edge and may creep beyond it."

Scheele and Meister [74] also carried out experiments with liquid-liquid systems to obtain the drop volume as a function of injection velocity and nozzle diameter. They experimented with systems in which the dispersed phase was of lower density than the continuous phase and observed that "There are four major forces which act on a drop during the process of formation at a nozzle. The buoyancy force due to the density difference between the two fluids and the inertial or kinetic force associated with fluid flowing out of the nozzle, act to separate the drop from the nozzle, while the interfacial tension force at the nozzle tip and the drag force exerted by the continuous phase act to keep the drop on the nozzle. When the lifting force exceeds the restraining force, the drop begins to break away from the nozzle."

By performing a force balance of the counteracting effects of these forces, they developed the following expression for predicting the volume of the falling drop:

$$V_f = F(r/V^{1/3}) \left[\frac{\pi \gamma D_n}{g \Delta \rho} + \frac{20 \mu Q D_n}{D_f^2 g \Delta \rho} - \frac{4}{3} \frac{\rho Q U_n}{g \Delta \rho} + 4.5 \left(\frac{Q^2 D_n^2 \rho \gamma}{(g \Delta \rho)^2} \right)^{1/3} \right]$$

(4.5)

where

V_f = Drop volume after break off from the nozzle [m^3]

D_n = Nozzle inside diameter [m]

$\Delta \rho$ = Difference between densities of dispersed and continuous phase [Kg/m^3]

μ = Viscosity of continuous phase [$Kg/m \cdot s$]

Q = Volume flow rate of dispersed phase [m^3/s]

D_f = Diameter of the drop which would form at the nozzle velocity U_j if a jet did not form [m]

U_n = Average nozzle velocity [m/s]

The terms in the equation account, respectively, for buoyancy and interfacial tension, drag force, kinetic force and volume added during necking. For continuous phases of low viscosity, such as air, the term due to the drag force may be neglected.

The condition for incipient jetting was derived to be

$$U_j = 1.73 \left[\frac{\gamma}{\rho D_n} \left(1 - \frac{D_n}{D_f} \right) \right]^{1/2} \quad (4.6)$$

where U_j = Nozzle velocity at which a jet first forms [m/s]. The numerical coefficients $4/3$ and 1.73 , apply when the velocity profile in the jet at the orifice is parabolic; coefficients of 1.0 and 2.0 respectively should be used for a flat velocity profile. The parabolic velocity profile applies for Reynolds numbers in the nozzle smaller than 2100 (the Reynolds number is the ratio of the inertial to the viscous forces).

They remark that "Although the constants were obtained only from data in which the dispersed phase was less dense than the continuous phase, the theoretical analysis should also be valid in the reverse situation so long as the injection is in the vertical plane. The only difference in the two situations is the direction of the pressure gradient in the continuous phase relative to the direction of dispersed phase injection." They concluded that the volume of the drop formed depends on the viscosity of the dispersed phase.

As the flow rate through the nozzle is increased, a critical velocity called the jetting velocity is reached,

above which a jet of liquid issues from the nozzle into the atmosphere and eventually breaks up into drops under the action of disturbances of its equilibrium.

Rayleigh [75] made an analytical study of the collapse of a liquid jet in the varicose region of jet flow. Assuming axial symmetry, irrotational flow, and a non-viscous liquid, he showed that a small disturbance symmetrical about the axis of the jet would cause breakup when the amplitude of the disturbance grew to 4.4 times the diameter of the undisturbed liquid jet. He considered a water jet issuing into air and by neglecting the viscosity of both phases, he found that the diameter of the drop generated by the jet breakup is approximately 1.89 times the diameter of the undisturbed jet. Rayleigh's breakup theory predicts one drop size with no distribution.

Rayleigh's analysis assumed that surface tension was the force that controls jet breakup, and therefore, the viscosity of the liquid was not considered. Some time after, Rayleigh [76] modified his theory to take into account the viscosity, which resulted in a reduction of the rate of growth of the optimum disturbance.

Tyler and Watkin [77] carried out experiments and observed modifications in the characteristics and upper critical velocity, as a result of increased viscosity. They concluded that "Viscosity and surface tension of the jet fluid are the prime factors controlling the upper critical

point, drop formation disturbance produced at the disruption point of the jet, gaining access to the nozzle, is the cause of the lower."

Marshall [78] refers to researches of Ohnesorge who, using mathematical analysis, correlated the jet breakup behavior in terms of the type of liquid, orifice size and Reynolds number. The results are illustrated in Figure 4.4 where the three zones of breakup are identified as follows: Zone I, the mode of breakup follows the Rayleigh mechanism. Individual drops are formed; Zone II, The breakup follows a lateral motion with increasing amplitude. The jet has a twisted or sinuous appearance; and Zone III, the jet disappears and the breakup occurs close to the nozzle (atomization).

The effects of nozzle diameter in jet breakup were investigated by Merrington and Richardson [79]. They carried out experiments with liquid-air systems and found that "In every case the mean drop size was found to depend only on the relative speed, V , of the jet to the air and on the viscosity of the liquid. Here again, d (mean drop diameter) was inversely proportional to V . The nozzles used varied in diameter from 0.4 to 0.7 inch, and also gave identical results independent of nozzle size."

A small drop size distribution around the expected single diameter, predicted by Rayleigh, was observed by Marshall.

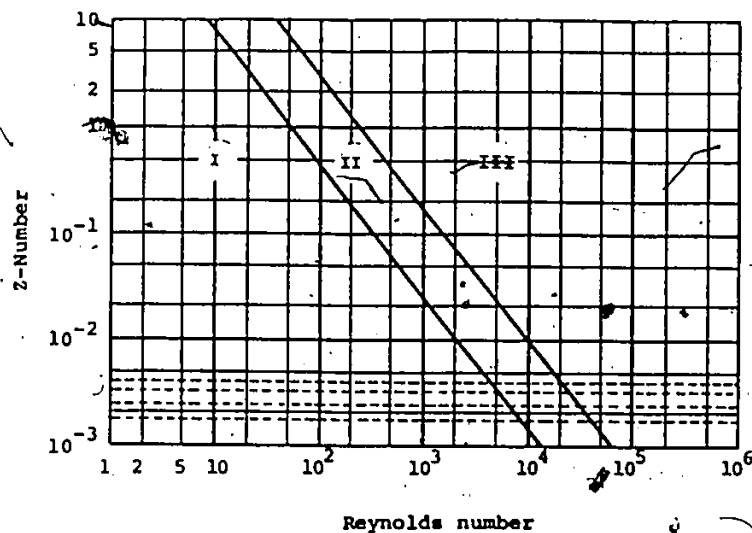


Figure 4.4 Flow-Area plot suggested by Ohnesorge.
 (The Z-number is a function of the type of liquid
 and tube dimensions). (From Marshall, [78])

Working with liquid-liquid systems, Keith and Hixson made observations which showed that just above the jetting point the drop size is very uniform and reproducible. They stated that "Uniformity is definitely a function of the flow rate for all the nozzles. Uniformity is better for smaller nozzles but is also good for lower rates with larger nozzles." A decrease in nozzle length decreases uniformity in the low flow rate range when compared to a longer nozzle. They concluded that a decrease in interfacial tension is insufficient to produce a change in the uniformity of drop

size and that viscosity had no effect on jet breakup.

Christiansen and Hixson [80] observed that "At flow rates, below the maximum area point, jet velocity is such that nodes form too frequently. Drops formed below the critical flow rate were of two sizes; one equal to the ideal one-wave-length drop and one double that size". Figure 4.5 shows the jet breakup at various flow rates where the nodes can be appreciated at the end of the jet. They found that the calculated jet diameters for small nozzles occasionally exceeded the nozzle diameter.

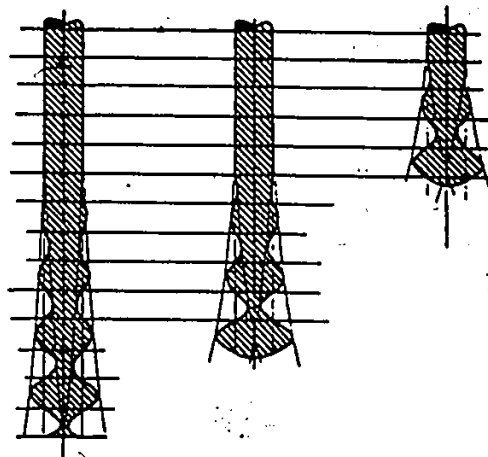


Figure 4.5 Jet breakup at various flow rates
(From Christiansen and Hixson, [80])

Lee [81], using nonlinear analyses, predicted the formation of satellite droplets (see Figure 4.3). The volume of the droplets predicted is about four percent of the volume of the main drop.

The main cause of the production of secondary drops is the surface tension; it forces the cylinder into a spherical pattern. The viscosity of the material, however, determines the length and diameter of the jet, and thus the size and number of secondary drops.

4.2 SUMMARY

Basically three types of behavior are observed when a liquid flows through a simple nozzle: (1) at low flow rates, individual drops are formed directly at the nozzle tip. Drop size is uniform and reproducible; (2) at intermediate flow rates, a jet of liquid issues from the nozzle and eventually breaks up into drops. The drops formed are less uniform than in the previous stage; and (3) at fast flow rates, a nonuniform spray of droplets is produced.

Many equations and models have been proposed for predicting drop volume, jet length and diameter, and volume of the secondary drops. Even though these empirical approaches were verified, they should be used with caution outside the operating conditions under which they were obtained.

In the low flow velocity region, mean drop size depends to a high degree on nozzle diameter. It increases with an increase of nozzle diameter. To a lower degree, drop size increases with: an increase of flow rate and surface tension and a decrease of dispersed phase temperature.

To the lowest degree, drop size depends on: viscosity of both dispersed and continuous phase, difference of density between the phases, capillary tension, and buoyancy force.

Drop size and drop size uniformity are sensitive to nozzle design, being more sensitive to variations or imperfections as the nozzle decreases in radius. The nozzle must be truly flat, circular, and perpendicular to the vertical axis, and with truly sharp edges.

Depending on the interface dispersed phase-nozzle material, the dispersed phase may or may not wet the nozzle. The pendant drop hangs from a number of sections of the nozzle relying on the type of interface.

For nozzle diameters smaller than 5 mm, the pendant drop diameter, in general, is greater than the nozzle diameter.

The formation of secondary drops depends on nozzle design and type of dispersed phase. For water-air systems and nozzle diameters smaller than 3.4 mm, drops detach without the formation of secondary drops. Their volume is, on average, 3.12 percent of the main-drop volume and increases with a decrease of surface tension and it is not affected by the viscosity of the dispersed phase.

In the intermediate flow velocity region prior to the critical point, individual drops are formed. Drop size is uniform and reproducible under certain given conditions and depends on the relative speed of the jet to the air, the

viscosity of the liquid, and nozzle design.

Drop size uniformity depends on the velocity of the dispersed phase through the nozzle, being better for low velocities and for large nozzle lengths. It is not affected by surface tension or viscosity of both phases.

In general and for small nozzle diameters, the jet diameter is smaller than the nozzle diameter and increases with an increase of nozzle diameter.

The process of creation of secondary drops is governed by surface tension and viscosity of the dispersed phase. In general, the volume of the secondary drops is approximately 4 percent of the main-drop volume.

PART TWO: INSTRUMENTATION SYSTEM DEVELOPMENT

CHAPTER 5

DROP COUNTER PRECIPITATION SENSOR

The drop counter precipitation sensor (DCPS) described in this thesis is a rate-of-rainfall rain gauge. The high resolution and fast response of the sensor provides an accurate means of estimating the instantaneous rainfall rate and the time of onset and cessation of a precipitation event. The information gathered from the sensor can also be used to estimate total amounts of precipitation by time intervals. Due to the low cost and fast response of the sensor, it can be used in dense rain gauge networks for the study of spatial and temporal distribution of rain, or storm dynamics. Cell speed and direction can be derived from the data.

This chapter presents a detailed description of the precipitation sensor and its operation. Experimental results obtained with the sensor and the dependency of its response to various parameters such as nozzle size and rainfall rate and temperature are discussed.

5.1 SENSOR DESCRIPTION

During rainfall, the precipitation sensor collects rain water in a funnel which channels it through a stainless steel tube. A stainless steel tube was chosen to avoid oxidation. The water is released from the tube in the form of drops, which are of almost constant volume. The falling drops close an electric circuit resulting in the drops being counted. Given the drop volume and the number of drops counted during a certain time interval, the amount of rainfall can be determined.

The DCPS is contained in two cylinders, denoted (1) and (2) in Figure 5.1. Cylinder (1) contains the sensor while cylinder (2) is used as the base. The cylinders are easily assembled. The precipitation sensor housing is a totalizer raingauge used by the Atmospheric Environmental Service (AES) of Environment Canada. The use of these rain-gauges simplify the comparability of measurements with existing networks. The DCPS includes a standard graduated rainfall totalizer (3) which is used to measure total amounts of rainfall collected by the sensor. The rim of cylinder (1) has a sharp edge which is bevelled on the outside and falls vertically on the inside.

Inside cylinder (1) there is a plastic funnel (4) whose function is to collect the rain and which is shaped to prevent loss due to splash. At the base of the funnel there is a machined nylon plug (5). This plug is held in place by

a rubber o-ring allowing easy removal of the plug for maintenance. The nylon plug is pierced by a stainless steel tube (6) that releases the collected water by drops of almost constant size.

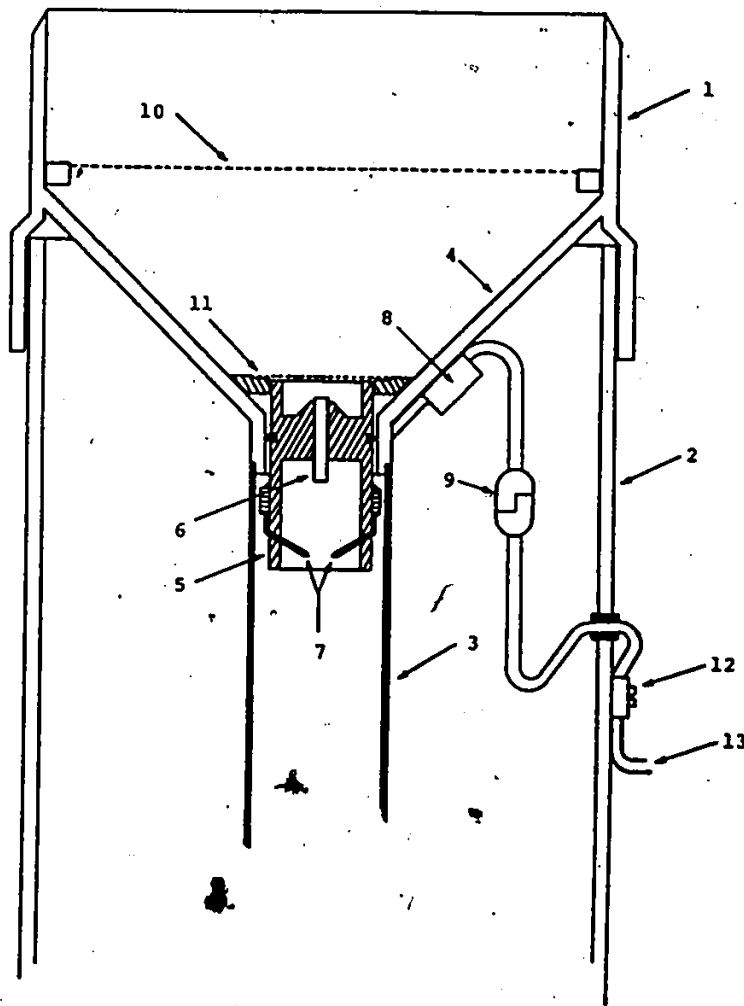


Figure 5.1 Drop counter precipitation sensor

The lower part of the plug supports the sensor (7) which consists of two electrically conducting points. The points are mass-produced pins which are gold plated to avoid oxidation. The drop presence is detected by enabling an electrical current to flow from one test point to the other through the water drop.

The sensor points are connected to an amplifier (8) which boosts the electrical signal produced when the drop is in contact with the sensor points. Connector (9) is mounted inside cylinder (1) and provides access to the electrical signal from the amplifier. Cylinder (1) may be separated mechanically as well as electrically from cylinder (2).

At the top of the funnel, inside cylinder (1), there is a removable coarse mesh screen (10) whose function is to trap leaves and bugs. Under this screen, there is a removable fine mesh screen (11) to prevent dust from entering the stainless steel tube.

A clamp (12) secures the two-conductor cable (13) to cylinder (2). The cable feeds the electrical signal to the data acquisition system.

Figure 5.2 provides details of the plug. The test points point slightly downward, about 30 degrees from the horizontal, to reduce the chance of water drops hanging from the test points.

The length of the stainless steel tube and the distances between the test points and from the points to the

bottom rim of the tube were determined as follows: The distance between the test points must be smaller than the diameter of the drops released from the nozzle, but larger than the diameter of the water jet that issues at very high rainfall intensities. Test point separation determined in this way permits the drops to be counted and unwanted signals produced by the water jet to be neglected.

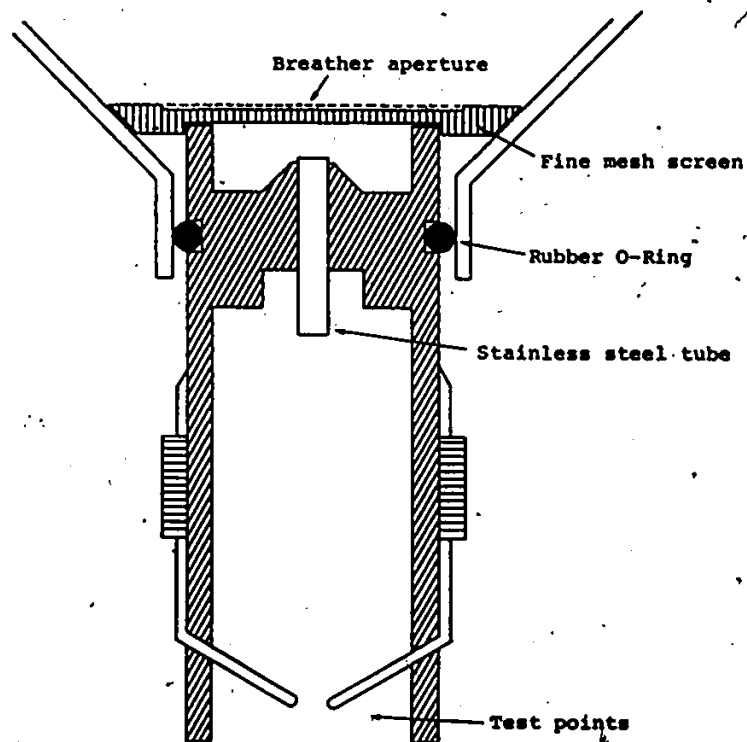


Figure 5.2 Narrow chamber drop generator plug

In the precipitation sensor design, the tube is made of stainless steel; the dispersed phase is water and the

continuous phase is air. Consequently, a nonwetting behavior takes place and the nozzle's inside diameter is considered in the calculations.

The nozzle diameter is 1.83 mm (0.072") and the diameter of the drops released, assuming a spherical shape and a volume of 46 cubic millimeters, is approximately 4.45 mm. The jet diameter for this size of nozzle occasionally exceeds the nozzle diameter and therefore, they are considered to be equal.

Various experiments were performed to corroborate the validity of the theory and it was found that a separation of 2 to 3 mm is appropriate and satisfies the requirements referred to above. A separation of 2 mm was adopted.

Even with these considerations a problem in the drop detection process remains: the nodes and drops produced at the end of the jet. As described in Chapter 4, for flow rates above the jetting velocity a jet of liquid issues from the nozzle into the atmosphere and eventually breaks up into drops under the action of disturbances of its equilibrium. The jet length depends on the flow rate through the nozzle as illustrated in Figure 4.5. The diameter of the drops and nodes produced is approximately 1.89 times the diameter of the undisturbed jet.

For short length jets, the nodes and drops produced may appear at the test points resulting in an erroneous reading. One characteristic of this phenomena is the short

time interval between consecutive nodes or drops. This characteristic is used in the data acquisition system input to avoid the nodes or drops being counted if they appear very close in time (5 milliseconds or less).

The distance between the test points and the bottom rim of the nozzle was established as follows: it must be larger than the length of the pendant drop, such that the drops are detected only after drop detachment. However, the distance should be kept short to avoid excessive splashing and the detection of long jets. A distance of 12 mm is used.

It was found experimentally, that nozzle lengths between 10 and 15 mm have no effect on drop size distribution, but in order to reduce tube blockage caused by dust, a tube of 10 mm is used.

The stainless steel tube protrudes from the nylon plug at both ends. At the top the surface configuration of the plug provides a settling reservoir that reduces dust entering the tube. At the bottom, it avoids the capillary effect and provides a constant area for drop generation. The bottom rim of the tube is flat and polished.

The DCPS, since its inception, has been modified several times. The modifications were made to avoid the obstruction of the drop generation tube, to produce drops of more constant size and to ease manufacturing and maintenance.

Two types of plugs are currently being used: "narrow chamber" and "wide chamber" shown in Figures 5.2 and 5.3 respectively. It is intended that in the near future only the wide chamber plug will be used. The step-like shape of the wide chamber plug provides a spacious lower chamber and a fixed position of the plug inside the funnel.

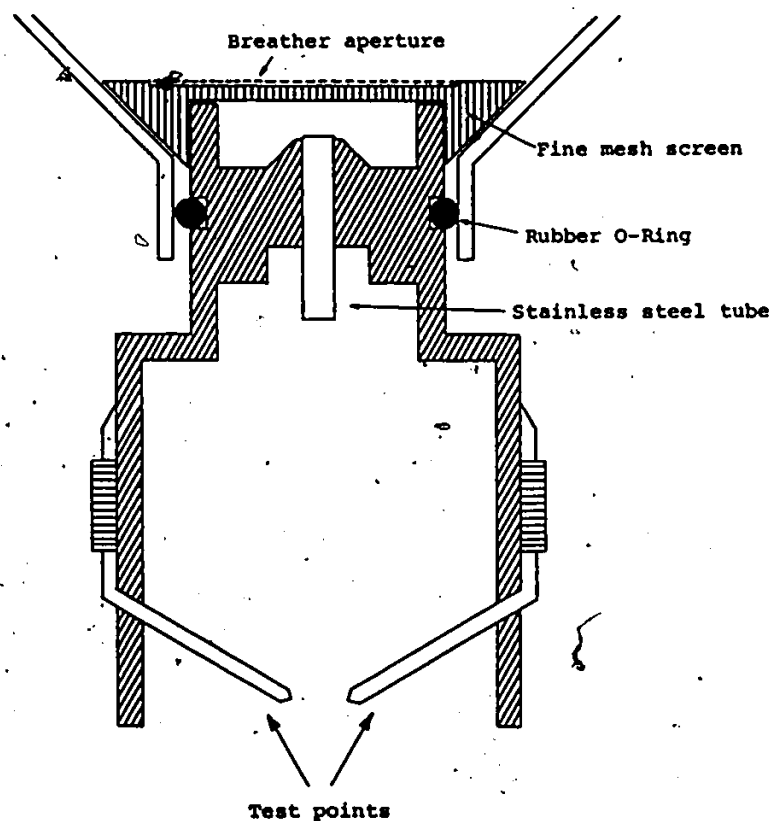


Figure 5.3 Wide chamber drop generator plug

The lower chamber walls are used to position the test points. When a drop falls and collides with the test points, small drops (droplets) splash in all directions.

Some of the droplets find their way to the walls of the chamber and adhere to it, while the rest fall away. It is possible for a large number of droplets attached to the walls to create a water path between the two test points. If the electrical conductor bridge occurs, the sensor will be unable to detect drops. The probability of occurrence of this phenomenon may be reduced by separating the test points as much as permitted by the drop size, hence reducing the amount of water splashed and by making the chamber as spacious as possible while keeping the test points protected.

The cavity created on top of the plug will always retain the same amount of water, if the plug is properly installed inside the funnel. The amount of water necessary to wet an initially dry sensor, is the water required to wet the fine mesh screen and the top of the plug. The amount of water held depends to a high degree on its cleanliness. It is suggested that the DCPS's in the field be cleaned frequently; preferably at least once a month.

After the sensor has been wetted, some water must build up above the plug before a drop is released from the tube. The stored water creates a pressure head on top of the steel tube. Drops are released from the tube when the pressure head is greater than the forces acting upwards on the drop.

In spite of the fact that other methods of detecting drops exist, the method described was chosen because it pro-

vides more data about the rain than just the amount and intensity. The average time a drop remains in contact with the test points is approximately 15 milliseconds, for water drops of about 46 cubic millimeters. During this time, it is possible to measure the conductivity of the water drop to estimate the concentration of total dissolved ionizable inorganic solids, which is an important parameter in rainfall quality analysis. In the present design only the drop presence is sensed but an interesting subject for future improvements has been established.

The field instrumentation installed employs the DCPS described above. At present, tests are being carried out on a plug that uses optoelectronic devices to detect the drops. Instead of the test points, the new design uses an infrared light emitter diode and a phototransistor aligned in the drop falling path. When the water drop falls, it interrupts the light beam and the phototransistor senses the disruption of light. Figure 5.4 shows the wide chamber plug and optoelectronic sensor.

Problems such as water splash and test point oxidation are completely avoided with the optoelectronic plug because there is no contact with the water. Although the optical method has some advantages over the contact method, there are also some disadvantages due to the possible drop breakup during drop formation. As explained in Chapter 4, depending on various physical factors, the drops can break

into smaller fragments. The number and size of these fragments vary widely. If breakup occurs when the drop is detected, the optical sensor may detect more than one drop. This phenomenon is avoided in the contact method by placing the test points in such a way that their position and separation constitute a drop size discriminator, such that only drops of a given size or larger can close the electric circuit between the two points. Errors introduced by splash are avoided for the same reason.

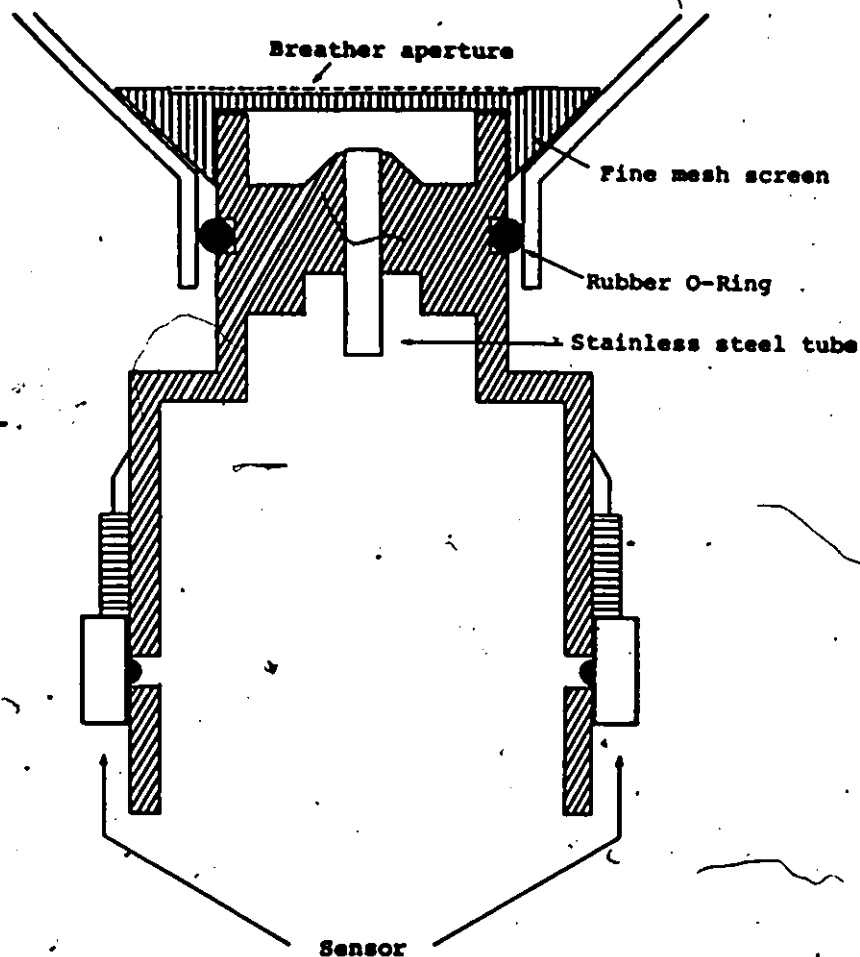


Figure 5.4 Wide chamber drop generator plug and optoelectronic sensor

The electrical signal produced by the phototransistor is a positive square pulse, similar to that produced by the test points. If the water is clear, a low voltage level appears momentarily at the center of the pulse. This sudden change in the voltage level of the signal is produced by the lens effect of the drop when it is aligned with the light beam path. Figure 5.5 shows the voltage signal generated by the optoelectronic sensor.

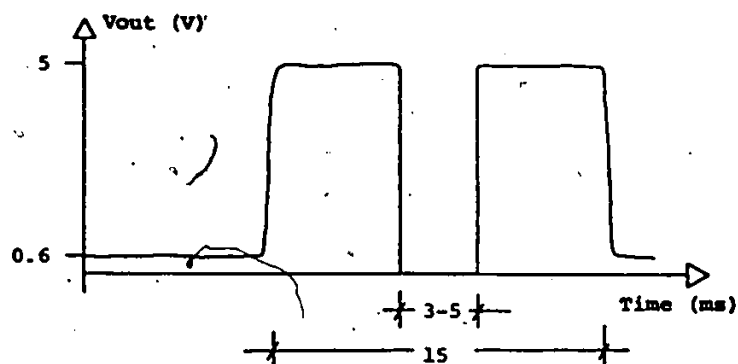


Figure 5.5 Voltage signal generated
by optoelectronic sensor

5.2 SUMMARY OF TESTS PERFORMED

Over 6000 tests were carried out. Depending on the purposes for which the tests were performed, they have been divided into four categories, as follows:

1. Tests performed to determine the dimensions and

- characteristics of the sensor, such as nozzle diameter and length, probe separation and drop generator plug shape.
2. Tests carried out to determine the performance of the final design under specific conditions.
 3. Tests performed to determine which parameters, such as rain water temperature, affect the performance of the sensor. The degree to which these parameters affect the response was also estimated.
 4. Tests to corroborate the performance of the system were carried out with various sensors assembled for the field program.

The main objective in most of the tests was to determine the effects of the factors considered on the relationship between drop size and rainfall intensity. In order to obtain reliable data from the DCPS the drop size produced must not vary significantly with the intensity of rainfall, when all other factors such as water temperature are held constant.

5.2.1 TEST PROCEDURE

Since the DCPS measures rainfall intensity, a method for simulating different intensities was needed in order to

test and calibrate the instrument. Rainfall intensities were simulated using a 10 ml pipette clamped to a retort stand as shown in Figure 5.6. By adjusting the slope of the pipette, different intensities may be obtained. For lower intensities than can be obtained with the pipette, two custom-made funnels with reduced nozzle diameter were used. The funnels were filled with 10 ml of water using the pipette. Tap water was used for all the experiments.

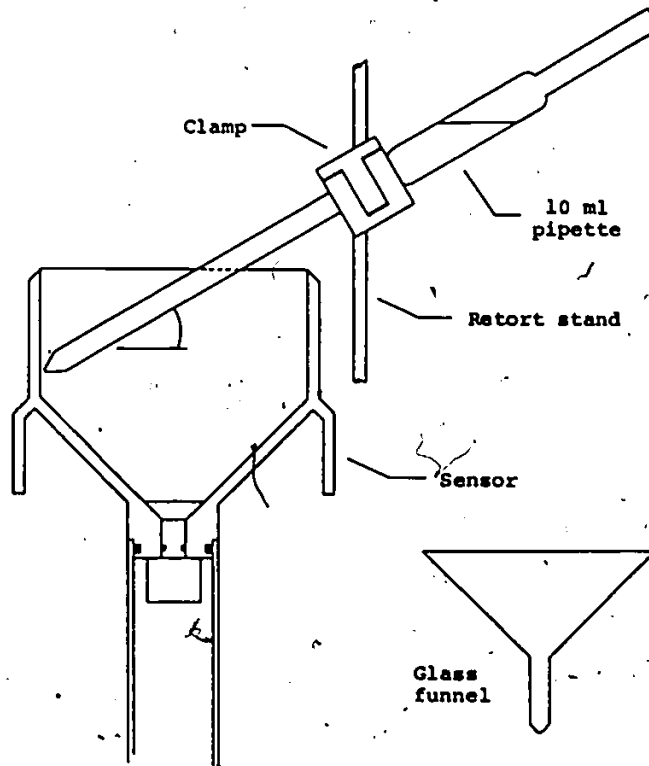


Figure 5.6 Testing apparatus

The simulated rainfall intensities were calculated

using the time for the first one hundred drops to cross the test points and the total number of drops for the 10 ml of water used. In the balance of this report, this method for rainfall intensity estimation will be referred to as the 100-Drops method.

The information required to estimate the intensity was obtained with the aid of a hand held stopwatch and a modified version of the data acquisition system, which displays the number of drops counted. 10 ml of water was used for the tests because this amount corresponds to 1 mm of rain collected over the collection area of the sensor (10 000 square millimeters).

The simulated rainfall intensity in millimeters per hour was calculated by converting the 100 drops into mm of rain (i.e., dividing by number of drops in one mm of rain), and then dividing this result by the time, in hours, for the 100 drops counted. For example, if 100 drops were counted in 10.2 seconds and the total number of drops for 1 mm of rain was 219.9, then the intensity would be $(100/219.9)/(10.2/3600)$ or 160.5 mm/hr.

The rainfall intensities simulated for the tests were intensities corresponding to 100 drops in approximately 10, 16.5, 20, 26.5, 50 and 100 seconds. Later these times were changed to approximately 10, 15, 25, 35, 50 and 100 to obtain a more even distribution of intensities. The first four times were obtained by adjusting the slope of the pi-

ette and the last two by using the two glass funnels.

To verify the above procedure for calculating the simulated rainfall intensities the following tests were performed. For each simulated rainfall intensity, water was placed in the pipette and released into the sensor's funnel. The number of drops counted at 5 second intervals was recorded. This was repeated 10 times for each intensity. The results of this test for an intensity corresponding to 100-Drops in 10 seconds is shown in Table 5.1.

For each 5 second interval, the average of the drops counted during the interval was calculated. The number of drops (incremental) was converted to mm of rain by dividing by the average from the 10 trials of the total number of drops for 10 ml of water and from this result, the equivalent rainfall rate was calculated for each 5 second interval.

The intensities during the last 5 second intervals were lower than the intensities during preceding intervals for the 6 simulated intensities. This behavior is due to the large loss in hydrostatic pressure which occurs as the water level in the pipette reaches the lower end of the nozzle. This effect is more significant for higher intensities than for lower intensities, since at lower intensities the difference of hydrostatic pressure between the top of the pipette is not as large as the difference for higher intensities. The last column indicates the total number of drops

per 10 ml.

In Figure 5.7 the solid line shows a plot of the number of drops counted versus time in 5 second intervals for an intensity corresponding to 100 drops in 10 seconds. The dashed line shows the number of drops per mm that would form at the nozzle for a rainfall rate of 164.4 mm/hr (1 drop is equivalent to 0.0046 mm of rain). Similar plots for the remaining intensities are presented in Appendix A.

The rainfall intensities for the first 4 tests are properly approximated by the intensities obtained using the 100-Drops method. This approximation is acceptable up to 85% of the test duration and can be considered representative of the simulated intensity. For the two tests in which the glass funnels were used an opposite response is observed; the rainfall intensity calculated for 50 seconds underestimates the real intensity, whereas the intensity calculated for 100 seconds overestimates.

From these observations, it is possible to conclude that the 100-Drops method provides a good approximation for determining the simulated rainfall intensities.

5.2.2 TESTS TO DETERMINE SENSOR DESIGN

Six tests were performed to determine the choice of nozzle inside diameter. Four different diameters were tested: 1.19, 1.6, 1.83, and 1.98 millimeters.

Table 5.1
 Simulated rainfall intensity test results
 corresponding to 100 drops in 10 seconds
 (Number of drops at 5 second intervals)

TEST	TIME					TOTAL
	5s	10s	15s	20s	25s	
1	52	95	145	190	212	218
2	53	103	147	189	215	223
3	52	99	146	190	213	218
4	55	99	146	189	212	217
5	50	98	145	188	211	217
6	51	98	145	187	210	216
7	54	99	146	191	215	222
8	52	99	145	190	213	218
9	53	100	146	190	214	220
10	54	98	144	188	212	218
Avg.	52.6	98.8	145.5	189.2	212.7	218.7
S.D.	1.5	2.0	0.9	1.2	1.6	2.3
Inc.	52.6	46.2	46.7	43.7	23.5	6.0
Rate	173.2	152.1	153.7	143.9	77.4	

Equivalent rainfall rate = 164.50 mm/hr

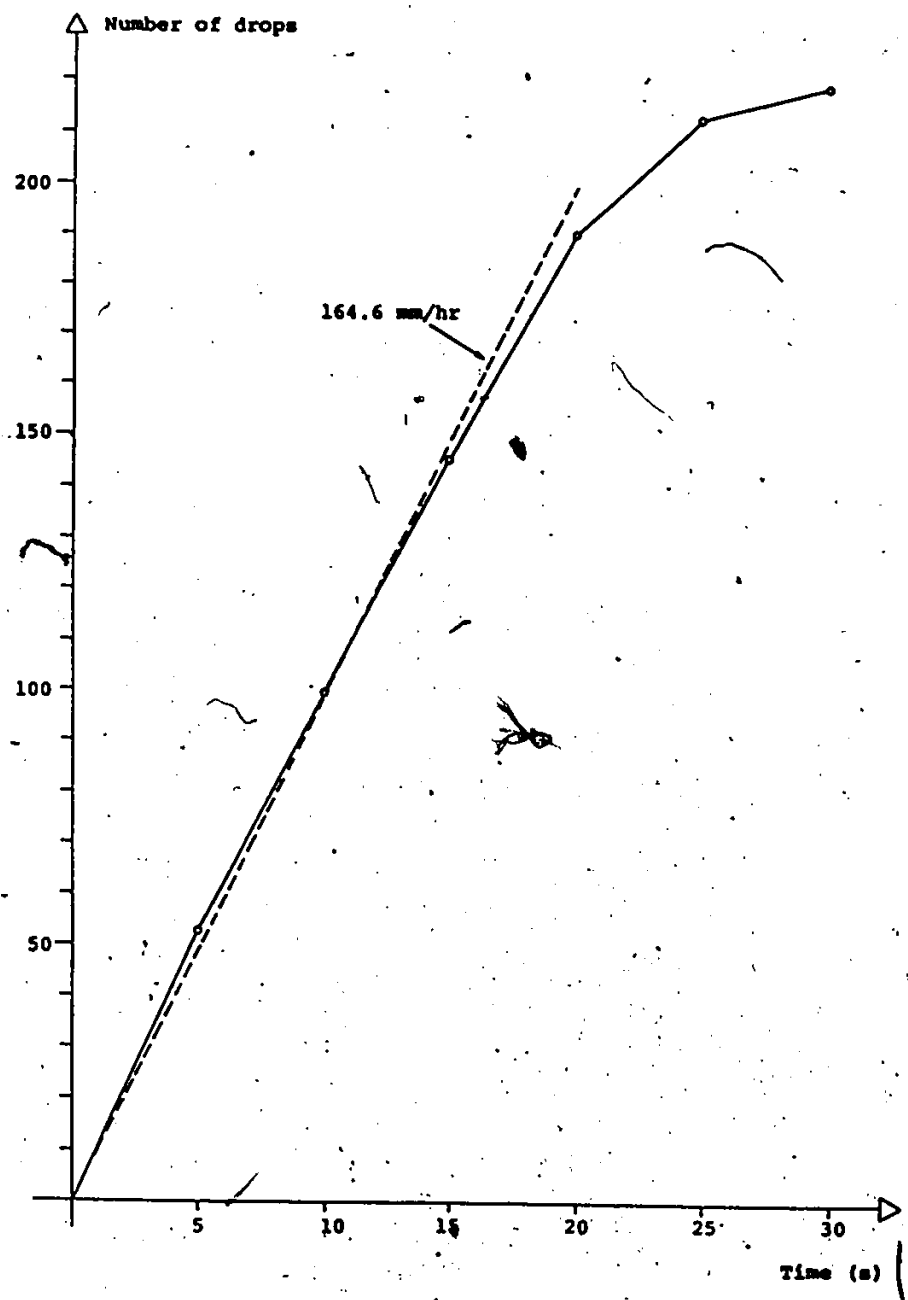


Figure 5.7 Rainfall intensity test results corresponding to 100 drops in 10 seconds

Test procedure was as described previously, but rainfall intensities were determined in a different way (these tests were performed before the 100-Drops method was established). Intensities were obtained by considering the time to drain all of the pipette water instead of the first 100 drops. The rates obtained using this method are up to 12% below the rates obtained using the 100-Drops method.

The results of these tests are shown in Figure 5.8. It is observed that drop size increases with increase in nozzle diameter. Also, as the nozzle diameter is varied, drops at high intensities compared to low intensities are larger for large diameters and smaller for small diameters. The smallest drop size variation in the rainfall intensity range tested was found for the nozzle of 1.83 mm; consequently this nozzle diameter is used in the final design of the sensor.

Similar tests were carried out to establish the length of the nozzle. Three different lengths were tested: 10, 12.5, and 15 mm. The equivalent rainfall rates were determined using the 100-Drop method.

The results of these tests are shown in Figure 5.9. It is observed that there is no appreciable difference among the results obtained. Although the 15 mm nozzle seems to produce larger drops, the difference is so small that it is not considered to be significant. A length of 10 mm was selected to reduce the probability of nozzle blocking.

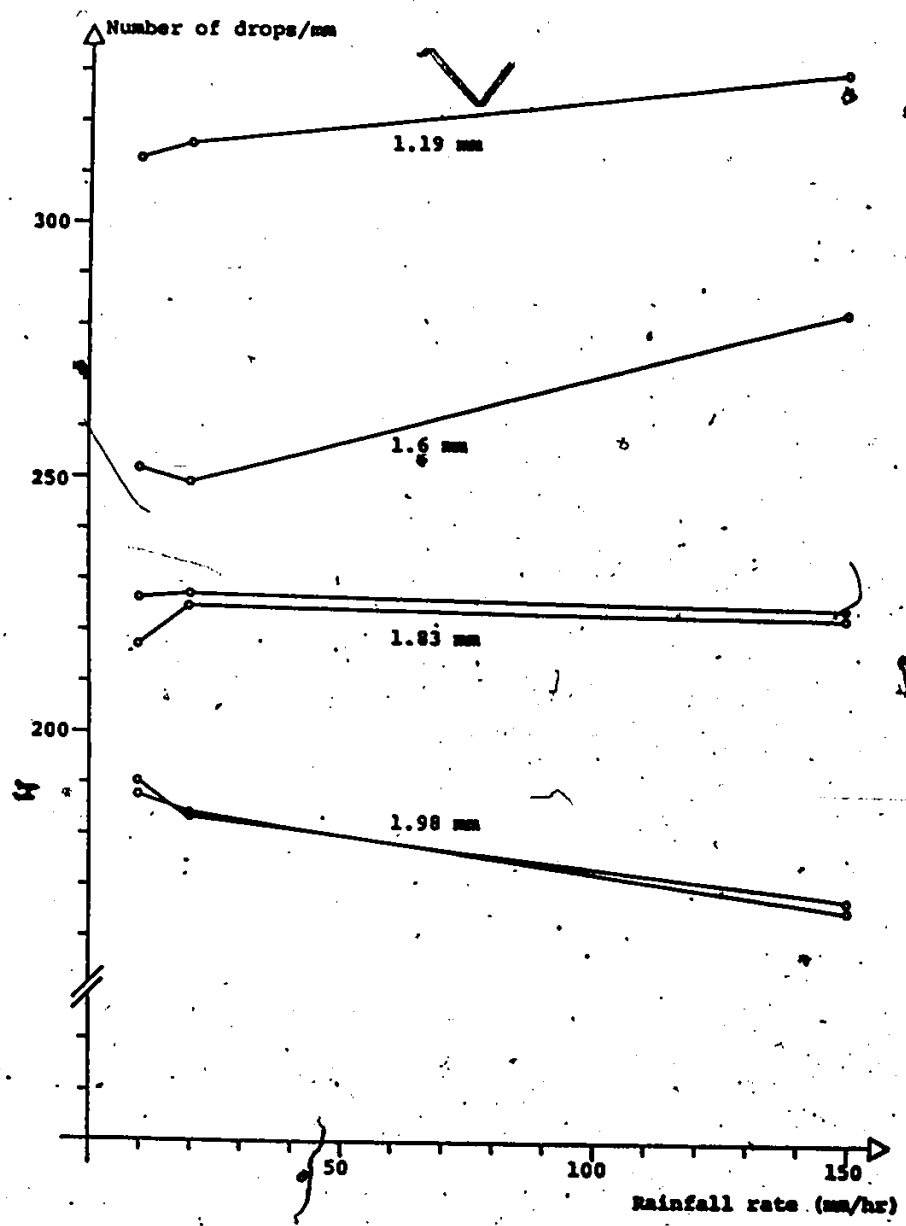


Figure 5.8. Nozzle inside diameter test results

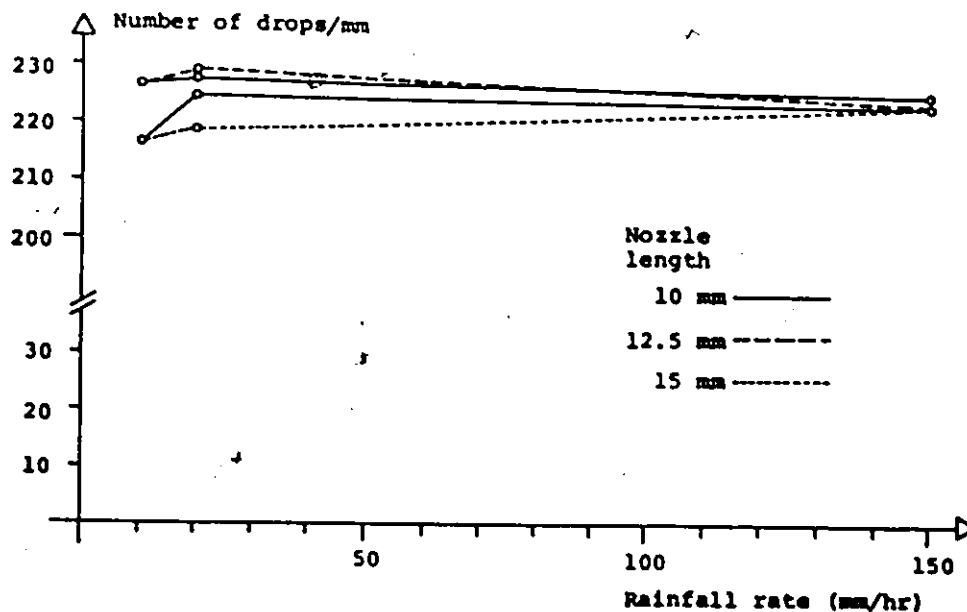


Figure 5.9 Nozzle length test results

A precipitation sensor that is initially dry needs to collect some water on top of the plug before one or more drops can pass through the nozzle and collide with the test points. At the end of a rainfall event, the water collected on top of the plug usually evaporates before the next event. Consequently the amount of water retained must be kept small for accurate time detection of the beginning of a rainstorm. This feature will also reduce the amount of water collected but not counted.

Various tests were performed to determine the amount of water retained by the sensor. The test procedure was as follows: the water from a 2 ml pipette was allowed to drip into a dry sensor. The amount of water placed in the funnel before the first drop fell from the nozzle as well as the

number of first drops were recorded. The remainder of the water in the pipette was poured and the total number of drops recorded. This procedure was repeated with the sensor wet. It was found that, when using the flat mesh screen shown in Figure 5.2, approximately 17.5 drops (0.08 mm of rain) are retained on top of the plug.

To reduce the amount of water retained, the screen design was modified so that the space below the screen was filled, as shown in Figure 5.3. The previous test was repeated using the new screen. The results obtained are shown in Table 5.2. The amount retained with the new screen was reduced to 11.4 drops (0.05 mm of rain). This feature improves the ability of the sensor to respond rapidly, especially during low intensity rainfalls, since less water is needed to wet a dry sensor.

5.2.3 TESTS TO DETERMINE SENSOR PERFORMANCE

Ten tests were conducted to characterize the performance of the sensor at various simulated rainfall intensities. All the tests were carried out with the same sensor, plug, and fine mesh screen and under controlled conditions. That is, water temperature, ambient temperature and simulated rainfall intensities were kept constant. The results obtained are considered to be the standard performance of the sensor. They are the basis of comparison when variations in parameters, such as water temperature, are tested.

Table 5.2
Wetting test results.
(Conical-shaped fine mesh screen)

ml WATER BEFORE DROP	NUMBER OF DROPS	DROPS FOR 2 ml	ml WATER BEFORE DROP	NUMBER OF DROPS	DROPS FOR 2 ml
0.67	1	36	0.02	1	48
0.62	1	37	0.05	1	49
0.63	3	37	0.05	1	48
0.68	1	36	0.12	2	47
0.65	1	36	0.05	1	48
0.65	1	35	0.08	1	48
0.56	1	37	0.03	1	47
0.63	2	38	0.04	1	47
0.61	1	36	0.03	1	48
0.65	1	37	0.05	1	49
AVERAGE					
0.64	1.3	36.5	0.05	1.1	47.9

Difference 11.4 drops

The plug used was a narrow chamber type with a nozzle inside diameter of 1.83 mm, an outside diameter of 2.41 mm and a length of 10 mm. A flat type fine mesh screen was used.

The data gathered from the tests was recorded on data sheets shown in Figure 5.10 (only one of the three pages of test results is shown). These data sheets are also used to record the calibration test results of the sensors assembled for the field program. Each calibration test includes 60 single trials, 10 for each one of the 6 rainfall intensities tested.

The first page of Figure 5.10 summarizes all the information pertaining to the test performed. The information includes the nozzle inside diameter, plug identification number, lower chamber inside diameter, which screens were used for the tests, the material the plug is made of and whether the fine mesh screen contained a breather aperture and tube lead-in wire (used in earlier designs). The remainder of the front page summarizes the results recorded on the three pages of test results, the average and standard deviation obtained in the test and the slope and Y-intercept of the linear regression equation. The slope of the linear regression equation is indicative of variations in drop size for variations in rainfall intensity.

A summary of the 10 tests, where average drop size by test can be compared is depicted in Table 5.3.

DROP COUNTER PRECIPITATION SENSOR

DROP SIZE CALIBRATION TEST No. 1Test done by Haro and Merlo Date 22.06.83

Tube diameter 1.83 mm Plug No 2
 Light/Contact contact Lower chamber I.D. 9.52 mm
 Coarse screen no Nylon/Acrylic nylon
 Fine screen yes Breather aperture yes
 Tube lead-in no

TEST SUMMARY:

TIME [SECONDS] (100 DROPS)	NUMBER OF DROPS MEAN	DROPS DEVIATION	RATE (MM/HR)
<u>10.2</u>	<u>219.9</u>	<u>2.4</u>	<u>160.50</u>
<u>16.4</u>	<u>216.6</u>	<u>2.4</u>	<u>101.34</u>
<u>20.4</u>	<u>216.4</u>	<u>1.3</u>	<u>81.55</u>
<u>25.7</u>	<u>215.9</u>	<u>2.4</u>	<u>64.88</u>
<u>53.2</u>	<u>217.4</u>	<u>1.2</u>	<u>31.13</u>
<u>101.3</u>	<u>217.0</u>	<u>1.7</u>	<u>16.38</u>

Average per 1 mm. of rain..... 217.2 [Drops]Standard deviation..... 1.42 [Drops]

Linear regression:

Slope (M)..... 0.0167 [DR-HR/MM²]Y-intercept..... 215.93 [Drops/mm]REMARKS _____

Figure 5.10 Precipitation sensor calibration data sheets

Page 2Test No. 1

No DROPS	TIME (S) 100 DROPS		No DROPS	TIME (S) 100 DROPS
<u>215</u>	<u>10.4</u>		<u>221</u>	<u>16.8</u>
<u>218</u>	<u>10.0</u>		<u>216</u>	<u>16.2</u>
<u>221</u>	<u>10.0</u>		<u>216</u>	<u>16.6</u>
<u>221</u>	<u>10.2</u>		<u>215</u>	<u>16.3</u>
<u>223</u>	<u>10.3</u>		<u>216</u>	<u>16.0</u>
<u>222</u>	<u>10.0</u>		<u>216</u>	<u>16.2</u>
<u>219</u>	<u>10.5</u>		<u>221</u>	<u>16.7</u>
<u>221</u>	<u>10.1</u>		<u>215</u>	<u>16.8</u>
<u>221</u>	<u>10.2</u>		<u>215</u>	<u>16.1</u>
<u>218</u>	<u>10.3</u>		<u>215</u>	<u>16.0</u>
<u>219.9</u>	<u>10.2</u>	AVG.	<u>216.6</u>	<u>16.4</u>
<u>2.4</u>	<u>0.2</u>	S.D.	<u>2.4</u>	<u>0.3</u>

160.50 EQUIVALENT RATE (MM/HR) 101.34

COMMENTS _____

Figure 5.10 (cont)

Table 5.3

Summary of characterization test results

TEST	STANDARD			
	AVERAGE	DEVIATION	SLOPE	Y-INTERCEPT
	drops/mm	drops/mm	drops-hr/mm ²	drops/mm
1	217.20	1.42	0.0167	215.93
2	215.40	2.74	0.0438	211.93
3	215.96	1.32	0.0014	215.85
4	217.95	1.48	-0.0074	218.51
5	216.48	1.72	0.0009	216.41
6	216.42	2.80	-0.0285	218.61
7	219.42	3.69	-0.0589	223.89
8	214.88	4.00	-0.0752	220.68
9	218.38	3.48	-0.0377	221.29
10	218.05	5.30	-0.0838	224.50
Ave.	217.01	2.795	-0.0229	218.76
S.D.	1.436	1.331	0.0414	3.92

1 drop equivalent to 0.0046 mm of rain

The mean of the total number of drops per 10 ml of water is 217.01 which corresponds to 0.0046 mm of rain per drop. The standard deviation obtained for 10 ml is an index

of the precision of the instrument; the value of 3.49 drops per 10 ml is appropriate for most applications. The coefficient of variability is 1.6%.

A plot of the average performance of the sensor at 6 different rainfall intensities is given in Figure 5.11. It is seen that the number of drops per 10 ml of rain over the rainfall intensity range tested is almost constant. The standard deviation of the average number of drops at 6 different rainfall intensities is approximately 1.83 drops and the coefficient of variability is 0.84%.

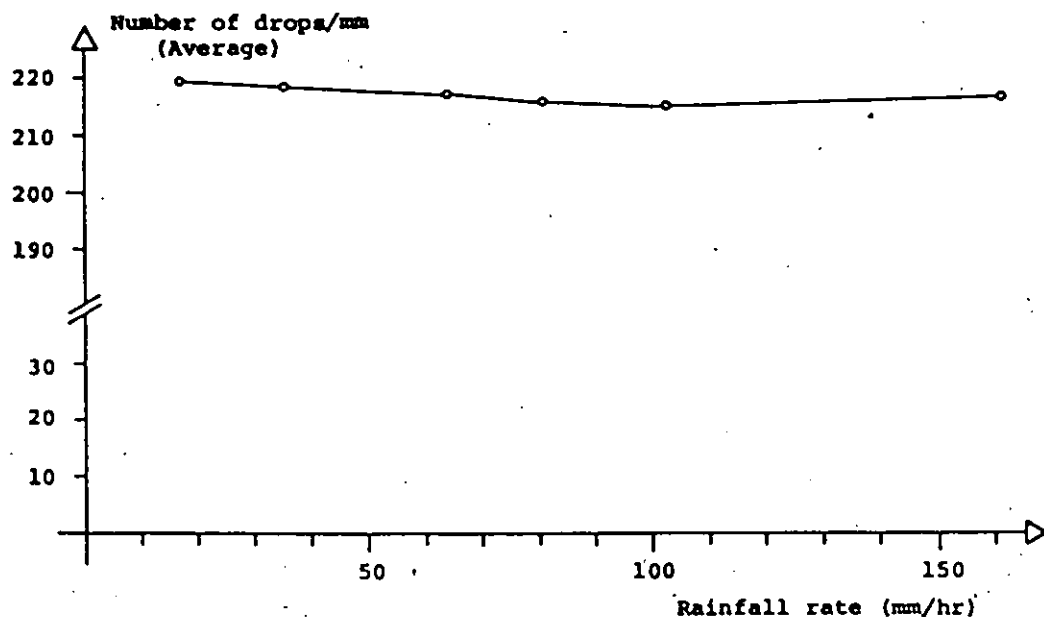


Figure 5.11 Precipitation sensor standard performance

To derive statistics on the drop size distribution, all individual results obtained in tests 1 to 10 are considered to be the total population. Assuming that the drop

size distribution is normal, the standard deviation is given by [82]

$$s = \left[\frac{\sum x^2 - (\sum x)^2/N}{N - 1} \right]^{1/2}$$

where

N = Number of samples

x = Sample value

$N-1$ = Number of degrees of freedom associated with s .

Using the properties of the normal distribution curve and the values obtained in the tests for the mean and the standard deviation, one obtains the probability of occurrence of a new observation. The following probabilities for 1 mm of rain are calculated using drop size $\bar{x} = 217$ drops/mm and standard deviation $s = 3.492$ drops/mm.

$(\bar{x} \pm 1\%)$	$P[215 \leq x \leq 219] = 0.4314$
$(\bar{x} \pm 2\%)$	$P[213 \leq x \leq 221] = 0.7478$
$(\bar{x} \pm 5\%)$	$P[207 \leq x \leq 227] = 0.9958$

In others words, the probability of obtaining between 207 and 227 drops for 1 mm of rain is 0.9958. Figure 5.12 shows the histogram of test result. The normal frequency curve corresponding to the above values of mean and standard deviation is represented by the dotted line.

The shape of the histogram conforms approximately to the normal curve. The following is obtained from the histogram:

58.66% of results are in the interval $215 \leq x \leq 219$
 83.88% of results are in the interval $213 \leq x \leq 221$
 99.33% of results are in the interval $207 \leq x \leq 227$

The confidence intervals are given by

99.7% confidence interval 217 ± 3.31 drops
 95.0% confidence interval 217 ± 2.16 drops
 88.3% confidence interval 217 ± 1.10 drops

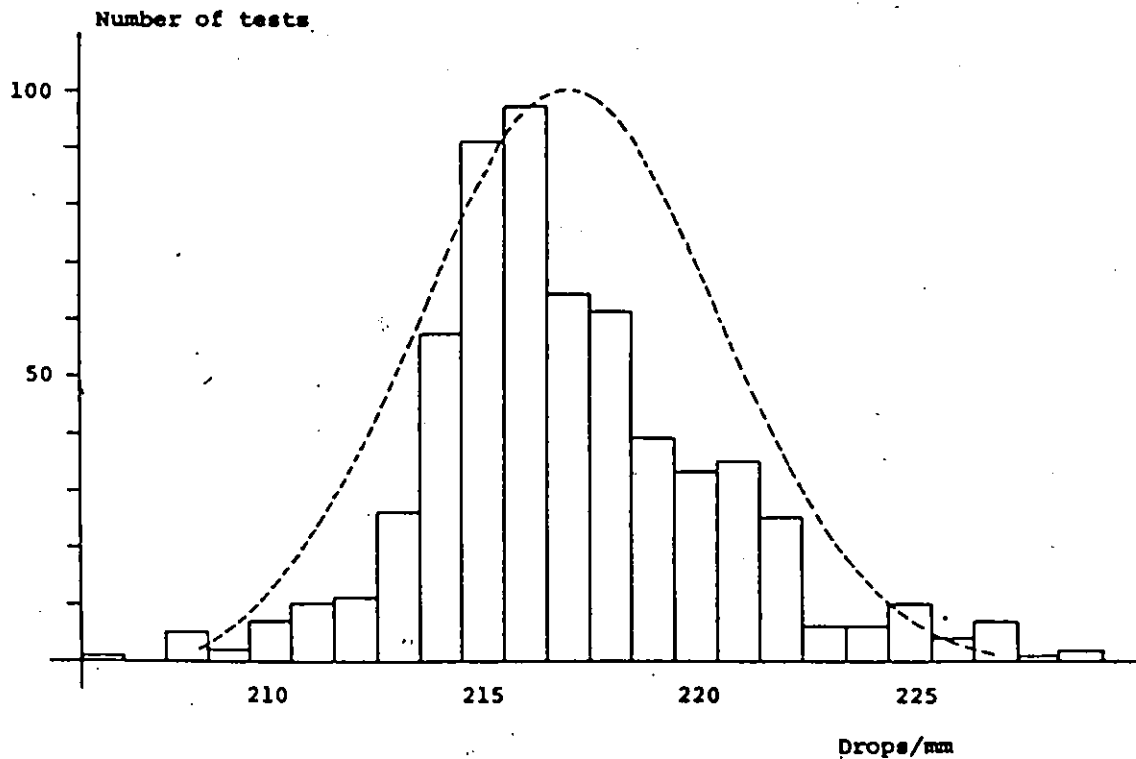


Figure 5.12 Histogram of test results

In other words, the assertion that the population mean value falls within the relative narrow interval of 214 to 219 has a probability of 0.95.

In addition to the tests previously described, various tests were undertaken to determine the maximum rainfall intensity (before jetting occurs) permissible in the precipitation sensor. The test procedure is described as follows: a 20 ml pipette was filled and held approximately 1 cm vertically above the sensor funnel. The water in the pipette was released and a stopwatch was started at the time the first drop was detected by the test points. The time and number of drops at the time the jet occurred were recorded. The time recorded was extrapolated to the corresponding time for 100 drops. The maximum rainfall rate was found using the values obtained and the 100-Drops method.

The results obtained are shown in Table 5.4. The large variation of the rainfall rates can be attributed to the nature of the experiment. There are several parameters that may affect the results obtained such as nodes and drops formed at the end of a liquid jet, satellite droplets produced by drop breakup, and inaccuracies of the measured time. If any of the first two cases occur, the number of drops counted will be larger than the number of drops expected for the volume of water released. If a larger number of drops is considered in the calculations, the maximum rainfall intensity calculated will be larger than the real in-

tensity permissible by the sensor.

The nature of the test is such that it is very easy to obtain erroneous time measurements. It is not difficult to determine the time at which the first drop reaches the tests points; the inaccuracy is mainly due to the manner in which the jet presence is determined. When a jet issues from the nozzle, the drop counter is not incremented because the jet diameter is smaller than the distance between the test points, and therefore the water bridge created between the points through the water drop is not formed. During the tests the jet presence was determined by observing the time at which the drop counter stops counting. The calculations do not take into account the fact that there is a reaction time between observing that the drop counter has stopped counting, and the observer stopping the stop watch.

The results obtained in these experiments are not truly representative of the real maximum rainfall rate. However the results obtained may be used to indicate this rate.

The complexity of the determination of the maximum rate is clearly seen. A better approach can be obtained if new experiments with more sophisticated equipment are designed. Equipment with the ability to supply and measure constant water flows with a precision of 27 cubic millimeters per second would be required to determine the maximum rainfall rate with a precision of 10 mm/hr.

Table 5.4
 Summary of maximum rainfall intensity test results

TEST	NUMBER OF DROPS	TIME (s)	TIME 100 DROPS	RATE mm/hr
1	93	4.5	4.8	345.6
2	68	3.5	5.1	325.3
3	65	3.1	4.8	345.6
4	56	3.2	5.7	291.1
5	79	3.9	4.9	338.6
6	61	3.5	5.7	291.1
7	68	3.2	4.7	353.0
8	82	4.1	5.0	331.8
9	75	4.0	5.3	313.0
10	92	4.8	5.2	319.0
11	66	3.2	4.8	345.7
12	73	3.5	4.8	345.7
13	84	4.0	4.8	345.7
14	88	4.9	5.6	296.3
15	67	3.4	5.0	331.8
AVERAGE	74.4	3.78	5.09	326.22

Average maximum rainfall rate = 327.93 mm/hr

Literature reviewed in Chapter 4 on drop formation theory included several formulas to calculate drop weight and volume, and jetting velocity based on nozzle dimensions and liquid flow rate. A comparison of the drop volume and maximum rainfall rate obtained experimentally against the corresponding calculated values follows.

The following values are used in the calculations:

A	Sensor collection area	1 E-02	[m]
An	Nozzle area	2.63 E-06	[m ²]
Dn	Nozzle inside diameter	1.83 E-03	[m]
g	Gravity acceleration	9.81	[m/s ²]
t	Temperature	20	[°C]
V	Drop volume	46 E-09	[m ³]
	(From characterization test)		
Y	Water surface tension	7.36 E-02	[N/m]
σ	Water specific weight	9789	[N/m ²]
Δρ	Difference between densities of dispersed and continuous phase	996.98	[Kg/m ³]
ρ	Water density	998.2	[Kg/m ³]

The weight of the "Ideal" drop given by Tate (Eqn 4.1) is

$$W = Mg = 2\pi r\gamma$$

hence

$$W = 422.85 \times 10^{-6} \text{ (Kg}\cdot\text{m/s}^2\text{)}$$

where the volume is calculated by

$$V' = \frac{W}{\sigma} = 43.197 \times 10^{-9} \text{ (m}^3\text{)}$$

Thus the Harkins and Brown correction factor (Eqn 4.4) may now be calculated

$$F(r/V^{1/3}) = \frac{V}{V'} = 1.066$$

The drop volume calculated by means of Tate's formula is less than the volume obtained by experimentation; it was expected to be larger. Thus the correction factor is greater than unity (its range is expected between zero and one). This deviation may be attributed to the time of drop formation; Tate's and Harkins and Brown's formulas apply to drop growth times of at least 3 minutes, while for the drop volume obtained experimentally with the precipitation sensor, drops are formed in approximately 1/10 of a second for rainfall rates of 164 mm of rain per hour.

As noted in Chapter 4, when the drop growth time is faster than one drop in three minutes, some of the water streaming from the tube flows into the falling drop during the time of detachment and consequently a drop formed rapid-

ly is heavier than a drop formed slowly.

Using the experimental value of volume V , $r/V^{1/3} = 0.255$. The Harkins and Brown correction factor cannot be estimated from Figure 4.2 because it does not show values of $r/V^{1/3}$ below 0.3. For values under 0.3, $F(r/V^{1/3})$ tends to 1, indicating that the whole drop falls (No water is retained in the nozzle after drop detachment):

Rayleigh proposed the following expression to find the weight of the drop (Eqn 4.2)

$$W = 3.8 \gamma a$$

The ratio of radius of the nozzle used is approximately 1.32. Considering the external radius the drop volume is

$$V = 34.47 \times 10^{-9} \text{ (m}^3\text{)}$$

This value is 25% smaller than the drop volume obtained experimentally and the deviation may be attributed to the large radius ratio of the nozzle used in the sensor.

In the Scheele and Meister formula the term due to the drag force is negligible for low continuous phase viscosities (as in the DCPS) so that equation 4.5 becomes

$$v_f = F(r/V^{1/3}) \left[\frac{\pi \gamma D_n}{g \Delta \rho} - \frac{4 \rho Q U_n}{3 g \Delta \rho} + 4.5 \left(\frac{Q^2 D_n^2 \rho \gamma}{(g \Delta \rho)^2} \right)^{1/3} \right]$$

where the terms account, respectively, for buoyancy and interfacial tension, kinetic force and volume added during necking.

Table 5.5 shows the Harkins and Brown correction factor calculated at various flow rates (assuming that the flow rate through the nozzle (Q) is equal to the simulated rainfall rate).

TABLE 5.5

FLOW RATE [m ³ /s] (1 E-09)	EQUIVALENT RAINFALL RATE [mm/hr]	Vf/F(r/V ^{1/3}) [m ³] (1 E-09)	F(r/V ^{1/3})
47.22	17	51.17	0.900
225.00	81	63.41	0.727
458.33	165	68.98	0.668
700.21	252	66.43	0.693

These calculations are based on the drop volume obtained from the sensor characterization tests. The factor $V_f/F(r/V^{1/3})$ decreases with increase in flow rate. However it was observed in the tests performed that at least for the first three flow rates, the drop volume remains almost constant. The difference may be attributed to the water remaining in the nozzle after drop detachment.

The theoretical maximum rainfall rate permissible in the precipitation sensor is given by (Eqn 4.6)

$$U_j = 1.73 \left[\frac{\gamma}{\rho D_n} \left(1 - \frac{D_n}{D_f} \right) \right]^{1/2}$$

Due to the reduced size of the drops produced, one may assume that the drops have a spherical shape, so that $D_f = 4.45 \text{ E-}03 \text{ m}$. The Reynolds number at the nozzle is 19.2, therefore, a parabolic velocity profile is considered in the calculations. Substituting numerical values results in

$$U_j = 266.6 \times 10^{-3} \text{ (m/s)}$$

The volume flow rate of the dispersed phase through the nozzle is then given by

$$Q_j = U_j \times A_n = 700 \times 10^{-9} \text{ (m}^3\text{/s)}$$

This corresponds to 15.2 drops per second or a maximum rainfall rate of 252.1 millimeters of rain per hour.

Comparison of the theoretical value of the maximum rainfall and the rate obtained experimentally shows a difference of approximately 75 mm per hr which is large. As explained before, the experimental results may be far from the real maximum rate. The theoretical rate calculated should be employed with caution because the equation was obtained using liquid-liquid systems and under specific test

conditions.

The maximum rainfall rate cannot be determined more accurately until special instrumentation to perform the experiments is available. The maximum rainfall rate of 180 mm/hr specified in the precipitation sensor technical data sheet was obtained by means of the 100-Drops method in several of the tests performed for different purposes.

5.2.4 TESTS TO DETERMINE SENSOR SENSITIVITY

Various tests were undertaken to determine the effects on the relationship between drop size and rainfall intensity of the variation of parameters, such as water temperature, fine mesh screen and breather aperture position and size. A summary follows.

One test was performed to determine the sensor performance if no fine mesh screen is used. The test was carried out at 6 different rainfall intensities following the usual procedure.

When water is first applied, it builds up between the outside of the top of the plug and the inside wall of the funnel as shown in Figure 5.13 (a). As the inflow continues the water bulges over the inside edge of the plug as in Figure 5.13 (b). Just prior to drop formation, this water storage bursts and fills up the inside of the top portion of the plug, as illustrated in Figure 5.13 (c). At this point, drops begin to fall from the bottom of the noz-

zle and continue to fall until the rate of drop formation, i.e., the flow from the nozzle is larger than the flow of water into the sensor.

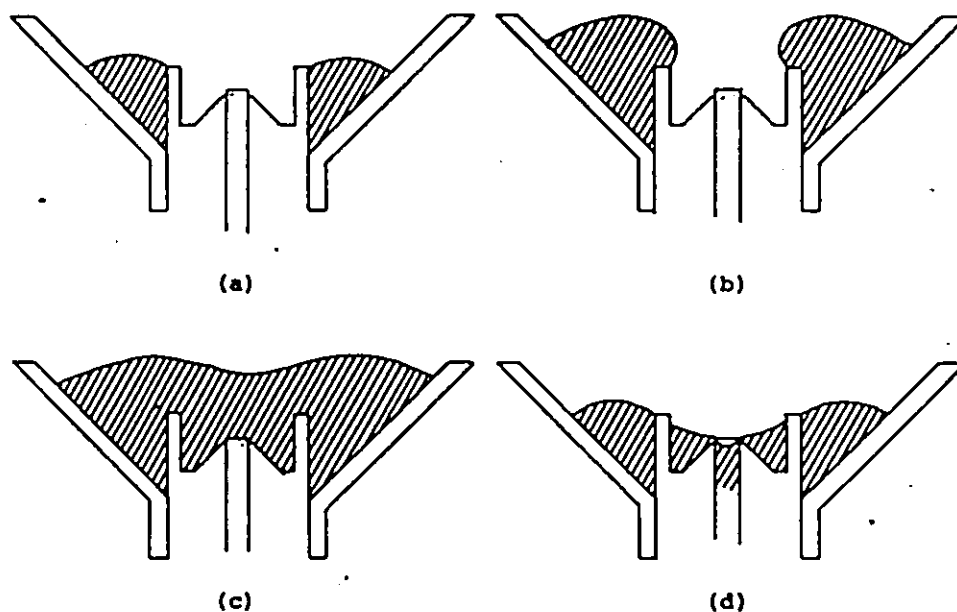


Figure 5.13 Precipitation sensor performance
without fine mesh screen (see text)

Figure 5.13 (d) shows the appearance of the sensor at the time the water has completed falling from the nozzle. As water continues to flow into the sensor, the build up of water around the top of the plug causes drop formation to commence again.

The average drop size produced when no fine screen is used, is approximately 34% smaller than the standard drop size. Very large variations in drop size were observed and the equivalent rainfall rates could not be calculated because of the above unsteady manner in which drops are pro-

duced.

From the above observations it was concluded that the fine mesh screen is needed to maintain a continuous flow of water into the nozzle in addition to stopping small particulates from entering the tube.

As described earlier in this chapter, the fine mesh screen has a breather aperture which appears to aid the flow of water through the screen and into the tube. This aperture consists of a hole 2.5 mm in diameter, placed near the centre of the screen. The hole evidently breaks up the film of water held on the screen. In order to determine if the breather aperture is needed and if so, to determine its size and position, four different screens were made. They had the following characteristics: screen No. 1 had no breather aperture, screen No. 2 had a 3 mm diameter breather aperture, screen No. 3 had a 3 mm aperture but placed closer to the centre of the screen and screen No. 4 had a 2 mm aperture placed in the same position as screen No. 2. Each screen was tested at 6 different rainfall intensities using the procedure previously described.

Figure 5.14 illustrates sensor performance for each of the above mesh screens. It is clear that the average drop size as well as the precision of the sensor are functions of the size and position of the breather aperture. Low precision and small size drops are observed when the fine mesh screen does not contain an aperture.

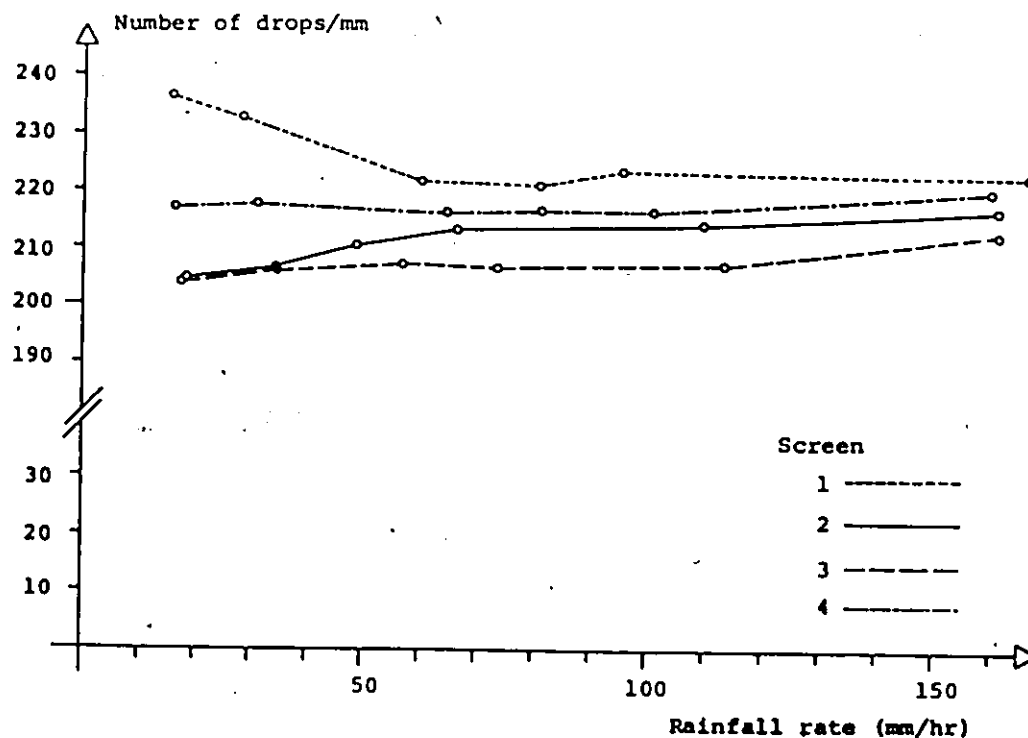


Figure 5.14 Effect of fine mesh screen breather aperture on sensor performance

The fine screen with an aperture diameter of 2 mm evidently produces drops of more consistent size over the rainfall intensity range tested. Little difference is observed when the aperture position is changed, but it seems that increasing the distance from the screen centre improves the drop size uniformity.

In the tests performed using the screen without a breather aperture, a small water build up on top of the screen was frequently observed. From these observations, it was decided to include an aperture of 2 mm in diameter placed far from the centre of the screen.

Five tests were performed to determine the effect of water temperature on drop size at different rainfall intensities. The tests were carried out at two different temperatures, 0 and 70 degrees Celsius, using the test procedure described previously.

Figure 5.15 shows a plot of sensor performance using water at the two temperatures as well as that obtained for the characterization test using water at 22 degrees. For water at 0 degrees, the average drop size is 4% larger than that at 22 degrees whereas, for water at 70 degrees, the average is just 0.8% larger. These results corroborate Guthrie's experiments (Chapter 4). The standard deviations obtained for 0 and 70 degrees are approximately the same, but they are larger than the standard deviation obtained at 22 degrees. The drop size variation was expected because surface tension is temperature dependent.

Because rainfall is formed by melting ice particles, rainfall temperature is, in general, slightly lower than the ambient ground-level temperature. Rainfall temperatures over 20 degrees is only likely to occur in summer.

In performing the above tests, it was found that the time for one hundred drops to cross the test points varied, depending on water temperature even though the position of the pipette and funnels were not changed. For water at 0 degrees Celsius, the times obtained are longer and hence the equivalent rainfall intensities lower whereas, for 70 de-

degrees the times are shorter and hence the intensities higher. This time variation is due to the temperature dependence of both the surface tension and viscosity of water; it is more noticeable at very low flow rates where water flows through capillaries in the glass funnels. Water is released from the glass funnels in the form of drops whose size also varies with water temperature.

The precipitation sensors are not intended for use below the freezing point and hence the temperature operating range is approximately from 0 to 20 degrees Celsius. A variation of about 4% in the drop size is expected in this temperature range; this is considered negligible in most Civil Engineering applications. This drop size variation can be corrected in the calculations of intensity and total precipitation if the ambient ground level temperature is known.

5.3 FIELD CALIBRATION TESTS

A field program was established. Several sampling sites were settled at different locations throughout the City of Hamilton. The instrumentation installed comprised a drop counter precipitation sensor and a data acquisition system. In some of the sampling locations tipping bucket raingauges were also included to compare the performance of both instruments. Data acquisition systems were used to store the rainfall data from the tipping bucket raingauges.

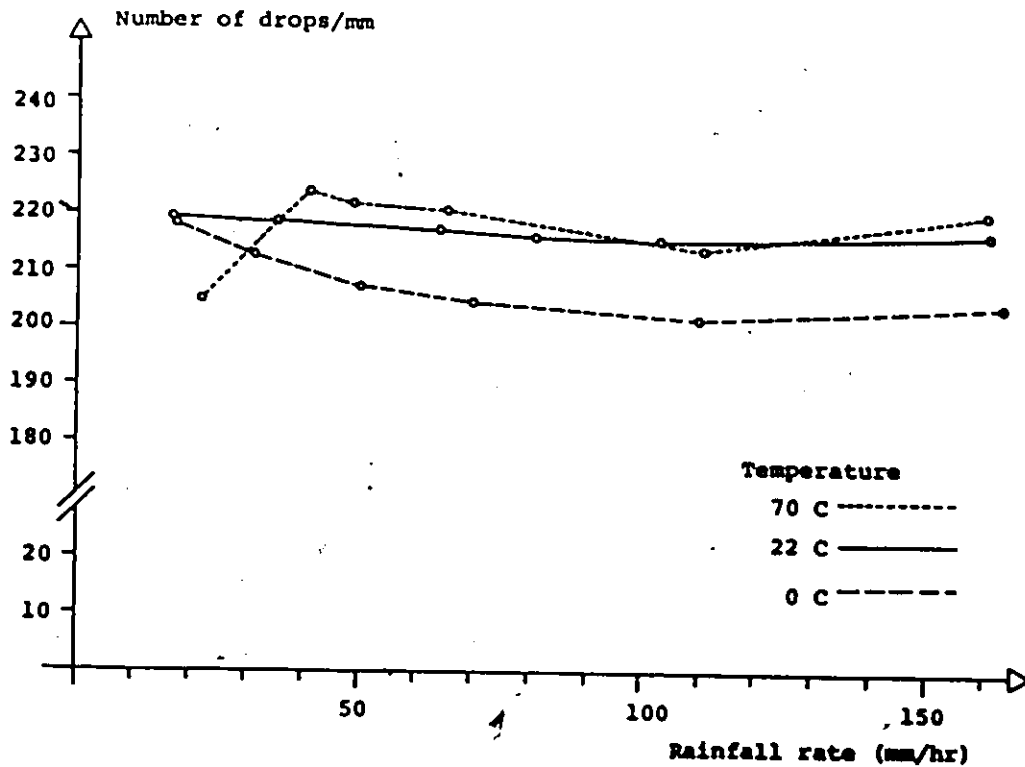


Figure 5.15 Effect of water temperature on sensor performance

Thirty nine precipitation sensors were constructed and calibrated as part of the field program. Twenty five sensors included 1.83 mm diameter nozzles (nozzle A) whereas, the remainder used 1.6 mm nozzles (nozzle B).

Seven sensors were operated in the City of Hamilton during the Summer of 1983, the remainder being used or evaluated in Ottawa (6), Halifax (16), Toronto (6), Calgary (1), Kentucky (U.S.A.) (1), Norway (1) and Mexico (1).

A summary of the calibration tests performed with the 39 sensors is presented in Appendix A; an evaluation of the results follows.

The sensors containing nozzle A were tested at 6 ra-

infall intensities using the test procedure described before. Because sensors using nozzle B were tested before the test procedure was standardized, they were tested at 3 rainfall rates. The rates were determined from the total number of drops per 10 ml and the time required to pour all the water into the sensor. The difference in the rainfall intensities estimated by both methods is under 12%.

Comparing the results herein obtained with the results obtained from the characterization test the following is observed: The average drop size produced by nozzle A is approximately 3.7% larger than the standard drop size whereas, the average drop size produced by nozzle B is 22.65% smaller. The standard deviation obtained for each test with nozzle B is large, i.e., the drop size is extremely non-uniform (as was observed in Figure 5.8), whereas, the average standard deviation with nozzle A (5.3 drops/mm) is similar to the standard deviation obtained in the characterization test (3.49 drops/mm).

From the results obtained with nozzle A, it is possible to infer that under specific conditions, the performance of a drop generator plug is similar to the performance of the characterized plug with a possible variation in drop size. In other words, any plug with the same diameter will lead to the same precision, standard deviation, and degree of confidence but possibly a different drop size. This difference has been attributed to variations in nozzle diam-

eter. It is expected that variations in average drop size will not be greater than 6%.

The precipitation sensor was tested at 6 different rainfall rates. The mean of the number of drops per millimeter of rain was 217 and the standard deviation was 3.49. These values are appropriate for most Civil Engineering applications. It was shown that the average drop size as well as the precision of the sensor are functions of the size and position of the fine mesh screen breather aperture and rain water temperature. The drop volume obtained experimentally was approximately 6% greater than the volume predicted by Tate's equation, the deviation has been attributed to the time of drop formation.

The experimental results obtained in the tests to determine the maximum rainfall rate permissible by the sensor are not representative of the real maximum rate. The accurate determination of this rate is not being undertaken until adequate instrumentation to perform the experiment is available. The value of 252 mm/hr was obtained using the equation for incipient jetting at the nozzle. The maximum rate of 180 mm/hr specified for the sensor was obtained in several of the tests performed for different purposes.

CHAPTER 6
DATA ACQUISITION SYSTEM

A data acquisition system (DAS) is a device designed to automatically collect large amounts of data from one or more sources and store or transmit the data for future or immediate processing. If continuous hydrometeorological data is to be stored at a fine time resolution, large quantities accumulate very rapidly and it is therefore essential that the mode of storage be computer compatible.

This chapter describes the operation of a low-cost, microcomputer-based data acquisition system designed to gather data from the drop counter precipitation sensor, partially process the data, and store the information on magnetic cassette tapes. The DAS contains only one acquisition channel, but it is possible to expand the system to include other measurements such as temperature, water conductivity, and pH.

Some of the advantages resulting from the use of a microcomputer include multiple sampling rates, data processing, continuous or intermittent operation, and programmability to cover other data acquisition needs.

6.1 CIRCUIT DESCRIPTION

The data acquisition system senses the drops and counts them over a programmable time interval, processes the time series and stores the results temporarily in the microcomputer data memory. When the memory is full, the information is stored on standard audio cassette magnetic tapes for future processing. Figure 6.1 shows a block diagram of the DAS.

The sensor interface block contains the electronic circuits necessary to transform the electrical signal produced by the DCPS into a positive voltage pulse compatible with the microcomputer specifications. The DAS circuit diagram is shown in Figure 6.2.

Every time a drop falls and collides with the test points, an electrically conducting bridge is created between the points. The current flowing through the drop is amplified by transistor Q2, placed inside the sensor, and transmitted to the DAS through an unshielded two-conductor cable.

The shape and duration of the pulse generated depends basically on

1. the volume of water in the drop that bridges the test points. This depends on the drop shape and volume, and on the test point shape and separation,

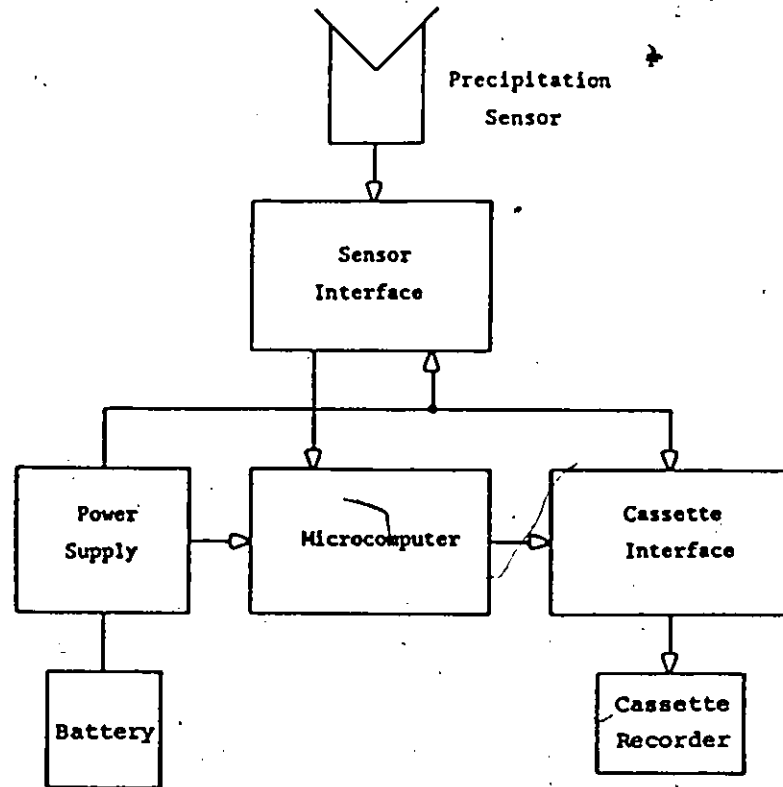


Figure 6.1 DAS block diagram

2. speed of the drop when it bridges the test points. The speed of the drop is a function of the rainfall rate, the stainless steel tube diameter, and the distance between the bottom rim of the tube and the test points.

The amplitude of the pulse depends basically on

1. water conductivity, which is a function of the ionizable inorganic dissolved solids,

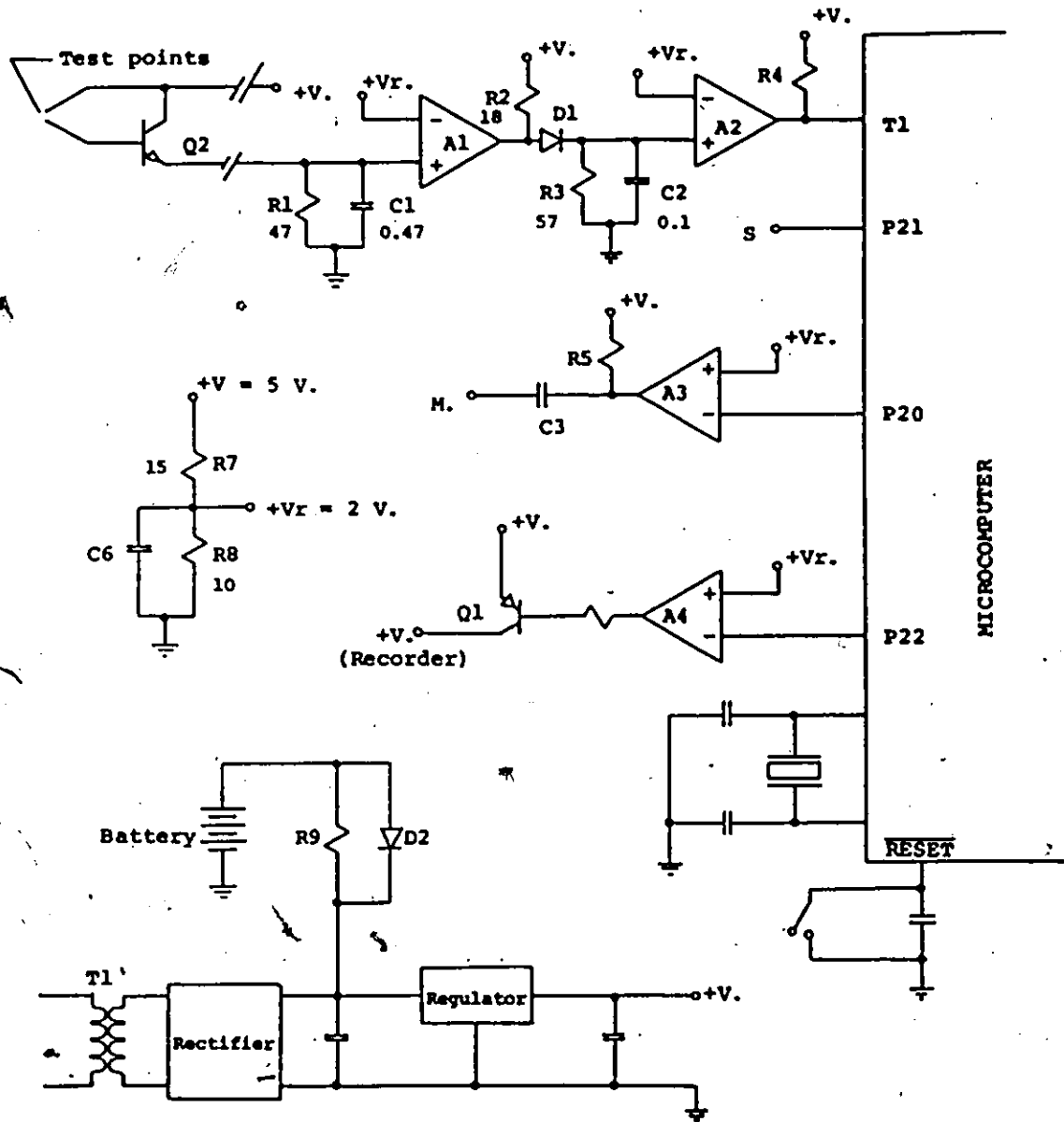


Figure 6.2 DAS circuit diagram. Capacitors are in microfarads and resistors in kilohms



2. the volume of the water that creates the electrical bridge between the test points,
3. test points separation and cleanliness.

There are other factors that determine the characteristics of the generated pulse, but those listed above are considered to be the most significant for this application. Figure 6.3 shows a typical pulse. On average, the pulse has a duration of 15 ms for a drop volume of 46 cubic millimeters.

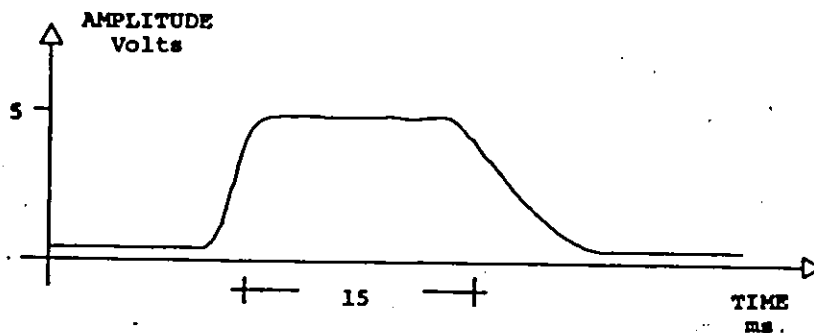


Figure 6.3 Typical signal generated by the presence of a drop

Referring to Figure 6.2, the input of the sensor interface includes resistor (R1), capacitor (C1), and voltage comparator (A1). R1 and C1 form a low-pass filter which attenuates unwanted high frequency components and converts the current signal into voltage. A1 compares the signal against the voltage reference V_r , derived by means of R7, R8, and C6. Because the output of the voltage comparator is an un-

committed collector, a pull-up resistor (R2) is included. R2 together with D1, R3, C2 and A2, constitute a retriggerable monostable multivibrator. This circuit avoids multiple counts, caused by a single drop, if drop breakup occurs.

When a drop builds a bridge between the test points, the output of A1 is high and capacitor C2 charges with a time constant $\tau_2 = R_2 \cdot R_3 \cdot C_2 / (R_2 + R_3)$ (neglecting diode resistance and voltage comparator input impedance). If the output of A1 remains high for at least 1 ms, the capacitor voltage will exceed V_r and the output of A2 will switch to high state. When the drop leaves the test points the output of A1 becomes low and C2 discharges mainly through R3 with a time constant $\tau_3 = R_3 \cdot C_2$. The output of A2 will switch to low if the output of A1 remains low for at least 5 ms. These times (1 and 5 ms) were determined based on the signal generated when drop breakup occurs which are pulses of approximately 0.1 to 0.3 ms following the signal generated by the main drop. The output of A2 is a positive pulse slightly delayed with respect to the drop generated pulse and with voltage levels compatible with the microcomputer I/O pins. This signal is fed to the microcomputer through input pin T1. R4 is a pull-up resistor.

The cassette interface contains the circuits needed to control the recorder power supply and to condition the signal to be recorded. The recorder is a mass-produced unit for audio purposes that has been modified slightly.

Standard audio cassette tapes are used.

The microcomputer turns the cassette recorder power supply on and off via output port 2, bit 2 (P22). Voltage comparator A4 drives transistor Q1 as an ON/OFF switch. The collector of Q1 is connected to the cassette recorder power supply.

In order to record the digital signal onto tape, Frequency Shift Keying (FSK) is used because of the limited frequency response of the recorder. The Kansas City Standard [83] for recording digital information on audio magnetic tapes is used. The frequencies of the carriers are 1800 and 2700 Hz for logical "0" and logical "1" respectively. The selection of these frequencies assures that a frequency transition always occurs during a voltage transition of the modulated signal.

The FSK signal is generated by the microcomputer using software, and transmitted to the recorder through P20. The ac-coupled amplifier comprising A3, R5 and C3 connects the microcomputer output pin to the cassette recorder input. The signal recorded is a square wave, but because the frequency response of the recorder is that of a band pass filter centered about 2000 Hz, the played-back signal is a distorted sinusoid.

The power supply includes a rectifier bridge, filters, a voltage regulator, and also a self-charging battery backup. When the primary power source is on, the bat-

tery charges through R9, D2 being reverse biased. In the event of primary power source failure, the battery provides the required current through D2.

The circuit is not intended for battery-only operation because its high power consumption would not allow this. However, the microcomputer can be replaced by its recently-introduced CMOS version, if desired.

The electronic components are assembled on a 5 cm by 7.5 cm single-sided printed circuit board. The circuit board, the transformer, the battery and the cassette recorder are housed in a 18 cm (W), 10 cm (H) and 30 cm (D) metal case.

The 8748 single-chip microcomputer [84] includes 64 bytes of program memory as depicted in Figure 6.4. The first 8 locations of the array are designated as working registers and are directly addressable by several instructions. The next 16 locations contain the program counter stack for up to 8 nested subroutines, and the data collected reside in the remaining 40 memory locations. All locations are indirectly addressable through either of two pointer registers R0 and R1.

The crystal-controlled oscillator is a high gain resonant circuit whose frequency has been set to 3.579525 MHz. The output of the oscillator is divided by 15 to provide a clock which defines an instruction cycle of 4.1905 microseconds. A TV colorburst crystal is used.

The reset input provides a means for initialization of the processor. A reset pulse is generated if push-button switch (S2) is depressed for at least 25 microseconds.

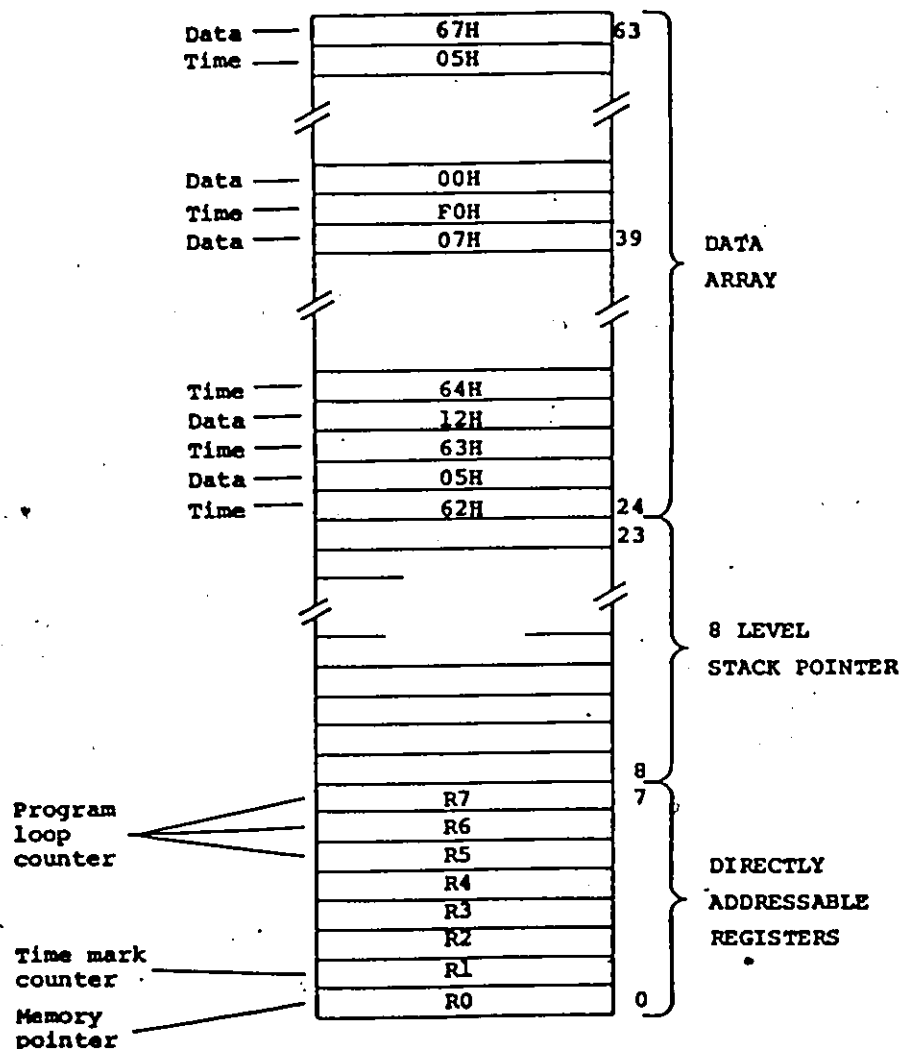


Figure 6.4 Data memory map

The microcomputer includes an 8-bit presettable timer/event counter which is used to count the number of drops detected by the sensor. Clocking of this counter is

via pin T1; high to low transitions on T1 cause the drop counter to increment. The maximum rate at which the counter may be incremented is once per three instruction cycles (approximately 80 kHz); there is no minimum rate. The increment from maximum count (FFH) to zero results in the setting of an overflow flag and the generation of an interrupt request. If the interrupt request is enabled, the counter overflow will cause a subroutine call to the counter service routine.

The microcomputer counts the number of drops during a time period known as rain integration time. At the end of this time the count is stored in the microcomputer RAM together with a time mark. Each data word occupies one byte so that the largest number that can be stored is 255. However, the precipitation sensor is capable of detecting more than ten drops per second, which is more than 600 drops for a rain integration time of one minute. To cope with this number, we would require 10 bits registers, so an alternative was chosen: two 8-bit counters, named DCL (timer/event counter) and DCH (R3) for low and high order respectively, are used to count up to 64K drops and the total number of drops is divided to reduce the range. A division by two is used for light and moderate rainfall (Chapter 2) areas and seasons whereas, a division by four is necessary for sampling heavy rainfalls. The division result will be smaller than 255 and therefore it can be stored in

one memory location. Counter DCH is incremented in the counter service routine when counter DCL overflows.

The instrument resolution (with division by 4) is 0.0184 mm of rain per count. Events over 3 mm per minute (180 mm/hr) are very unlikely in the areas where the systems are operating at present (once in 25 years with a duration of 5 minutes). The resolution obtained after division is satisfactory for the present central site data processing software which was designed to take data from tipping bucket raingauges where the resolution is lower. The microcomputer performs the division using software; it may therefore be modified as required by simple program changes.

Every count stored in memory is accompanied by a time mark (data set), as shown in Figure 6.4. In order to save space in memory and on tape, the acquisition system represents the acquisition time as an incrementally-coded time mark. The time mark represents "the elapsed time since start" and ranges from 1 to 240.

The microcomputer stores data into memory only when rainfall is detected or when the time mark counter equals 240. The integration time is software generated and is therefore easily modified to meet unusual requirements. In the present system it is one minute.

Every time the memory space is full, the microcomputer turns on the cassette recorder power supply and, at the same time, it starts recording 50 synchronization char-

acters. Approximately, 20 of these characters are recorded properly because of the time required by the tape transport mechanism to reach its nominal velocity. After the synchronization block has been recorded, the information block is fetched from memory and transferred to tape. At the end of the recording, the microcomputer turns off the recorder power supply, but some tape is wasted because the tape transport mechanism does not stop instantly. Because of the tape wasted, the tape-use efficiency is just over 50%. The efficiency may be improved if circuitry to achieve faster start and stop of the recorder drive mechanism is incorporated. Figure 6.5 shows a plot of tape speed versus time. By replacing the 8748 microcomputer by its pin compatible 8749, which contains 128 locations of data memory, the tape-use efficiency may be improved to 75% since larger data blocks can be recorded.

At the same time as the modulated signal is recorded on tape, the microcomputer transmits the unmodulated signal through pin P21. In the present design, this signal is not being used but it can easily be coupled to modems, radio transmitters or to a line for the transmission of the collected data.

Every character recorded or transmitted comprises eight bits of information, one start bit, one parity bit and one stop bit. The control bits are used in the data recovery stage.

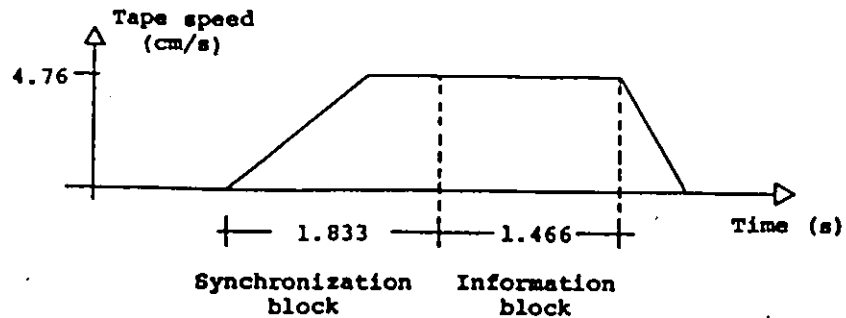


Figure 6.5 Plot of tape speed against time

The unattended time period of the system depends basically on the tape capacity. The DAS stores approximately 17 blocks of information (340 minutes of rain or 1360 hours of no rain) on one minute of tape. The amount of data recorded on tape depends on the duration of rain and not on the amount of rain. When the integration time is programmed to be one minute, the system can be left unattended for more than 7 days of continuous rain or more than 4 years of no rain using C-60 tapes. Details of the data acquisition system are given in table 6.1.

The microcomputer is fully dedicated to data acquisition and storage. However, these tasks use only a small fraction of the available time, so the remaining time may be used to perform some data processing. The microcomputer program and a description of its operation are detailed in appendix B.

Table 6.1 Data acquisition system technical data

Microcomputer.....	Intel 8748.
Storage media:	
Magnetic cassette tape.....	Audio.
Modulation.....	Frequency Shift Keying. (FSK).
Carriers.....	1.8 kHz for logical "0", 2.7 kHz for logical "1".
Baud rate.....	300 bits per second.
Format.....	50 bytes per block, 11 bits per byte.
Data block.....	10 bytes of synchronism, 20 bytes of data, 20 bytes of timing.
Error relation.....	Less than 1 error in 1 E06 bits stored.
Integration time.....	Programmable.
Period of unattended operation..	7 days of rain (tape C-60 one side).
Operating temperature.....	+10 to + 50 degrees C.
Power requirements:	
Steady state.....	75 mA @ 5 V.D.C.
Peak.....	225 mA @ 5 V.D.C. For 3.5 seconds when data is transferred to tape.

Battery back-up.....17 hrs. Six "C" size
rechargeable.

Dimensions:

Height.....10 cm

width.....18 cm

Depth.....30 cm

6.2 DATA ACQUISITION SYSTEM VERSIONS

Various versions of the data acquisition system were designed to satisfy different data collection needs. A description of the characteristics of these versions and of the differences between them and the original system follows.

One of the desirable objectives in the design of the different versions was to maintain the original design, thereby leading to ease the construction, operation and maintenance of the systems.

6.2.1 LOW-POWER VERSION

A version of the DAS (DAS-LP) that consumes small amounts of power and may be operated by battery, was developed to be able to collect rainfall data at locations where a primary power source is not available.

In order to reduce the power consumption, CMOS integrated circuits were used (the DAS-LP was designed before the CMOS version of the microcomputer became available). CMOS integrated circuits are well known for their low power

supply requirements, high noise immunity, and operation under large variations of power supply voltage.

The difference between the DAS-LP and the original version is basically that the CMOS microcomputer, although pin by pin compatible, does not include program memory. Therefore program memory is contained in a CMOS Erasable-Programmable Read-Only Memory (EPROM). Figure 6.6 shows the circuit diagram of the interconnection between the microcomputer and the memory. The latch is used to time demultiplex the address/data bus of the microcomputer.

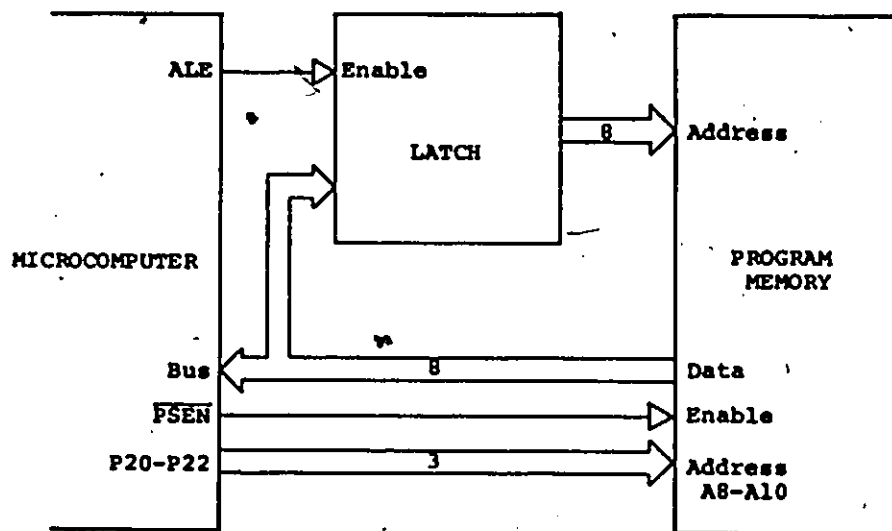


Figure 6.6 DAS-LP circuit modification diagram

The address/data bus transmits the 8 least significant bits of the program counter and receives the addressed instruction during a program memory fetch. All memory fetches generate the control signal Address latch enable.

(ALE) and Program Store Enable ($\overline{\text{PSEN}}$). Figure 6.7 shows the time diagram of the control signals. ALE indicates the time at which the address in the bus is valid. The trailing edge of this signal is used to latch the address. $\overline{\text{PSEN}}$ is used to enable the program memory and the microcomputer receives the instruction on its trailing edge.

Lines P20 to P23 contain the 4 high order bits of the program counter. In the present design only lines P20 to P22 are used due to the size of the program memory (2K by 8 bits).

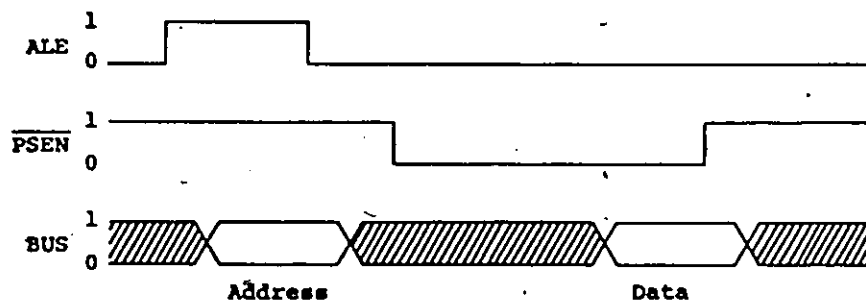


Figure 6.7 DAS-LP control signals timing diagram

The modulated signal to be recorded on tape, the serial signal intended for data transmission and the control signal that controls the recorder power supply are available through output lines P10 to P12 respectively. This change was necessary because lines P20 to P22 are now being used to address the external memory.

The power supply includes a rechargeable battery and a low-dropout voltage regulator. The power consumption of

the system while collecting data is less than 7 mA and approximately 200 mA when data is being recorded on tape. The unattended time period depends on the capacity of the battery as well as on the amount of rain collected.

The remaining portions of the circuit are identical to those of the original system. The electronic components are assembled on a 7.5 cm by 12 cm double-sided printed circuit board. The circuit board, the battery and the cassette recorder are contained in a 18 cm (W) by 10 cm (H) by 30 cm (D) metal case.

The software used by the microcomputer in the DAS-LP version is basically the same, except for minor modifications required to accommodate the output port change.

6.2.2 PRECIPITATION COLLECTOR VERSION

Originally, the data acquisition system included only one acquisition channel intended to collect data from the drop counter precipitation sensor. In support of the Acidic Precipitation in Ontario Study (APIOS) and upon request from the Ontario Ministry of the Environment (MOE) a new version of the DAS was developed. This (DAS-MOE) includes an additional acquisition channel for an automatic sensing wet/Dry Precipitation Collector (W/DPC). The DAS-MOE was used in a quality assurance audit program of the precipitation collector.

Basically the W/DPC consists of a rainfall sensor,

two containers, an automated container lid, and electronic circuitry [85]. The purpose of the precipitation collector is to collect rainfall (wetfall) in the wet sample container and dust-fall (dryfall) in the dry sample container. The samples collected are analysed to determine the amounts of atmospheric deposition of persistent organic chemicals [86].

The precipitation collection procedure is performed in the following fashion: On the "Dry collection status", the container lid covers the wet container, so dust-fall is collected in the dry container. When rainfall is detected by the sensor, the lid automatically moves to cover the dry container and thus rainfall is collected in the wet container, that is "Wet collection status". The W/DPC rainfall sensor is provided with a heater so that the accumulated rain on the sensor is evaporated, and approximately three minutes after rain stops, the sensor is dry and the lid moves back to cover the wet container.

The instrumentation was required to perform the following tasks [87]:

1. To record the performance of the APIOS's precipitation sampler, i.e., whether it opens or closes properly in response to precipitation. The actual time of opening or closing should be accurate to the nearest minute, NRC atomic clock time.

2. To record rainfall intensity accurately to one minute, NRC atomic clock time.

3. To be serviced and checked at least twice a month.

Originally, the precipitation collector provided an electrical signal indicating the collection status. This signal supplies approximately 18 V.D.C. when the lid covers the dry container (wet collection status). However, the true wet collection status should also include information on the lid movement between the dry and wet containers. The lid takes approximately eight seconds to move from the top of one container to the top of the other. Therefore, to include the lid movement, the signal supply point was changed.

With the supply point rewired, the signal is approximately 18 V.D.C. when the lid covers the wet container and less than 1 V.D.C when the lid is in any other position. Therefore, an electronic circuit was required to discriminate between the two voltage levels. The alternative use was a voltage comparator with the configuration shown in Figure 6.8. Here S0 is the output signal from the precipitation collector and S1 is the conditioned signal that is transmitted to the microcomputer.

R1 and R2 constitute a voltage divider with $R1 = 2.7$ R2, so that the incoming signal is divided by a factor of 3.7. R3 and R4 constitute another voltage divider for the threshold voltage in which the input signal is compared.

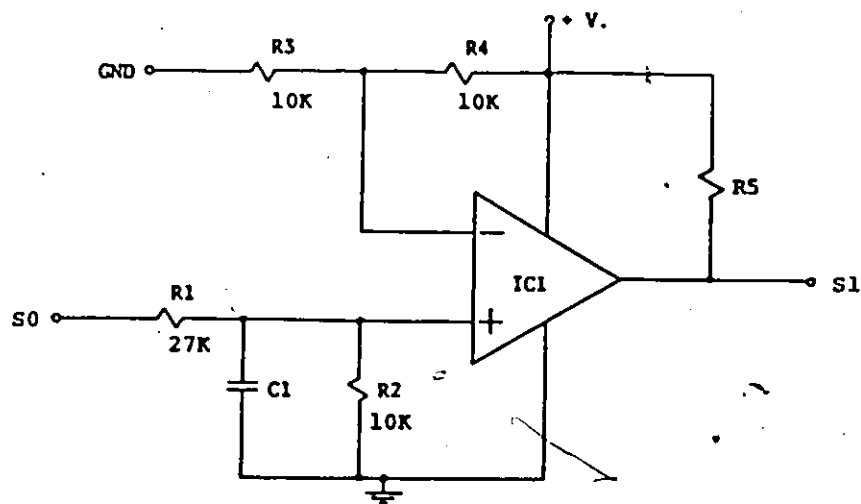


Figure 6.8. DAS-MOE circuit modification diagram

The signal S1 is high (logical "1") to indicate the dry collection status and low (logical "0") for the wet collection status. The time diagram of these signals is shown in Figure 6.9. Signal S1 is transferred to the microcomputer through an output pin testable using conditional transfer instructions.

The main circuit board used for the DAS-MOE is otherwise the same as that used in the original version. The electronic components of the interface board are assembled on a 2 cm by 6 cm single-sided printed circuit board. The signals common to both boards are S1, Ground and +Vcc. The printed circuit boards, the cassette recorder, the transformer and the backup battery are contained in a metal case with the same dimensions as the DAS case.

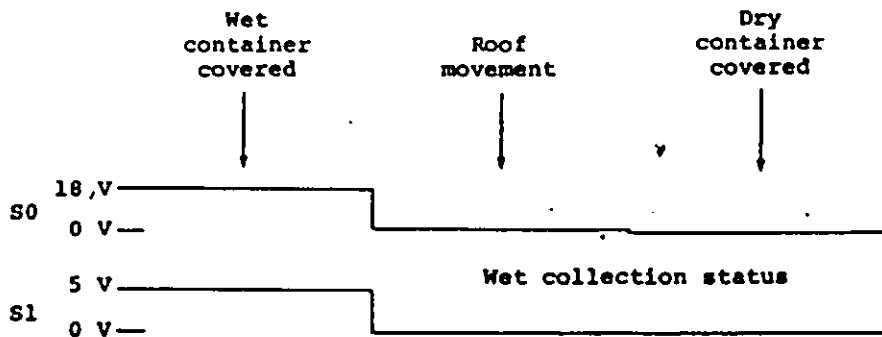


Figure 6.9 DAS-MOE data signals timing diagram

The microcomputer program was modified to satisfy the new data collection needs. The data collection procedure is as follows: every minute on the minute, the microcomputer tests the precipitation collector status and reads the drop and time mark counters; the microcomputer stores data in memory, and therefore on tape, when the time mark equals 240, and/or rainfall has been detected, and/or the precipitation collector is in the wet collection status.

Because the precipitation collector has only two states (wet and dry collection status), only one bit of information is required. But in order to increase the resolution of the rainfall data by removing the division of the drops counted, an extra byte of information was used. Each data set for this version comprises three bytes: one for the time mark, one for the 8 least significant bits of the drop counter and the third for the collection status and the high order bits of the drop counter. The collection status

is represented by the most significant bit and the 2 most significant bits of the drop counter correspond to the 2 least significant bits of the third byte.

The unattended time period of the system can be extended if the remaining 5 bits of the third byte are used to extend the time mark capacity. Since the systems were serviced at least twice a month, this extension was not necessary.

The information is stored in memory and on tape by blocks, each block comprising 40 bytes. Therefore in each block there are 13 data sets plus one byte. This byte is placed at the end of the block and is always zero. Because the time mark is never zero, three consecutive null bytes should never appear as valid information. All these characteristics are tested when the data is retrieved from tape.

The remainder of the software used in this version is equivalent to the software of the original version.

6.2.3 TIPPING BUCKET RAINGAUGE VERSION

A version of the acquisition system was developed to collect information from tipping bucket raingauges (DAS-TBRG). Usually, tipping bucket raingauge data is recorded on strip charts. The chart recorders have many disadvantages: they are expensive to purchase and to maintain; under field conditions, problems may be experienced with the delicate parts of the instruments; also, as

with all autographic records, data reduction is demanding of human resources, and gives rise to errors when the recorder strip charts are translated manually into time series to be analysed.

The only difference between this version and the original system is that the division of the number of drops has been removed.

Various DAS-TBRGs were constructed and are operating satisfactorily in the Hamilton area, as part of the hydrometeorological field program of the Computational Hydraulics Group at McMaster University. Some of these instruments are operating at the same sampling sites as the DCPS in order to compare the performance of the two devices. Results of these comparisons are discussed in the following chapters.

CHAPTER 7

DATA DECODER

Depending on the length of monitoring time the amount of data stored on tape can be large; over 40,000 8 bit words on a single tape. This data requires further processing before being input to mainframe computers, where program packages for simulating the various phases of the hydrological cycle are available.

This chapter describes a microcomputer-based data decoder (DD) that was designed to retrieve automatically the information stored on tape, verify its validity, and transmit it to the central computer where the data processing is performed. The automation of this process has led to considerable improvements over manual methods previously used, including the prevention of random errors and the reduction of time needed to transfer the information to the computer.

7.1 CIRCUIT DESCRIPTION

The played-back signal is a distorted sinusoidal signal modulated in frequency and amplitude that includes low frequency noise due to power line interference, white noise inherent in all electronic components, unwanted high

frequencies generated in the modulation process, and finally, undesired carrier modulation (modulation noise) due to the nonuniform speed of the tape transport (wow and flutter). This signal is recovered after it has passed through the recorder pre-amplifier and before the amplifier. In this way, the volume level of the recorder has no effect on the amplitude of the signal reproduced.

Before performing the signal demodulation, noise and unwanted frequency components are removed using a second order band-pass filter. A block diagram of the data decoder is shown in Figure 7.1. Because the amplitude of the played-back signal is rather small (about 0.2 Volts) it is desirable that the filter, in addition to attenuating the unwanted frequency bands, should amplify both carriers.

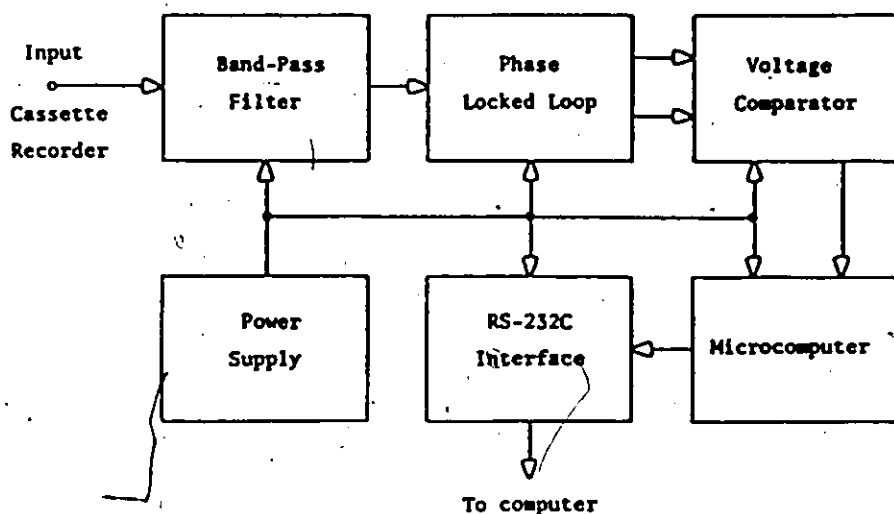


Figure 7.1 DD block diagram

The band-pass filter has been implemented using a high-pass filter followed by a low-pass filter instead of a single band-pass. This approach has been used because it is easier to tune the two separated filters in order to obtain a frequency response in accordance with that of the cassette recorder. The type of filters used are Sallen and Key active RC filters [88], which are classified as Voltage Controlled Voltage Source (VCVS) filters.

The general structure of each one of the two filters used is shown in Figure 7.2. The type of filter (low-pass or high-pass) is determined by the type of components used to implement the network. The transfer function of the network is given by

$$\frac{V_2}{V_1} = \frac{\mu Y_2 Y_1}{(Y_2 + Y_4)(Y_1 + Y_2 + Y_3) - \mu Y_2 Y_3 - Y_2^2} \quad (7.1)$$

The filter implemented in the decoder input is a high-pass filter. The general form of a second-order high-pass filter transfer function is given by [89]

$$\frac{V_2(s)}{V_1(s)} = \frac{\mu s^2}{s^2 + 2\zeta W_n s + W_n^2} \quad (7.2)$$

where

W_n = Natural frequency

ζ = Damping factor

μ = Voltage gain

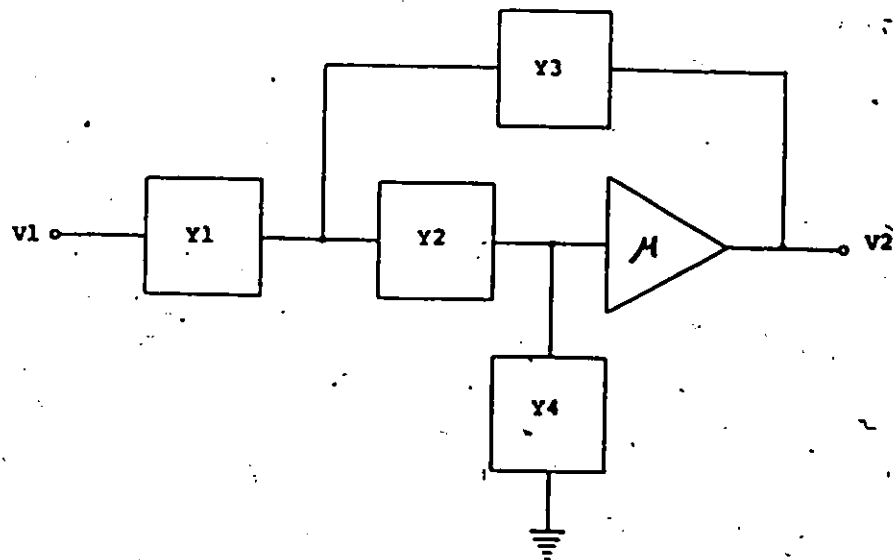


Figure 7.2 Filter block diagram

Matching equations 7.1 and 7.2, the components were selected as follows:

Capacitor (C1s)	for admittance Y1
Capacitor (C2s)	for admittance Y2
Resistor (R1)	for admittance Y3
Resistor (R2)	for admittance Y4

Substituting these components into equation 7.1 and simplifying gives

$$\frac{V_2(s)}{V_1(s)} = \frac{\mu s^2}{s^2 + s \left[\frac{1}{R_1 C_1} (1-\mu) + \frac{1}{R_2} \left(\frac{1}{C_1} + \frac{1}{C_2} \right) \right] + \frac{1}{R_1 R_2 C_1 C_2}} \quad (7.3)$$

A version of this filter that offers very low sensitivity to component-value drifts and is easily tuned is

known as "Equal-component-value Sallen and Key". The component values can therefore be selected:

$$R_1 = R_2 = R \qquad C_1 = C_2 = C$$

Substituting in equation 7.3 results in

$$\frac{V_2(s)}{V_1(s)} = \frac{\mu s^2}{s^2 + s \left[\frac{1}{RC} (3 - \mu) \right] + \frac{1}{R^2 C^2}} \quad (7.4)$$

and the designing equations are

$$\omega_n = \frac{1}{RC}$$

$$\zeta = \frac{3 - \mu}{2}$$

The filter voltage gain is determined by resistors R_3 and R_4 connected as shown in Figure 7.3, where

$$\mu = 1 + \frac{R_3}{R_4}$$

In other words, the natural frequency of the filter can be determined independently, but the filter gain depends on the damping factor selected, or viceversa.

In order to reduce the amplifier offset voltage the resistance to ground of both inputs must be equal so that

$$R = \frac{R_3 R_4}{R_3 + R_4}$$

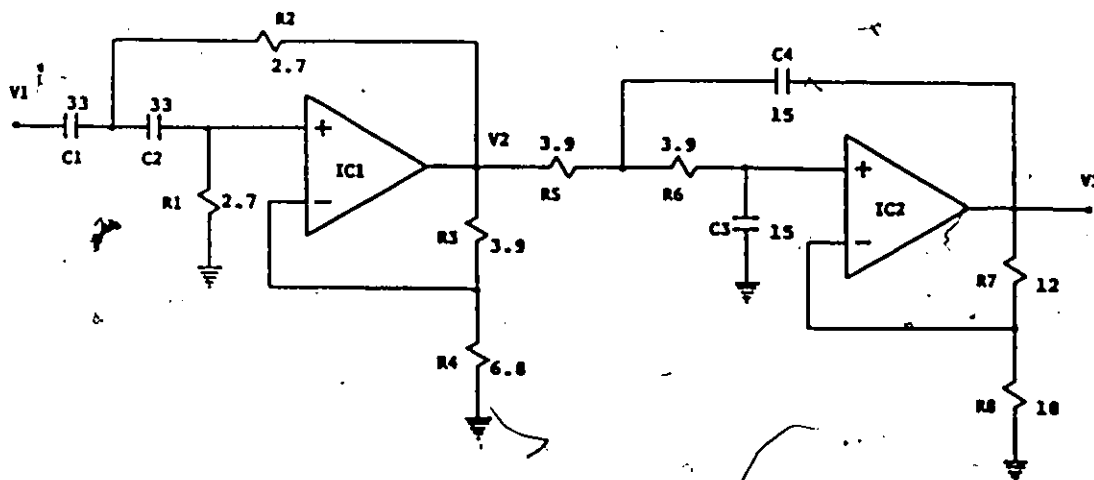


Figure 7.3 Filter circuit diagram.

Capacitors are in nanofarads and resistors in kilohms

The values shown for the high-pass filter in Figure 7.3 correspond to a natural frequency of 1.8 kHz, a damping factor of 0.71, and a resultant filter gain of 1.55.

The low-pass filter was designed in a similar way. The general form of a second-order low-pass filter transfer function is

$$\frac{V_2(s)}{V_1(s)} = \frac{\mu W n^2}{s^2 + 2\zeta W n s + W n^2} \quad (7.5)$$

Matching equations 7.1 and 7.5 and considering equal-component values as follows:

Resistors (R) for admittances Y1 and Y2

Capacitors (C) for admittances Y3 and Y4

the network transfer function is given by

$$\frac{V_2(s)}{V_1(s)} = \frac{\frac{\mu}{R^2 C^2}}{s^2 + s \left[\frac{1}{RC} (3 - \mu) \right] + \frac{1}{R^2 C^2}} \quad (7.6)$$

and the designing equations are

$$\omega_n = \frac{1}{RC}$$

$$\mu = 1 + \frac{R_7}{R_8}$$

$$\zeta = 1 + \frac{R_7}{2R_8}$$

The corresponding value of resistor R, in order to reduce the amplifier offset voltage is given by

$$2R = \frac{R_7 R_8}{R_7 + R_8}$$

The component values shown in Figure 7.3 correspond to a natural frequency of 2.7 kHz, a damping factor of 0.67, and a resultant filter gain of 1.66.

A Phase-Locked Loop (PLL) is used to demodulate the signal and, together with a voltage comparator, convert it into voltage levels compatible with the microcomputer input specifications. A PLL consists of a double balanced phase detector (PD), a loop filter, and a linear

voltage-controlled oscillator (VCO) [90] as illustrated in Figure 7.4.

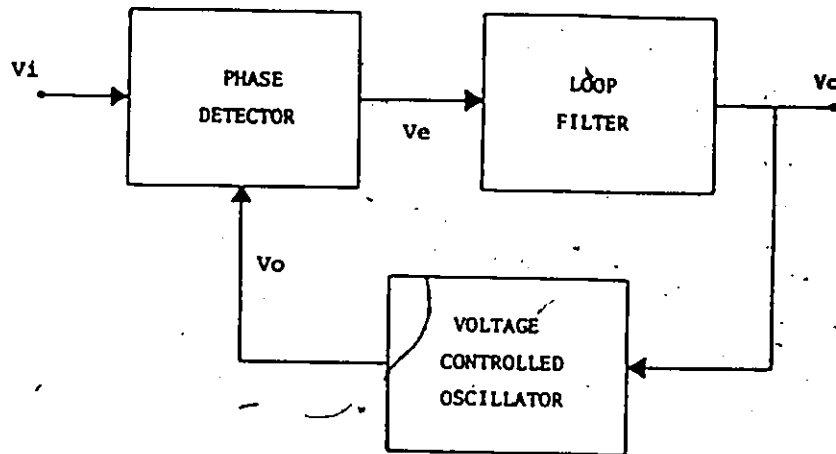


Figure 7.4 PLL block diagram

Assuming that the loop is locked, the control voltage (V_c) is such that the VCO output signal (V_o) is a sinusoidal of the same frequency but different phase of the input signal (V_i), where

$$V_i(t) = \sqrt{2} \cos(\omega t + \theta_i)$$

$$V_o(t) = \sqrt{2} \cos(\omega t + \theta_o)$$

and the output of the phase detector is given by

$$V_e(t) = V_i(t) \cdot V_o(t) = 2K_d \sin(\omega t + \theta_i) \cos(\omega t + \theta_o)$$

$$V_e(t) = K_d \sin(\theta_i - \theta_o) + K_d \sin(2\omega t + \theta_i + \theta_o)$$

where

K_d = Phase detector gain factor (Volts per radians)

To maintain the control voltage needed for lock, it is generally necessary to have a nonzero output from the phase detector. Consequently, the loop operates with some phase error present. As a practical matter, however, this error tends to be small in a well designed loop.

Error voltage (V_e) is filtered by the low-pass loop filter. Noise and high frequency signals, such as the second harmonic of the carrier, are suppressed. The filter transfer function is given by $F(s)$. The resulting output of the filter is

$$V_c(t) = K_d \sin (\theta_i + \theta_o)$$

The control signal is a D.C. voltage which is a function of the phase difference between V_o and V_i . Assuming $(\theta_i - \theta_o) \ll \pi/2$ (this is close to the condition of lock and gives the usual linearized version of the phase-locked loop) then

$$V_c(t) = K_d (\theta_i + \theta_o)$$

This approximation is most accurate near $(\theta_i - \theta_o) = 0$. The deviation of the VCO from its center frequency is given by

$$\Delta\omega \approx K_o \cdot V_c(t)$$

where

K_o = VCO gain factor (radians per second-volt).

Since frequency is the derivative of phase, the output of the VCO is related to its input by

$$\frac{d\theta_o}{dt} = K_o \cdot V_c(t)$$

taking the Laplace transform gives

$$\theta_o(s) = \frac{K_o \cdot V_c(s)}{s}$$

In other words, the phase of the VCO output is linearly related to the integral of the control voltage. Combination of these equations results in the basic loop equations

$$\frac{\theta_o(s)}{\theta_i(s)} = H(s) = \frac{K_o \cdot K_d \cdot F(s)}{s + K_o \cdot K_d \cdot F(s)} \quad (7.7)$$

$$V_c(s) = \frac{s\theta_i(s)}{K_o} H(s) \quad (7.8)$$

where

$H(S)$ = Closed-loop transfer function.

Since, in the present application, an FM system employing square wave modulation is being used, the natural frequency of the loop must be chosen so that peak phase er-

rors do not exceed 90 degrees under all conditions.

For wide bandwidth applications where wideband data modulation must be followed, the loop filter can be implemented by just one capacitor [91]. The transfer function of the filter is simply

$$\frac{V_c(s)}{V_e(s)} = \frac{1}{1 + RCs}$$

Substituting into equation 7.7 results in

$$H(s) = \frac{\frac{K_o \cdot K_d}{RC}}{s^2 + \frac{s}{RC} + \frac{K_o \cdot K_d}{RC}}$$

where the natural frequency and damping factor are given by

$$\omega_n = \left[\frac{K_o K_d}{RC} \right]^{1/2} \quad (7.9)$$

$$\zeta = \frac{1}{2} \left[\frac{1}{K_o \cdot K_d \cdot RC} \right]^{1/2} \quad (7.10)$$

A monolithic phase-locked loop (LM565) is used in the implementation of the circuit, where the VCO free running frequency is given by

$$f_o = \frac{1}{3.7(R_{14} + R_{15})C_8}$$

The loop gain depends on the total supply voltage and is obtained by

$$K_o \cdot K_d = \frac{33.6 \cdot f_o}{V_c}$$

The range of frequencies that the loop remains in lock after initially being locked is given by

$$f_h = \pm \frac{8f_o}{V_c}$$

The circuit diagram of the PLL and voltage comparator is shown in Figure 7.5. Component values correspond to a free running frequency of 2250 Hz, a filter natural frequency of 150 Hz, and a damping factor of 1.36. These values were obtained with a power supply (V_c) of 30 Volts and R (the PLL internal resistor) equal to 3.6 kohms. Resistors R_{12} and R_{13} and capacitors C_6 and C_7 provide further filtering and therefore smoother operation of the circuit.

The output of the comparator is a distorted digital signal that contains the data recorded on tape. The distortion in the signal is due mainly to tape speed variations (wow and flutter) in the recording and play-back processes.

Two tests were performed to measure the amount of frequency shift in the played-back signal due to tape speed variations. The test procedure was as follows: A 2 kHz square wave signal was recorded onto the tape for 10 mi-

notes. A new cassette recorder and tape were used. To measure the frequency shift, the tape was played back twice. The reproduced frequency was measured over 1 second intervals but even with this long sampling interval, the readings were accurate only to the nearest Hz. A record of the measurements was obtained.

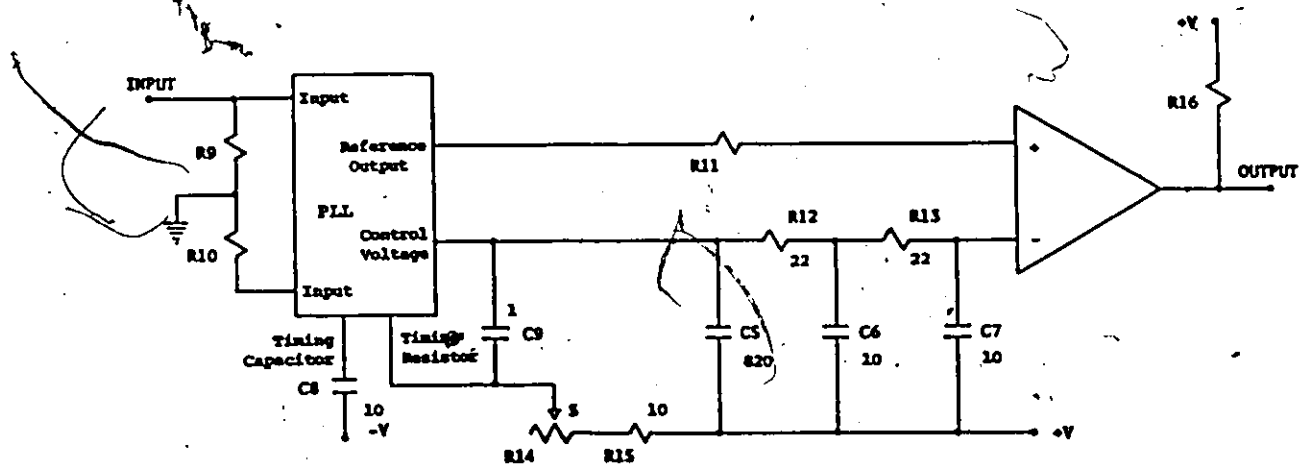


Figure 7.5 PLL and voltage comparator circuit diagram. Capacitors are in nanofarads and resistors in kilohms

The collected data were analysed and the following was found: the average reproduced frequency was 2008.3 Hz (+0.42 %) with a standard deviation of 11.8 Hz. Frequencies as high as 2040 Hz (+2 %) and as low as 1970 Hz (-1.5 %) were observed but combined, they occurred in less than 2% of the measurements. No frequencies higher than 2040 Hz or lower than 1970 Hz occurred. The frequency shifts are due to the

combined tape speed variations during recording and play back. With the equipment used one cannot determine the effects due to each of them separately.

The digital signal at the output of the comparator is fed into the microcomputer through pin T0. The logical value of this pin can be tested using conditional jump instructions. This pin allows inputs to cause program branches without the need to load an input port into the accumulator [84]. Figure 7.6 shows the circuit diagram of the microcomputer and line driver. A 6 MHz crystal is used to obtain an instruction cycle of 2.5 microseconds.

Every block of information recorded on tape is comprised of at least ten synchronization characters and forty data characters. The numeric value of a synchronization character is zero. One character is comprised of 11 bits: one START bit (Logical "0" or space), eight bits of information, one parity bit (even parity), and one STOP bit (logical "1" or mark), in that order. Figure 7.7 shows a time diagram of the information recorded onto tape and the word structure used.

The microcomputer needs to receive at least 5 synchronization characters before the data block is read. After receiving the synchronization block, the microcomputer considers the first character different from zero as data (The first data character is always different from zero, and two characters of zero value never appear together as valid

information).

The algorithm used to sample the serial data was designed to minimize the effects of signal distortion. The distortion manifests itself as small amounts of pulse-to-pulse jitter and frequency shifts produced by the variations in tape speed.

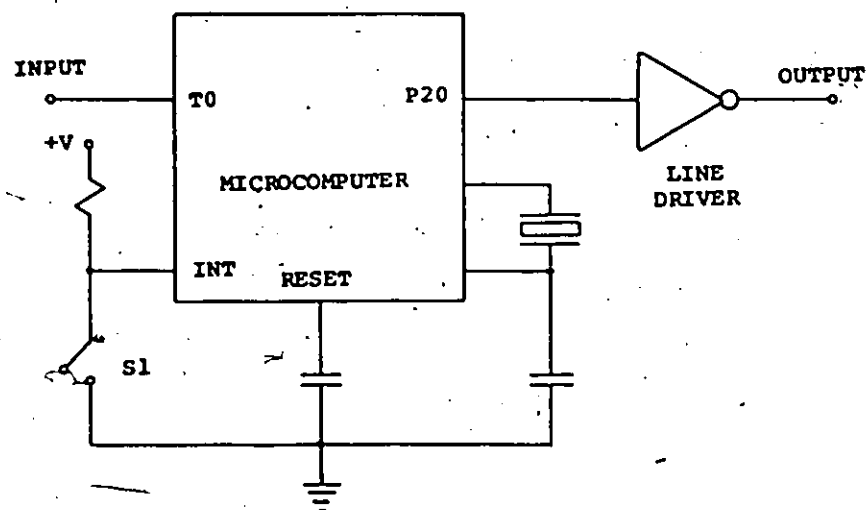


Figure 7.6 Microcomputer and line driver circuit diagram

To read one character from tape, the program detects the leading edge of the start bit by means of a 5 microsecond test loop. This time is used as a reference point to sample the subsequent bits as close to the centre of occurrence as possible. After the start bit has been detected, a delay of one half bit the bit time (1665 microseconds) is produced to test its validity. Subsequent time delays of one bit time (3332.5 microseconds) are performed to sample the remaining 10 bits of the character.

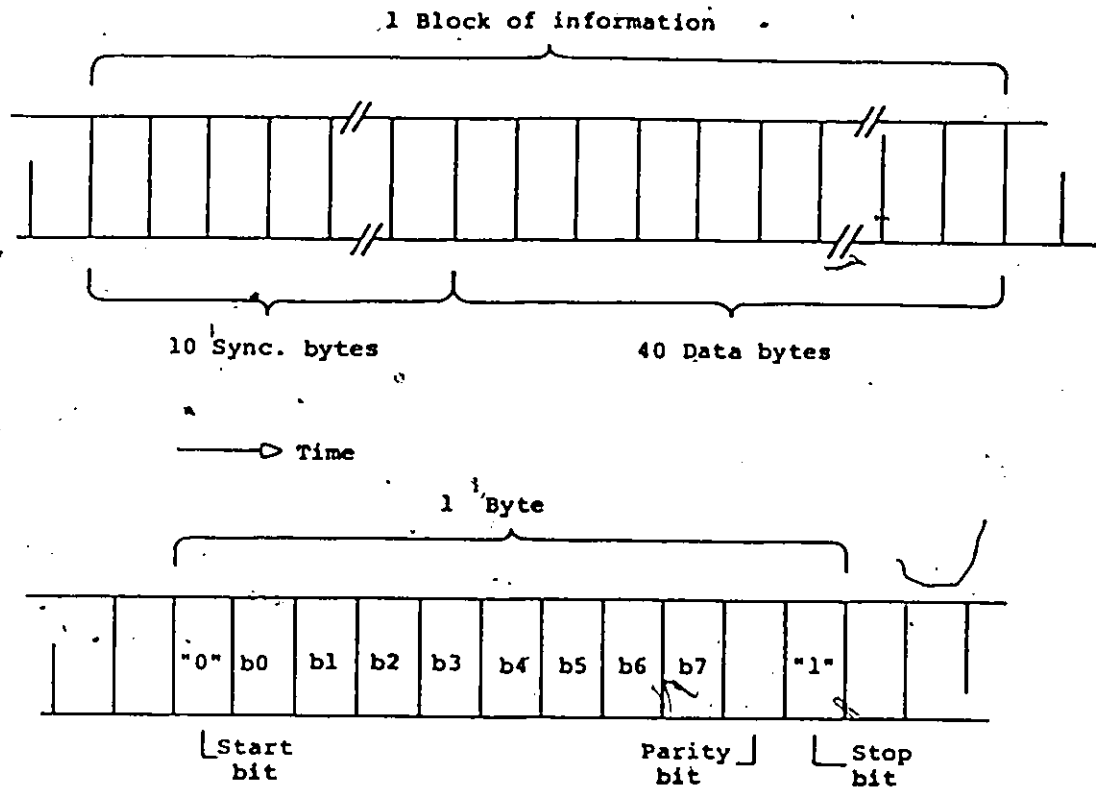


Figure 7.7 Tape information and word structure timing diagram

This algorithm is appropriate if frequency variations of the played-back signal are small. A cumulative error of one half of the bit time will result in erroneous reception [92]. The maximum timing error which can be tolerated and still allow proper detection of an 11 bit character is

$$t_{\max} = \frac{0.5 \cdot \text{bit time}}{11} = 0.15 \text{ ms}$$

Comparing this result with the results obtained from the tests on tape speed variations, it is seen that this al-

gorithm can be used with confidence but should be modified if tape speed variations increase due to recorder use.

After the character has been read, the software checks the validity of the information using the parity bit. The algorithm used for parity calculation is presented, together with the program description, in Appendix C. If an error is detected, the program informs the user and continues with the next block of information. If no error is detected, the data is stored temporarily in memory.

After the last characters have been received and stored, the block of information is converted into ASCII code and transmitted to the central computer. The transmission is through pin P20 and the line driver. The signal is transmitted asynchronously at 1200 bits per second and the output is RS-232C compatible.

The time required to transmit one block of information is shorter than the time between blocks of information retrieved from tape. The transmission is therefore complete and the program is ready before the next block is played back.

The microcomputer indicates to the central computer the end of the file by sending the control character "CNTRL-Z". An interrupt request and the subsequent transmission of the control character is produced by depressing push-button S1.

The algorithm for Serial transmission is simpler

than the algorithm for serial reception since no synchronization is required. All that is required is to generate time delays at the desired bit rate and output the data to be transmitted at an output pin. Appendix C lists the Data Decoder program and gives a description of its operation.

Various tests were carried out to determine the performance of the complete system: that is, data recorded on tape by the data acquisition system was recovered by the data decoder and verified to determine the error rate. The test procedure was as follows: simulated blocks of information (40 bytes per block) were recorded on tape by a DAS. Each block of information consisted of the numbers 1 to 20 for the time marks and 33 to 52 for the number of drops. 5 cassette tapes were recorded with the same information, each tape contained about 50,000 bits of information (including 5 synchronization characters).

A microcomputer program was developed to retrieve the data from tape and compare it against the data recorded. The program indicates when an error is detected and the time mark associated with it. If an error was detected the block of information was played back up to 9 times to attempt to retrieve the information correctly.

The five tapes were played back 4 times each, corresponding to about 1 million bits. A total of 20 errors were observed. In 11 cases the block of information was recovered properly after several times of playing it back. In

the remaining 9 cases the block could not be retrieved without error. Eight of these errors always appeared in the same two tapes every time the tapes were played back; they were attributed to flaws in the tapes. The remaining error appeared only once, even though the tape was played back 4 times. This error is included in the system error rate specifications.



CHAPTER 8

DATA PROCESSING

The final component in the rainfall monitoring network is the synthesis of all data collected through analysis and interpretation. This results in a product for the user in a format that is compatible with his application. The final result obtained may be data for models to predict runoff or to determine other water-related problems.

The uses for which precipitation data is intended determine the type of data processing to be performed. The rainfall time series may be processed to produce intensity-duration-frequency curves, tables or maps of rainfall. The data processing should be able to integrate the time series into data bases to be used by computer program packages, such as those described in Chapter 2.

8.1 DATA COLLECTED

After the block of information has been converted into ASCII format by the microcomputer in the data decoder, each of the 20 data sets comprises 2 numbers of 3 decimal digits each. The first number of each data set represents the acquisition time and the second the amount of rain sensed during the acquisition time indicated. The range of

FB

the acquisition time mark is from 1 to 240 while for the amount of rain is from 0 to 255.

A block of information has the following characteristics: the first number is never zero and valid collected data can never contain two consecutive zeroes or two consecutive numbers greater than 240.

A block of information contains a trailing string of zeroes as a result of dumping an incomplete block from memory onto tape in the DAS. This string is always contained in the last block recorded and indicates the end of the file.

The data decoder transmits a string of 255's to indicate the occurrence of an error during data recovery. The data decoder has the capability to detect two different types of errors: (a) when the parity bit recorded on tape does not match with the parity bit calculated, and (b) when the stop bit is not detected at the end of a character.

To convert the series of numbers into meaningful information, it is necessary to know the date and time at which the tape was installed in the field. This data is written on the cassette tape case at the time the system is initialized. Figure 8.1 shows one complete block of simulated information (20 data sets) and its interpretation. It can be observed that high rainfall intensity was detected at the start and end of this block. The intensity increases, then tails off and ceases for 10 hours, 11 minutes before another onset.

Figure 8.1 One complete block of information and its interpretation. The first number represents the acquisition time and the second the amount of rain.

Starting time: October 5, 18:30 hrs.

One drop is equivalent to 0.0046 mm of rain

098005099018100042101046102040

103021104007105007240000240000

236017237063238098239140240153

001165021490314100004128005103

FIRST NUMBER	SECOND NUMBER	TIME	DAY	DROPS	mm OF RAIN
098	005	20:08	5	10	0.0460
099	018	20:09	5	36	0.1656
100	042	20:10	5	84	0.3864
101	046	20:11	5	92	0.4232
102	040	20:12	5	80	0.3680
103	021	20:13	5	42	0.1932
104	007	20:14	5	14	0.0644
105	007	20:15	5	14	0.0644
240	000	22:30	5	00	0.0000
240	000	2:30	6	00	0.0000
236	017	6:26	6	34	0.1564

237	063	6:27	6	126	0.5796
238	098	6:28	6	196	0.9016
239	140	6:29	6	280	1.2880
240	153	6:30	6	306	1.4076
001	165	6:31	6	330	1.5180
002	149	6:32	6	298	1.3708
003	141	6:33	6	282	1.2972
004	128	6:34	6	256	1.1776
005	103	6:35	6	206	0.9476

8.2 DATA PRESENTATION

Many hydrological problems require an analysis of time as well as areal distribution of storm precipitation. Maximum amounts of precipitation of various durations over areas of different sizes are usually determined by depth-area-duration analysis of storms.

The average depth of precipitation over a specific area is usually required in many types of hydrological problems. The simplest method of obtaining this is to average arithmetically the collected amounts of rain in the area. This method yields good estimates in flat catchment areas if the raingauges are uniformly distributed and the individual gauge records do not vary widely from the mean. An accurate method of averaging precipitation is the isohyetal method, in which contours of equal precipitation are plotted on a

map.

The data files created with the information collected are used in conjunction with a computer program known as FASTPLOT [93]. This program is used to receive, interpret, store, process, and present the information. Two types of processing are carried out using FASTPLOT: the first is the derivation of a hyetograph for each of the storms and for each monitoring site; the second is done in conjunction with computer programs for stormwater management modelling. These models are used in turn to determine average, daily, monthly, and annual amounts of stormwater runoff entering the receiving water. The models are also being used to investigate a wide range of design alternatives and strategies for minimizing pollutant overflows due to stormwater from the city of Hamilton. In the field program, rainfall intensity, stormwater quality and quantity samples are collected from various field stations located through the city. Figure 8.2 shows a sample run of FASTPLOT.

Individual raingauge data may be processed to produce hyetographs (plots of rainfall intensity in mm/hour against time in hours). Hyetographs are plotted at various integration time intervals, usually 1 minute for the DCPS and 5 to 10 minutes for tipping bucket raingauges.

Long integration time intervals can be very misleading regarding instantaneous rainfall intensity, because a given integration time value can cover widely varying

```

@DLO:[1,10]FASTPLOT4
>;
>; *****
>; FASTPLOT4
>; *****
>;
>;
>* WHICH DISK DRIVE IS BEING USED? (0 R:0-4 D:1): 1
>PIP DL1:FOR001.DAT;*,FOR002.DAT;*,FOR003.DAT;*,FOR004.DAT;*/DE
PIP -- NO SUCH FILE(S)
DL1:[57,1]FOR001.DAT;*
PIP -- NO SUCH FILE(S)
DL1:[57,1]FOR002.DAT;*
PIP -- NO SUCH FILE(S)
DL1:[57,1]FOR003.DAT;*
PIP -- NO SUCH FILE(S)
DL1:[57,1]FOR004.DAT;*
>PIP DL1:FOR007.DAT;*,FOR008.DAT;*/DE
PIP -- NO SUCH FILE(S)
DL1:[57,1]FOR007.DAT;*
PIP -- NO SUCH FILE(S)
DL1:[57,1]FOR008.DAT;*
>* ONLY PLOTTING TO BE DONE? [Y/N]:N
>* WHICH DATA FILE IS TO BE TRANSLATED? (S): CIRDRP2
>;
>;
>PIP DL1:FOR002.DAT-DL1:CIRDRP2.DAT
>RUN DLO:[1,10]INTERP4

ENTER TYPE OF DATA TO BE PROCESSED (RAIN, DISCHARGE OR POLLUTANTS)
RAIN

ENTER GAUGE IDENTIFICATION
CIRCLE D

ENTER GAUGE UNIT NUMBER
001

ENTER UNITS TO BE USED (METRIC/IMPERIAL)
METRIC

ENTER DATA SOURCE ("CHARTROLL" OR "CASSETTE")
CASSETTE

WAS A RAINFALL SAMPLER ASSOCIATED WITH THE RECORDER (Y/N)
N

ENTER STARTING TIME (YEAR MO DY HR MIN)
1983 07 26 14 10

ENTER OBSERVED TOTALIZER VOLUME (mm,in)
28.7

ENTER TYPE OF GAUGE (DROP COUNTER/TIPPING BUCKET)
DROP COUNTER

ENTER TYPE OF DROP COUNTER "BLACK" OR "WHITE"
WHITE

ENTER INTER-EVENT PERIOD (MINUTES)
60

ENTER TIME-STEP FOR PLOTTING HYETOGRAPH (MINUTES)
1

```

Figure 8.2 Sample run of FASTPLOT

PROCESSED RAINFALL DATA FOR 1983 FOR CIRCLE D UNIT NO. 1

MONTH	DAY	HOUR:MINUTE	RAINFALL		EVENT	
			VOLUME (mm)	INTENSITY (mm/hr)	VOLUME (mm)	(min)
7	26	18:10	0.0000	0.0000		
7	26	22:10	0.0000	0.0000		
7	27	2:10	0.0000	0.0000		
7	27	6:10	0.0000	0.0000		
7	27	10:10	0.0000	0.0000		
7	27	14:10	0.0000	0.0000		
7	27	18:10	0.0000	0.0000		
7	27	22:10	0.0000	0.0000		
7	28	2:10	0.0000	0.0000		
7	28	6:10	0.0000	0.0000		
7	28	10:10	0.0000	0.0000		
7	28	14:10	0.0000	0.0000		
7	28	15:50	0.0062	0.3720		
7	28	15:51	0.0062	0.3720		
7	28	15:52	0.0062	0.3720		
7	28	15:53	0.0062	0.3720		
7	28	15:57	0.0062	0.3720	0.03	8
7	28	18:10	0.0000	0.0000		
7	28	21:17	0.0558	3.3480		
7	28	21:18	0.0434	2.6040		
7	28	21:20	0.0062	0.3720		
7	28	21:44	0.0062	0.3720		
7	28	21:47	0.0186	1.1160		
7	28	21:48	0.0124	0.7440		
7	28	21:49	0.0496	2.9760		
7	28	21:50	0.0558	3.3480		
7	28	21:51	0.0998	5.9520		
7	28	21:52	0.0620	3.7200		
7	28	21:53	0.0062	0.3720		
7	28	21:54	0.0124	0.7440		
7	28	22:10	0.0000	0.0000	0.43	38
7	29	1:14	0.0806	4.8360		
7	29	1:15	0.5580	33.4800		
7	29	1:16	0.9238	55.4280		
7	29	1:17	0.4774	28.6440		
7	29	1:18	0.3782	22.6920		
7	29	1:19	0.2108	12.6480		
7	29	1:20	0.1364	8.1840		
7	29	1:21	0.1240	7.4400		
7	29	1:22	0.0868	5.2080		
7	29	1:23	0.0248	1.4880		
7	29	1:24	0.0372	2.2320		
7	29	1:25	0.0186	1.1160		
7	29	1:26	0.1240	7.4400		
7	29	1:27	0.0620	3.7200		
7	29	1:28	0.0248	1.4880		
7	29	1:29	0.0124	0.7440		
7	29	1:31	0.0372	2.2320		
7	29	1:35	0.0806	4.8360		
7	29	1:36	0.0372	2.2320		
7	29	1:37	0.0124	0.7440		
7	29	1:38	0.0062	0.3720		
7	29	1:47	0.0062	0.3720		
7	29	1:56	0.0124	0.7440		
7	29	2:10	0.0000	0.0000		
7	29	2:35	0.0186	1.1160		
7	29	2:36	0.0310	1.8600		
7	29	2:37	0.0062	0.3720		
7	29	2:38	0.0062	0.3720		
7	29	2:39	0.0124	0.7440		
7	29	2:44	0.0124	0.7440		

Figure 8.2 (cont)

instantaneous intensities. This kind of data tends to underestimate the short-period rainfall at high intensity and overestimate the low-intensity rainfall. At present, the data collected from the DCPS is processed using the same software package as the data from the tipping bucket rain-gauges.

There are a large number of storm characteristics important to urban hydrology. Accurate information concerning these characteristics in time and space is indispensable for the cost-effective design of hydraulic structures.

An inspection of rainfall distributions illustrates the wide variety of shapes a hyetograph can assume. There is no typical rain sequence even though the average sequence might consist of a rapidly increasing rate of rainfall with a maximum intensity reached in the first 15 minutes of a short-duration storm, followed by a period in which intensity decreases to zero or becomes inappreciable [94]. An "average" design storm is illustrated in Figure 8.3.

To compare the performance of the drop counter precipitation sensor and the tipping bucket rain-gauge, both instruments were placed in various locations during the rainfall monitoring field program within 3 m of each other. The hyetographs obtained are shown in Figures 8.4 to 8.6. The data from the tipping bucket rain-gauge was collected by means of a DAS-TBRG version. The rainfall integration time used was 1 minute.

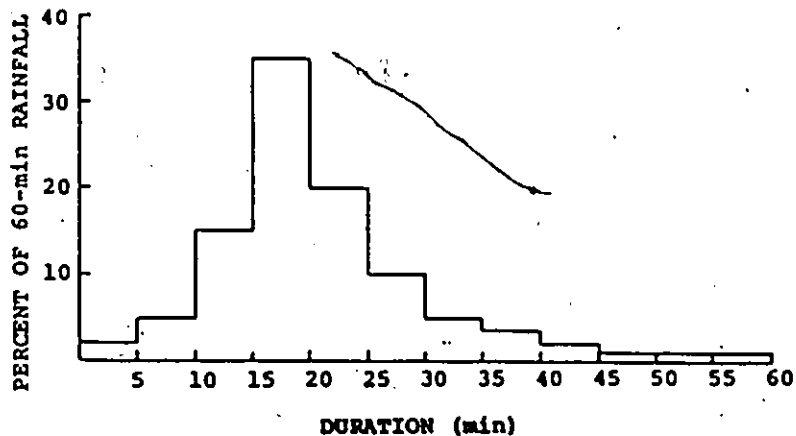


Figure 8.3 "Average" time distribution model

Hyetographs with the identifier "CIRCLE D" correspond to the information collected by the DCPS, the information from the tipping bucket rain gauge is illustrated by hyetographs identified simply by "CIRCLE".

Figure 8.4 shows the hyetographs plotted using 10 minute time-step. It can be seen that the total amount of rainfall collected by each of the gauges is almost the same, within a 6% difference. The general shapes of the hyetographs are similar, but the better resolution of the DCPS can be easily appreciated. The event times for the graphs are seen to be the same.

Hyetographs plotted in time-steps of 5 minutes are shown in Figure 8.5 where the superior resolution of the DCPS is more evident.

For the hyetographs plotted using time-steps of 1 minute, shown in Figure 8.6, the similarity of the shapes is almost lost. Event timing is maintained and the high resolution of the DCPS is fully exposed. Note that the vertical scales are not the same for these graphs.

The quantitative resolution provided by the drop counter precipitation sensor, in conjunction with the high time resolution of the data acquisition system, may greatly improve the results obtained from the computer program packages mentioned earlier. As shown in the hyetographs, it is easier to determine the characteristics of a rainstorm event (i. e. time of onset and cessation of rain, maximum intensity and timing of rainfall) from data collected by means of the precipitation sensor and data acquisition system than from data collected with the tipping bucket raingauge.

Figure 8.4 (a)

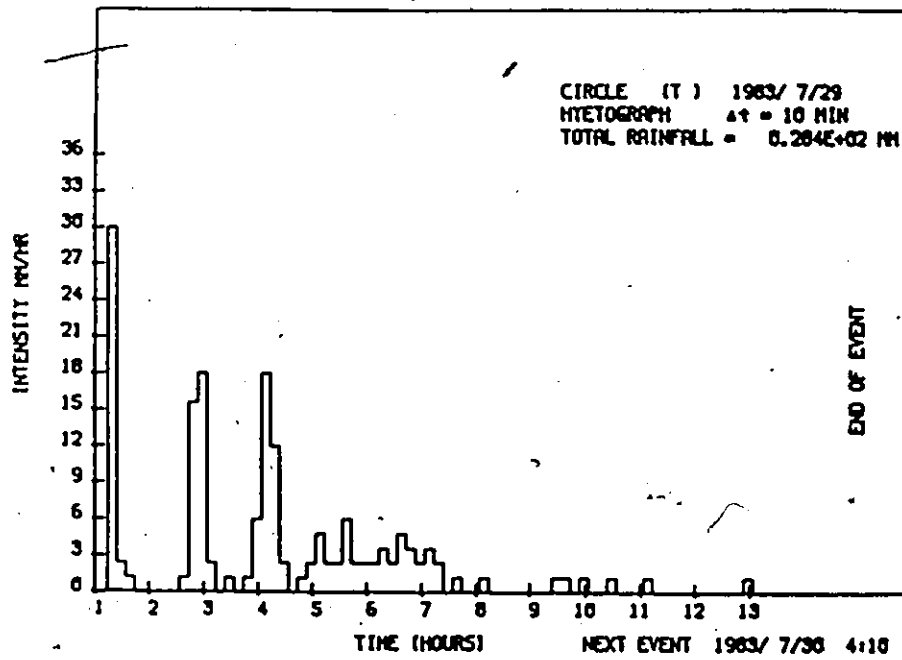


Figure 8.4 (b)

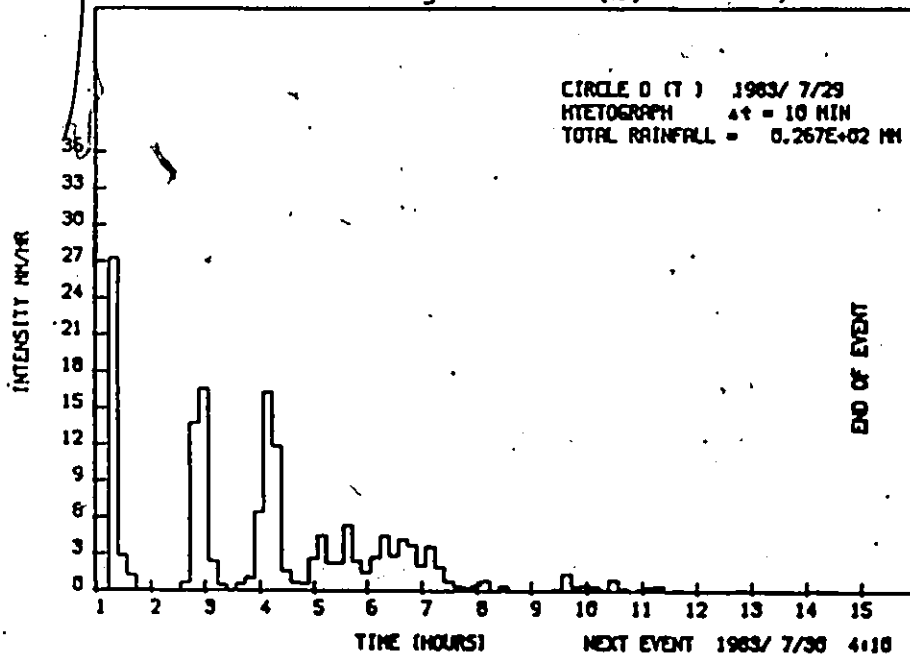


Figure 8.4 Hyetograph using 10 minute time-step:
(a) tipping bucket rain gauge, (b) drop counter precipitation sensor

Figure 8.5 (a)

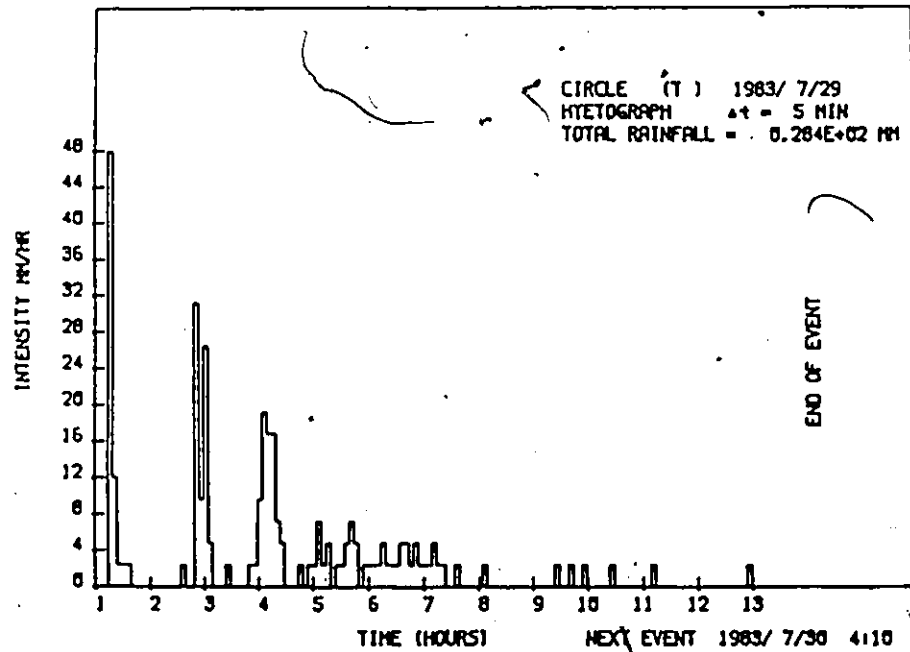


Figure 8.5 (b)

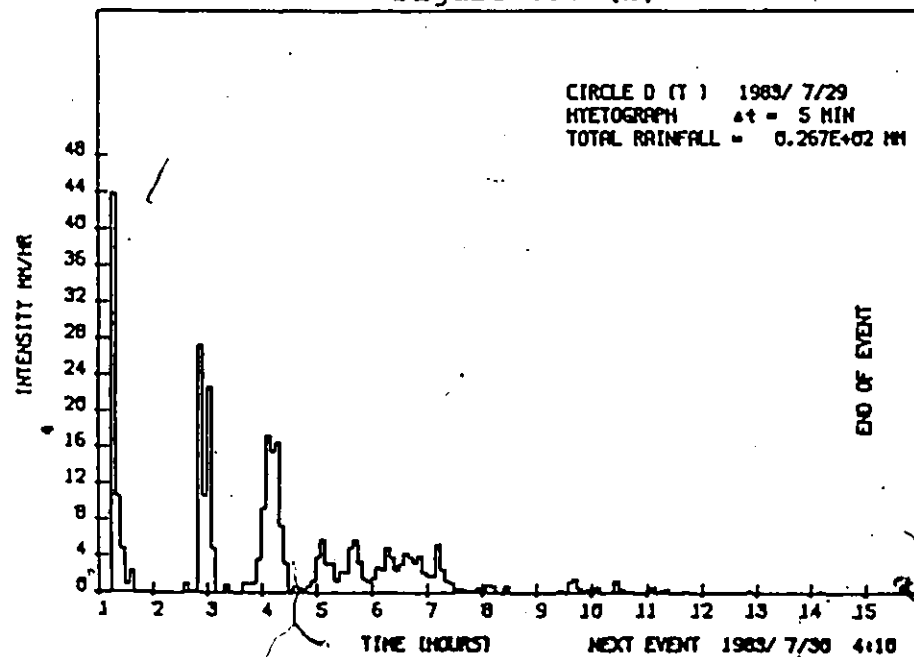


Figure 8.5 Hyetograph using 5 minute time-step:
 (a) tipping bucket rain gauge, (b) drop counter
 precipitation sensor

Figure 8.6 (a)

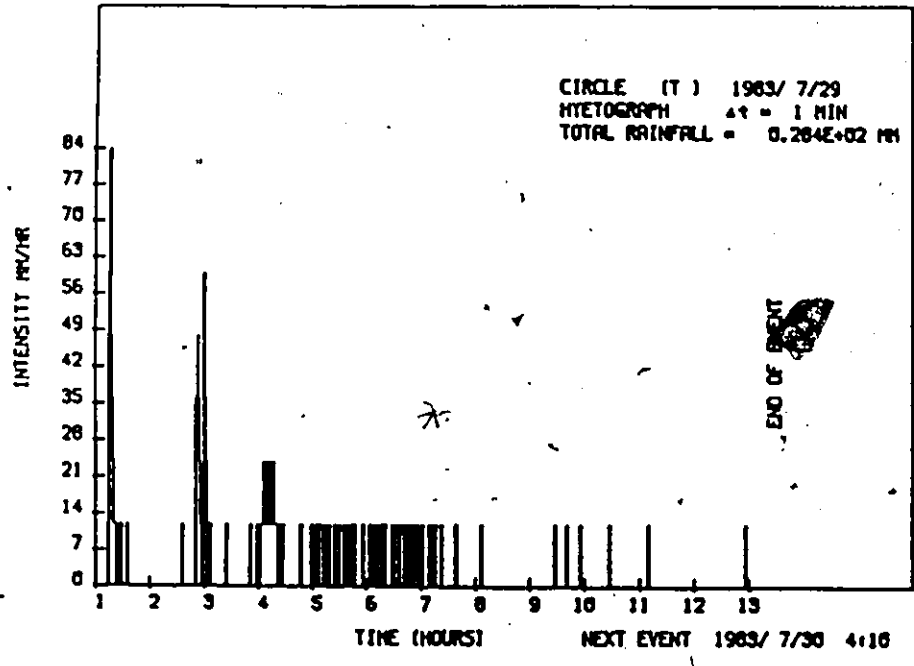


Figure 8.6 (b)

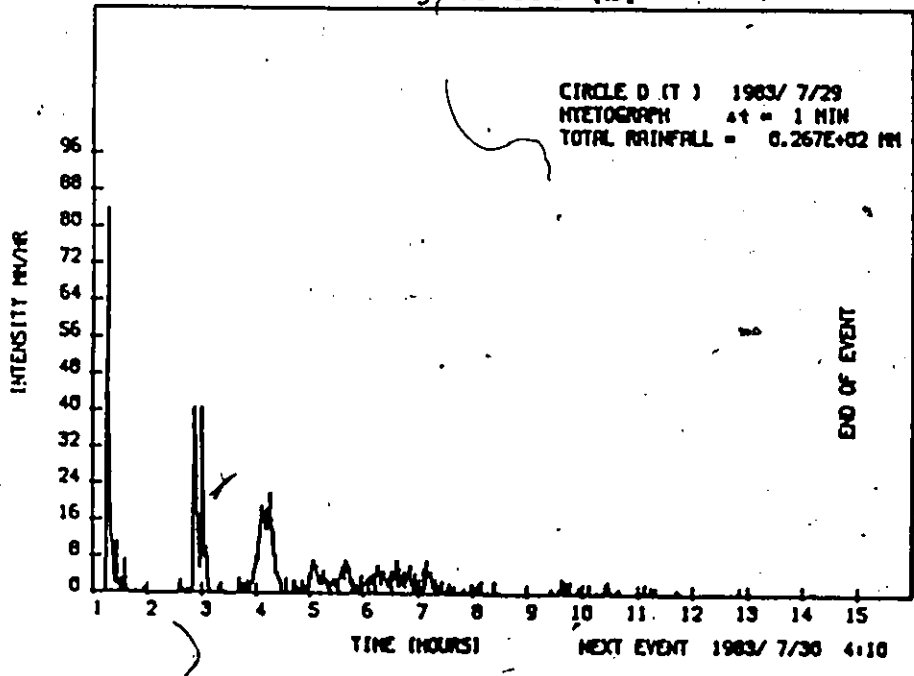


Figure 8.6. Hyetograph using 1 minute time-step:
(a) tipping bucket rain gauge, (b) drop counter precipitation sensor

PART THREE: CONCLUSIONS

CHAPTER 9 CONCLUSIONS

Precipitation is the most important factor governing the urban runoff pattern. Accurate data on amounts and time and space distribution are essential for effective financial and physical planning, implementation and evaluation of urban stormwater systems. Stormwater management is complicated by several factors such as the continuous growth of urban areas, water quality regulations, the need for control of urban flooding and economical use of hydroelectric potential. As a result, hydrometeorologists need better instrumentation to collect, store, communicate, and process rainfall information.

Typically, hydrometeorologists use a simplistic approach to estimate the average precipitation over an area. This methodology is based on assumptions such as uniform spatial distribution of rain over significantly large catchment areas. The use of such a methodology is due to the high cost of instruments in present use. Advanced storm analysis, such as dynamic tracking of storms, storm models,

based on kinematics of cells within the rainstorm, and similar improvements, have had to await the advent of better spatial and temporal sampling of rainfall.

It has been shown that precipitation instrumentation can be constructed by using low-cost mass-produced components. The only components that needed to be fabricated were the drop sensor and the printed circuit boards for the electronic components. The low cost of the instrument and the lengthy period over which it may be left to operate unattended open the way to the deployment of many more rainfall gauges over a catchment area than has hitherto been economically possible. Improved spatial resolution permits new theoretical development on the spatial distribution of rainfall, and more realistic models of thunderstorm dynamics. This in turn allows total rainfall to be estimated much more accurately for stormwater control and for anti-pollution measures. A second and significant advantage is that failure of any one or two gauges does not affect the measurement system as a whole to any particularly significant extent.

Rainfall instrumentation systems often fall victim to vandals who destroy the comparatively expensive tipping buckets all too frequently, no matter how remotely and unobtrusively they may be situated. The small size of the drop counter system, compared with the tipping bucket, also helps to make it inconspicuous.

Comparative measurements using the drop counter gauge and the tipping bucket gauges show that the drop counter is more sensitive, leading to a superior signalling of the beginning and end of rain, and with comparable accuracy. Finally, the versatility of the microcomputer opens the way to a broader range of measures of atmospheric phenomena that share the same electronics and storage/communications.

After extensive testing of the drop counter precipitation sensor ~~it~~ was concluded that it performs adequately in terms of producing constant size drops. However, in spite of this more research may be performed into other factors which may affect sensor operation, such as the effect of wind on the amount of precipitation collected.

Adequate instrumentation is required to perform experiments to determine the maximum rainfall rate permissible by the sensor. One form of changing the maximum rainfall rate of the sensor is by changing its collection area; reducing the collection area by half will double the maximum rate.

The data acquisition system can be improved in several ways, including the replacement of the cassette recorder by solid state memory. The acquisition system temperature range specified is due mainly to the cassette recorder; replacing it by solid state memory will make it possible to use the instrument at lower temperatures (Even below the

freezing point if a heater is adapted to the precipitation sensor). The microcomputer is fully dedicated to data acquisition and storage. However these tasks use only a small fraction of the available time and program memory, so the remaining may be used to perform some data processing.

Further improvements of the instrumentation can be performed in several ways, including the addition of a radio communication link between the sampling sites and the central computer for real-time operation and the extension of acquisition channels. The new channels will be used to collect more information, using additional transducers for measurement of water depth in pipe discharges, water and ambient temperature, water conductivity and pH. It is envisaged that the real-time microcomputer control system would include the following, as depicted in Figure 9.1:

1. Remote monitoring and telemetering with microcomputer-based stations.
2. Radio communication link.
3. Microcomputer-controlled diversion structures for runoff control.
4. Central computer with display, operator control console and magnetic tape archive.

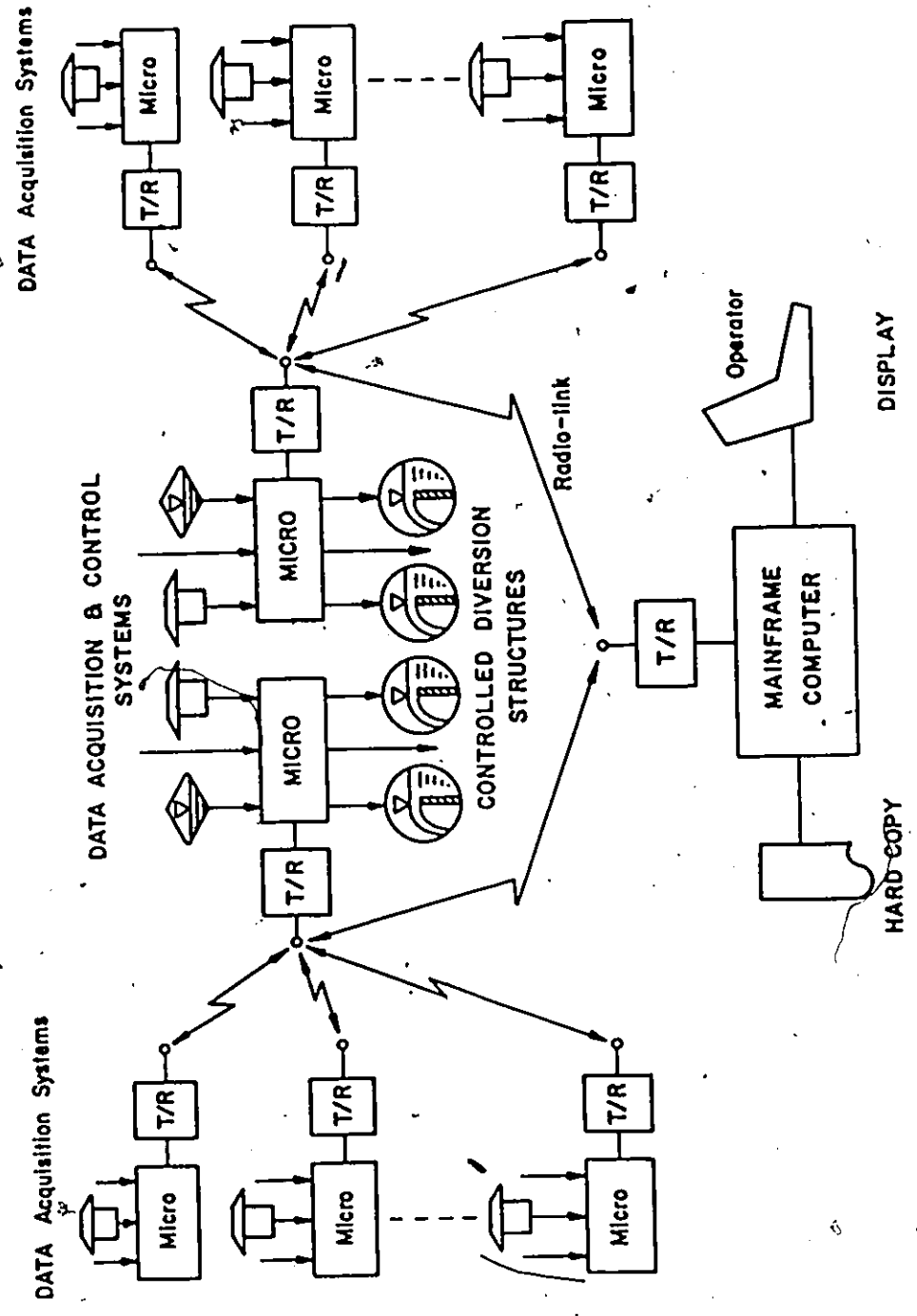


Figure 9.1 Envisaged real-time microcomputer-control system

REFERENCES

CHAPTER 1

[1] "Better Observation Network Needed: Weather Expert", The Spectator, Hamilton, Ontario, October 12, 1983, pp C9

[2] James, W. and Shtifter, Z., "Implications of Storm Dynamics on Design Storm Inputs", Proceedings of the conference on Water Quality and Stormwater Management Modelling, Niagara Falls, Ontario, U.S.E.P.A., October 1981, pp 55-78.

[3] H. Haro, R. Kitai, and W. James, "Precipitation Instrumentation Package for Improved Spatial and Temporal Sampling of Rainfall", IEEE Transactions on Instrumentation and Measurement, Vol. IM-32, No. 3, September 1983, pp. 423-429.

[4] H. Haro, "Inexpensive Microcomputer Based Precipitation Data Acquisition System", Conference on Emerging Computer Techniques in Stormwater and Flood Management, Niagara-on-the-Lake, Ontario, Canada, October 1983.

[5] H. Haro, R. Kitai, and W. James, "Precipitation Instrumentation Package for Sampling of Rainfall", Internation-

tional Workshop on Atmospheric Contamination, Mexico City, Mexico, May 1983, 27 pp.

[6] W. James, D. Henry, and H. Haro, "Integrity of Rainfall Time Series Input for Models of Existing Combined Sewer Systems", Proceedings of the Conference on Stormwater and Water Quality Model Users Group Meeting, Ottawa, Ontario, Canada, October 1982, 14 pp.

[7] W. James, H. Haro, M. A. Robinson, D. Henry, and R. Kitai, "Hydrometeorological Data Acquisition: Innovative, High-Resolution, Programmable Instrumentation for Stormwater Management", Proceedings of the Conference on Stormwater and Water Quality Management Modeling Users Group Meeting, Washington, DC., U.S.A., March 1982, pp. 128-151.

[8] W. James, M. A. Robinson, and H. Haro, "Specifications for Rainfall Instrumentation", Computational Hydraulics Group, McMaster University, Hamilton, Ontario, July 1983, 6 pp.

[9] W. James, H. Haro, A. Merlo, and W. Glass, "Drop Counter Precipitation Sensor User's Manual", Computational Hydraulics Group, McMaster University, Hamilton, Ontario, September 1983, 22 pp.

[10] W. James, M. A. Robinson, and H. Haro, "Data Decoder User's Manual", Computational Hydraulics Group, McMaster University, Hamilton, Ontario, November 1983, 52 pp.

[11] W. James, M. A. Robinson, and H. Haro, "Rainfall Data Acquisition; Manual for 110V Power Source", Computational Hydraulics Group, McMaster University, Hamilton, Ontario, November 1983, 81 pp.

CHAPTER 2.

[12] Linsley, R., Kohler, M., and Paulhus, J., "Hydrology for Engineers", McGraw-Hill Series in Water Resources and Environmental Engineering, 2nd. ed., 1975, 482 pp.

[13] World Meteorological Organization, "Guide to Meteorological Instruments and Observing Practices", 3rd. ed., Geneva, Switzerland, 1969, pp. 1.1-1.33 and 7.1-7.21.

[14] Atkinson, B. W., "The Effect of an Urban Area on the Precipitation from a Moving Thunderstorm", Journal of Applied Meteorology, Vol. 10, February 1971, pp. 47-55.

[15] Linsley, R. K., "A manual on Collection of Hydrologic Data for Urban Drainage Design", Hydrocomp Inc., Palo Alto,

California, 1973.

[16] Federal Council for Science and Technology, "Scientific Hydrology", Washington, June 1962.

[17] James, W., "Introduction to Computational Hydrology and Hydraulics", McMaster University, 1982, 526 pp.

[18] Private communication from A. Unal, Civil Engineering Dept., McMaster University, 1983.

[19] Robinson, M. A., and James, W., "Continuous SWMM Modeling of Summer Stormwater Runoff Quality in Hamilton: Analysis of Preliminary Output Time Series Based on Discrete-Event Calibrations from Non-Industrial Areas", Computational Hydraulics Group, Hamilton, Ontario, January, 1982, pp. 1-26.

[20] Robinson, M. A. and James, W., "Co-Ordinated Multiprocessing for Real-Time Control of Urban Drainage", Proceedings of Stormwater Management Model (SWMM) Users Group Meeting, January 1981, pp. 119-140.

[21] Private communication from M. A. Robinson, Civil Engineering Dept., McMaster University, 1983.

[22] Private Communication from B. Shivalingaiah, Civil Engineering Dept., McMaster University, 1983.

[23] Private communication from M. Stirrup, Civil Engineering Dept., McMaster University, 1983.

[24] R. Scheckenberger, and James, W., "RAINPAC Users manual", Computational Hydraulics Group, McMaster University, Hamilton, Ontario, May 1983, pp 1-65.

[25] Private communication from P. Nimmrichter, Civil Engineering Dept., McMaster University, 1983.

[26] James, W. and Shtifter, Z., "Implications of Storm Dynamics on Design Storm Inputs", Proceedings of the Conference on Water Quality and Stormwater Management Modelling, Niagara Falls, Ontario, Canada, October 1981, pp. 55-70.

[27] Kibler, D. F. and Aron, G., "Urban Runoff Management Strategies", Journal of the Technical Council, ASCE, Vol. 106, No. TC1, August 1980, pp. 1-12.

[28] Viessman, W. Jr., Knapp, J. W., Lewis, G. L. and Harbaugh, T. E., "Introduction to Hydrology", Harper Row, Publishers, IEP Series in Civil Engineering, (in Canada Fitzhenry, Whiteside, Ltd., Toronto), 2 ed., 1977, 704 pp.

[29] Huber, W. C., Heaney, J. P., Nix, S. J., Dickinson, R. E. and Polman, D. J., "Storm Water Management Model User's Manual", Version III, United States Environmental Protection Agency (USEPA), Cincinnati, Ohio, November 1981, pp. 1.1-8.1.

[30] James, W., "Program FASTSWMM User's Guide", Computational Hydraulics Inc., December 1979, 73 pp.

CHAPTER 3

[31] Middleton, W. E. K., "Invention of the Meteorological Instrument", The John Hopkins Press, Baltimore 1969, pp. 133-174.

[32] Middleton, W. E. K., "Catalog of Meteorological Instruments in the Museum of History and Technology", Smithsonian Institution Press, Washington 1969, pp. 73-76.

[33] Biswas, A. K., "History of Hydrology", North Holland Pub., 1970, 336 pp.

[34] Kautilya, "Arthashastra", Translated by R. Shamasastri, Government Press, Bangalore, India 1915. Reference obtained from [31], not confirmed.

[35] Sammadar, J. N., "Indian Meteorology of the Fourth Century B. C." Quarterly Journal of the Royal Meteorological Society, Vol. 38, 1912, pp. 65-66.

[36] The Mishnah, Translated by Herbert Danby, Oxford University Press, 1933. Reference obtained from [33], not confirmed.

[37] Needham, J., "Science and Civilization in China", Cambridge, University Press, Vol. 3, 1959. Reference obtained from [33], not confirmed.

[38] Stout, G. E., and Mueller, E. A., "Survey of Relationships Between Rainfall Rate and Radar Reflectivity in the Measurement of Precipitation", Journal of Applied Meteorology, Vol. 7, June 1968, pp. 465-474.

[39] Linsley, R., Kohler, M. and Paulhus, J., "Hydrology for Engineers", McGraw-Hill series in Water resources and Environmental Engineering, 2nd. ed., 1975, 482 pp.

[40] Wilson, J. W., "Integration of Radar and Gage Data for Improved Rainfall Measurements", Journal of Applied Meteorology, Vol. 9, June 1970, pp. 489-497.

[41] Seliga, T. A., Bringi, V. N. and Al-Khatib, H. H.,

"A Preliminary Study of Comparative Measurements of Rainfall Rate Using the Differential Reflectivity Radar Technique and a Raingage Network", Journal of Applied Meteorology, Vol. 20, November 1981, pp. 1362-1369.

[42] Huff, F. A., "Comparison Between Standard and Small Orifice Raingages", Transactions Am. Geophys. Union, Vol. 36, No. 4, August 1955, pp. 689-694.

[43] Jones, D. M. A., "Effect of Housing Shape on the Catch of Recording Gages", Monthly Weather Rev., Vol. 97, August 1969, pp. 604-606.

[44] McKay, G. A., "Precipitation", Handbook on the Principles of Hydrology, Canadian National Committee for the International Hydrological Decade, 1970, Section II, pp. 2.1-2.111.

[45] World Meteorological Organization, "Guide to Meteorological Instruments and Observing Practices", 3rd. ed., Geneva, Switzerland, 1969, pp. 7.1-7.21.

[46] Marsalek, J., "Instrumentation for Field Studies of Urban Runoff", Research report No. 42, Ministry of the Environment, Canada, 1973, 82 pp.

[47] Environment Canada, "Field Test of Accuracy for Bridge and Bucket Assemblies (Tipping Bucket Rain gauge)", Atmospheric Environment Services, Willowdale, Toronto, October 1980.

[48] National Weather Service, "Engineering Test of an Inexpensive Tipping Bucket Precipitation Gage (MISCO)", Sterling, Virginia, USA, March 1978, 12 pp.

[49] Parsons, D. A., "Calibration of a Weather Bureau Tipping Bucket Gage", Mon. Weather Rev., Vol. 69, July 1941, pp. 204-206.

[50] Freeny, A. E. and Semplak, R. A., "Measuring Rainfall", Bell laboratories record, December 1964, 6 pp.

[51] Seibel, R. R., "A Capacitor-Type Rain Gauge with DC Output and Improved Flow Characteristics", Rev. of Scientific Ins., Vol. 43, No. 8, August 1972, pp. 1081-1085.

[52] Kirkham, H., "Instantaneous Rainfall Rate: its Measurement and its Influence on High Voltage Transmission Lines", Journal App. Meteor., Vol. 19, January 1980, pp. 35-40.

[53] Adkins, C. J., "A Rate-of-Rainfall Recorder", Cavend-

ism Laboratory, Cambridge, USA, pp. 419-420.

[54] Venugopal, G. and Radhakrishnan, V., "A High-Resolution Electronic Rainfall Intensity Recorder and Totaliser", Indian Journal Met. Hydrol. Geophys., Vol. 27, No. 4, 1976, pp. 441-444.

[55] Norbury, J. R. and White, W. J., "A Rapid-Response Rain Gauge", Journal of Physics E.: Scientific Instruments, Vol. 41, 1971, pp. 601-602.

[56] Robinson, A. C. and Rodda, J. C., "Rain, Wind and the Aerodynamic Characteristics of Raingauges", Meteorological Magazine, Vol. 98, 1969, pp. 113-120.

[57] Sevruk, B., "Methods of Correcting for Systematic Error in Point Precipitation Measurement for Operational Use", World Meteorological Organization, Operational Hydrology, Report No. 21, WMO-No. 589, 1982, 91 pp.

[58] Warnick, C. C., "Experiments with Wind Shields for Precipitation Gauges", Trans. Am. Geophys. Union, Vol. 34, June 1953, pp. 379-388.

[59] "The Tipping Bucket Rain Gauge", Instrument manual No. 41, Department of Transport, Meteorological Division, Toron-

to, Ont., 1952, 34 pp.

[60] Kurtyka, J. C., "Precipitation Measurements Study", Illinois state water survey, Report of investigation 20, Urbana, Ill., 1953.

CHAPTER 4

[61] Clift, R., Grace, J. R. and Weber, M. E., "Bubbles, Drops and Particles", Academic Press, New York, 1978, pp. 321-380.

[62] Keith, F. W. and Hixson, A. N., "Liquid-Liquid Extraction Spray Columns", Industrial and Engineering Chemistry, Vol. 47, No. 2, February 1955, pp. 258-267.

[63] Brodkey, R. S., "The Phenomena of Fluid Motions", Addison-Wesley Series in Chemical Engineering, 1967, pp. 539-618.

[64] Hauser, E. A., Edgerton, H. E., Holt, B. M. and Cox, J. T. Jr., "The Application of the High-Speed Motion Picture Camera to Research on the Surface Tension of Liquids", Journal of Physical Chemistry, Vol. 40, 1936, pp. 973-987.

[65] Guthrie, F., "On Drops", Proceedings of the Royal Society, London, Vol. 13, 1863-1864, pp. 444-483.

[66] Rayleigh, "Investigation in Capillarity:- The Size of Drops.- The Liberation of Gas from Supersaturated Solutions.- Colliding Jets.- The Tension of Contaminated Water Surfaces", Philosophical Magazine, S. 5, Vol. 48, October 1899, pp. 321-337.

[67] Harkins, W. D. and Humphery, E. C., "The Drop Weight Method for the Determination of Surface Tension", Journal of the American Chemistry Society, Vol. 38, 1916, pp. 228-246.

[68] Morgan, J. L. R., "The Drop Weight Method for the Determination of the Surface Tension of a Liquid", Journal of the American Chemistry Society, Vol. 37, 1915, pp. 1461-1467.

[69] Harkins, W. D. and Brown, F. E., "The Determination of Surface Tension (Free Surface Energy) and the Weight of Falling Drops: The Surface Tension of Water and Benzene by the Capillary Height Method", Journal of the American Chemistry Society, Vol. 41, 1919, pp. 499-524.

[70] Edgerton, H. E., Hauser, E. A. and Tucker, W. R.,

"Studies in Drop Formation as Revealed by the High-Speed Motion Camera", Journal of Physical Chemistry, Vol. 41, 1937, pp. 1017-1028.

[71] Andreas, J. M., Hauser, E. A. and Tucker, W. B., "Boundary Tension by Pendant Drops", Journal of Physical Chemistry, Vol. 42, 1938, pp. 1001-1019.

[72] Hayworth, C. B. and Treybal, R. E., "Drop Formation in Two-Liquid-Phase Systems", Industrial and Engineering Chemistry, Vol. 42, No. 6, June 1950, pp. 1174-1181.

[73] Izard, J. A. W., Cavers, S. D. and Forsyth, J. S., "Production of Liquid Drops by Discontinuous Injection", Journal of Chemical Engineering Science, Vol. 18, 1963, pp. 467-468.

[74] Sceelee, G. F. and Meister, B. J., "Drop Formation at Low Velocities in Liquid-Liquid Systems", AIChE Journal, Vol. 14, No. 1, January 1968, pp. 9-19.

[75] Rayleigh, "On the Instability of Jets", Proceedings of the Royal Society, London, Vol. 10, 1878, pp. 4-13.

[76] Rayleigh, "On the Instability of a Cylinder of Viscous Liquid Under Capillary Force" and "On The Instability of

Cylindrical Fluid Surfaces", Philosophical Magazine, S.5, Vol. 34, August 1892, pp. 145-153 and 177-180.

[77] Tyler, E. and Watkin, F., "Experiments with Capillary Jets", Philosophical Magazine, S.7, Vol. 14, No. 94, November 1932, pp. 849-881.

[78] Marshall, W. R. Jr., "Atomization and Spray Drying", Chemical Engineering Progress Monograph Series, Published by The American Institute of Chemical Engineers, New York, Vol. 50, No. 2, 1954, pp. 1-26.

[79] Merrington, A. C. and Richardson, E. G., "The Break-up of Liquid Jets", Proceedings of the Physical Society, Vol. 59, No. 331, January 1947, pp. 1-13.

[80] Christiansen, R. H. and Hixson, A. N., "Breakup of a Liquid Jet in a Denser Liquid", Industrial and Engineering Chemistry, Vol. 49, No. 6, June 1957, pp. 1017-1024.

[81] Lee, H. C., "Drop Formation in a Liquid Jet", IBM Journal of Research and Development, Vol. 18, No. 4, July 1974, pp. 364-369.

CHAPTER 5

[82] Bragg, G. M., "Principles of Experimentation and Measurement", Prentice-Hall, New Jersey, 1974, pp. 32-67.

CHAPTER 6

[83] Wobschall, D., "Circuit Design for Electronic Instrumentation", McGraw-Hill co., 1979, 390 pp.

[84] "MCS-48 Family of Single-Chip Microcomputers User's Manual", Intel Co., 1981.

[85] "Automatic Sensing Wet/Dry Precipitation Collector", Aerochem Metrics Model 301, Assembly and Operation Instructions, Aerochem Metrics, Miami, USA, 5 pp.

[86] Strachan, W. M. J. and Luneault, H., "Evaluation of an Organic Automated Rain Sampler", Environment Canada, Canada Centre for Inland Waters, Burlington, Ontario, Bulletin No. 128, 1982, 5 pp.

[87] Letter of Agreement between McMaster University and The Ontario Ministry of the Environment, Toronto, July 12, 1982.

CHAPTER 7

[88] Sallen, R. P. and Key, E. L., "A Practical Method of Designing RC Active Filters", I.R.E. Transactions on Circuit Theory, Vol. CT-2, March 1955, pp. 51-62.

[89] Johnson, D. E., "Introduction to Filter Theory", Prentice-Hall, Electrical Engineering Series, 1976, 306 pp.

[90] Gardner, F. M., "Phaselock Techniques", John Wiley and Sons, 1979, 285 pp.

[91] Linear Applications Handbook, National Semiconductors, 1978, pp. AN46.1 - AN46.12

[92] 8048 Family Applications Handbook, Intel Co., 1980, pp. 1.1-4.24.

CHAPTER 8

[93] Private communication from Eng. Mark Robinson, Computational Hydraulics Group, Dept. of Civil Engineering, McMaster University, Hamilton, Canada.

[94] Hershfield, D. M., "Some Statistical Properties of ~~Short~~-Duration Rainfall", Specialized Seminar on Rainfall as the Basis for Urban Runoff, Design and Analysis, Denmark, August 1983, 9 pp.

BIBLIOGRAPHY

(Literature providing background to the subject of the thesis)

Battan, L. J., "Radar Observations of the Atmosphere", University of Chicago Press, Chicago, Il., 1973, 324 pp.

Brandstetter, A. B, "Assessment of Mathematical Models for Storm and Combined Sewer Management", United States Environmental Protection Agency (USEPA), Cincinnati, Ohio, August 1977.

Cheng, L. and Cross, W. C., "Production of Single Liquid Drops of Controlled Size and Velocity", Rev. Sci. Instrum., Vol. 46, No. 3, March 1975, pp. 263-265.

Fordham, S., "On the Calculation of Surface Tension from Measurements of Pendant Drops", Proceedings Royal Society, London, Vol. 194A, July 1948, pp. 1-15.

Frisinger, H. H., "The History of Meteorology: to 1800", Science History Pub., 1977, pp. 89-91.

Green, M. J., "Effects of the Exposure of the Catch of the Rain Gauges", T. P. 67, Water Resources Assoc., July 1969.

APPENDICES

APPENDIX A
PRECIPITATION SENSOR TEST RESULTS

Since the precipitation sensor measures rainfall intensity, a method for simulating different intensities was needed in order to calibrate the instrument. The simulated rainfall intensities were calculated using the time for the first 100 drops to cross the test points and the number of drops for 10 ml of water. The rainfall intensity in millimeters per hour was obtained by converting the 100 drops into mm of rain and then dividing this result by the time, in hours, for the 100 drops counted.

To verify the above procedure the following test was carried out. For each simulated rainfall intensity, water was placed in the pipette and released into the sensor. The number of drops counted at 5 second intervals were recorded. This was repeated 10 times for each intensity. For each interval, the average of the drops counted and the equivalent rainfall rate were calculated.

In Figures A.1 to A.5 the solid lines show a plot of the number of drops counted versus time in 5 second intervals for intensities corresponding to 100 drops in 16.5, 20, 26.5, 50, and 100 seconds respectively. The dashed lines show the number of drops per mm that would form at the nozzle.

zle for the rainfall rates indicated.

Thirty nine drop counter precipitation sensors were constructed and calibrated as part of the field program. A summary of the calibration tests performed is presented in Table A.1. Twenty five sensors included 1.83 mm diameter nozzles whereas, the remainder used 1.6 mm nozzles. Each calibration test included 60 single trials, 10 for each one of the 6 rainfall intensities tested. The table shows the average and standard deviation obtained in the tests and the slope and Y-intercept of the linear regression equation. The standard deviation is indicative of the precision of the instrument and the slope is indicative of variations in drop size for variations in rainfall intensity.

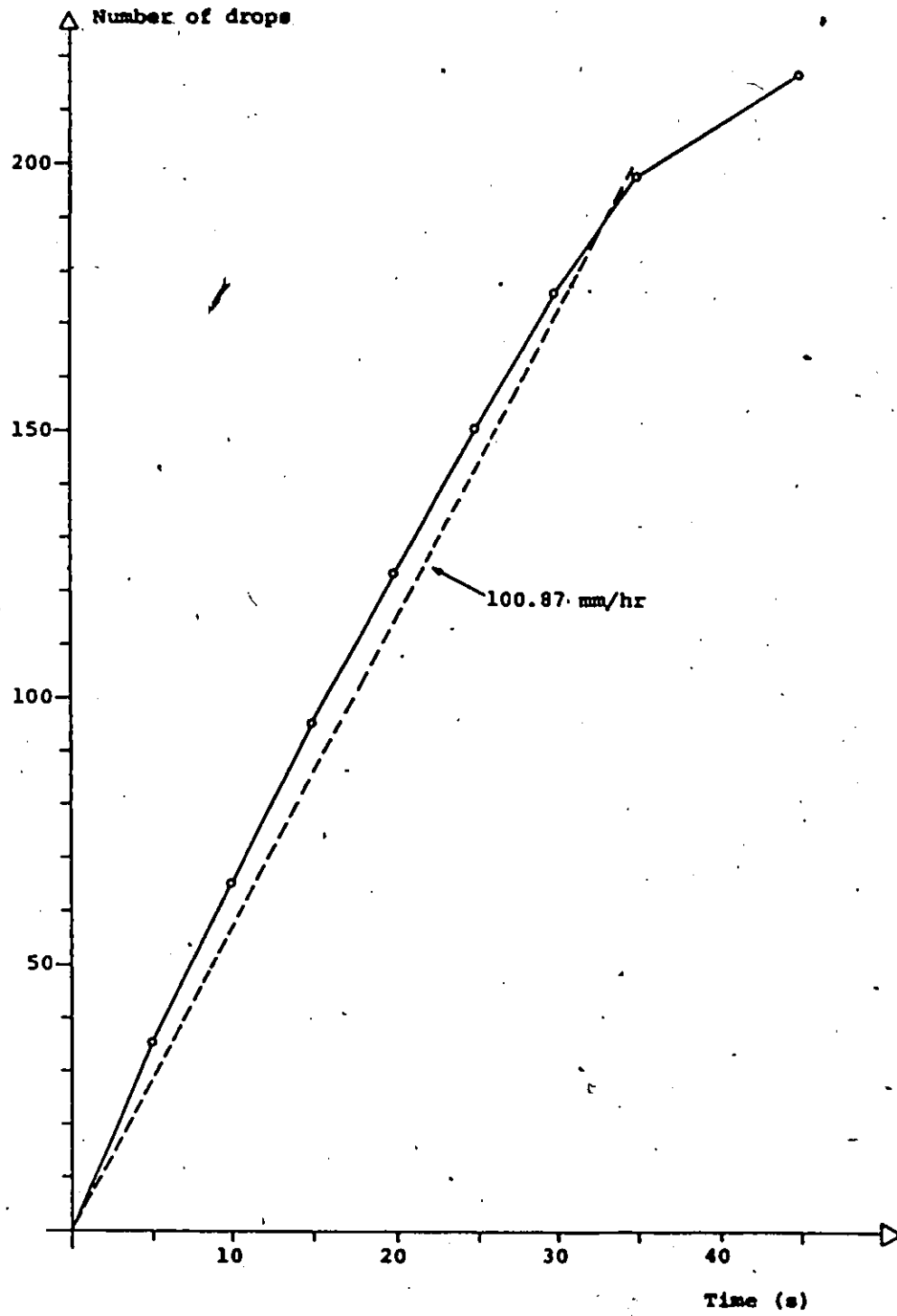


Figure A.1 Simulated rainfall intensity test results.

100 drops in 16.5 seconds

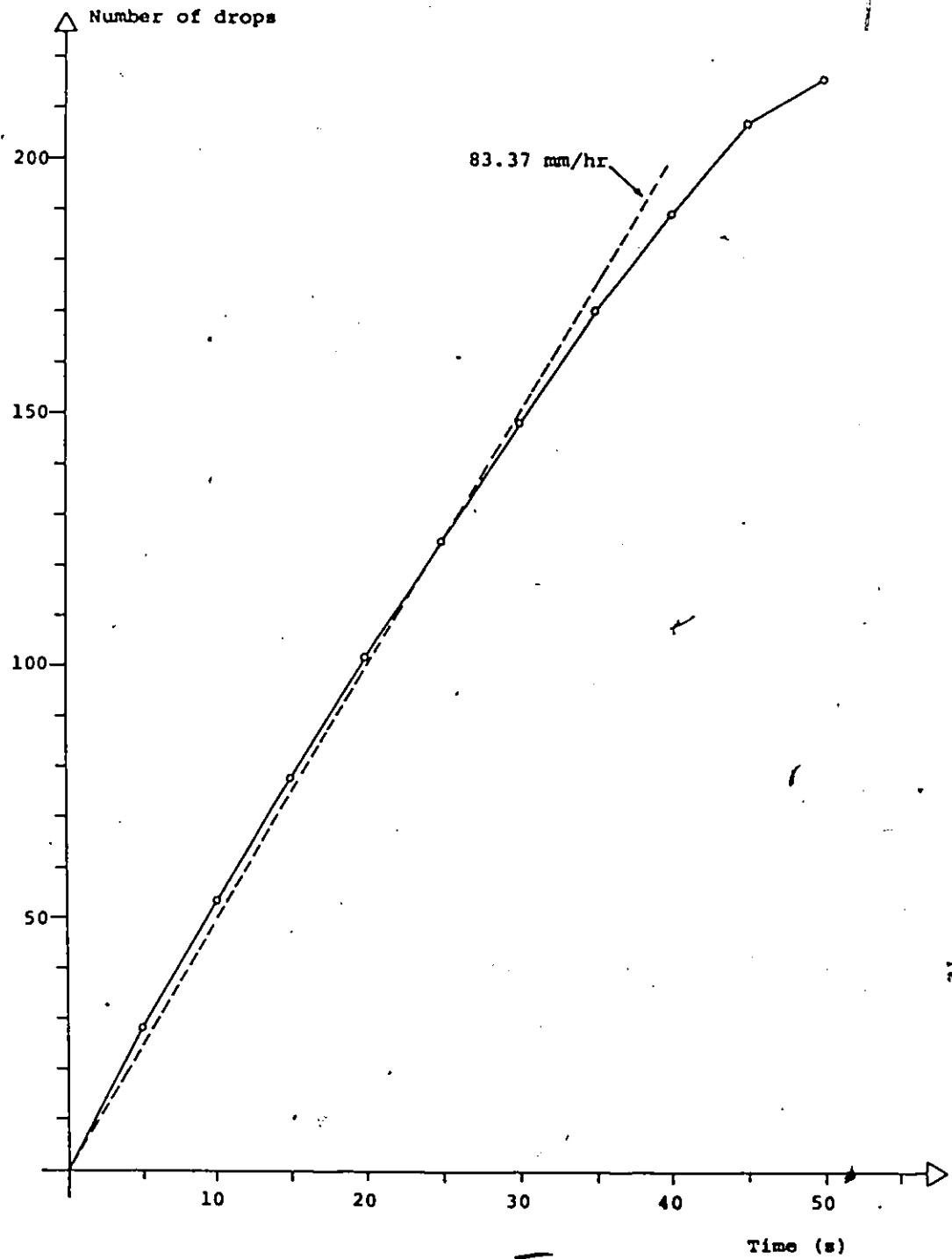


Figure A.2 Simulated rainfall intensity test results.

100 drops in 20 seconds

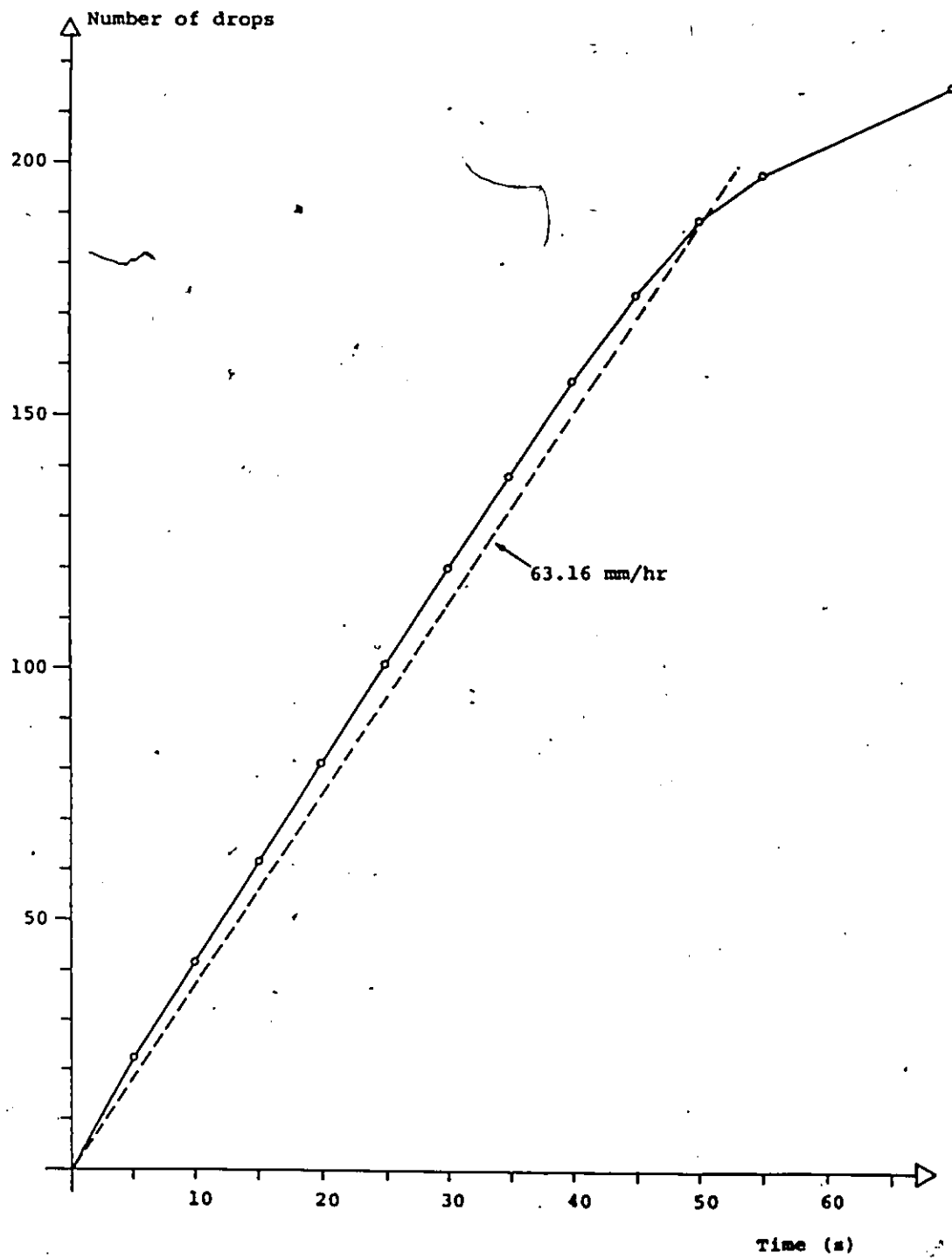


Figure A.3 Simulated rainfall intensity test results.

100 drops in 26.5 seconds

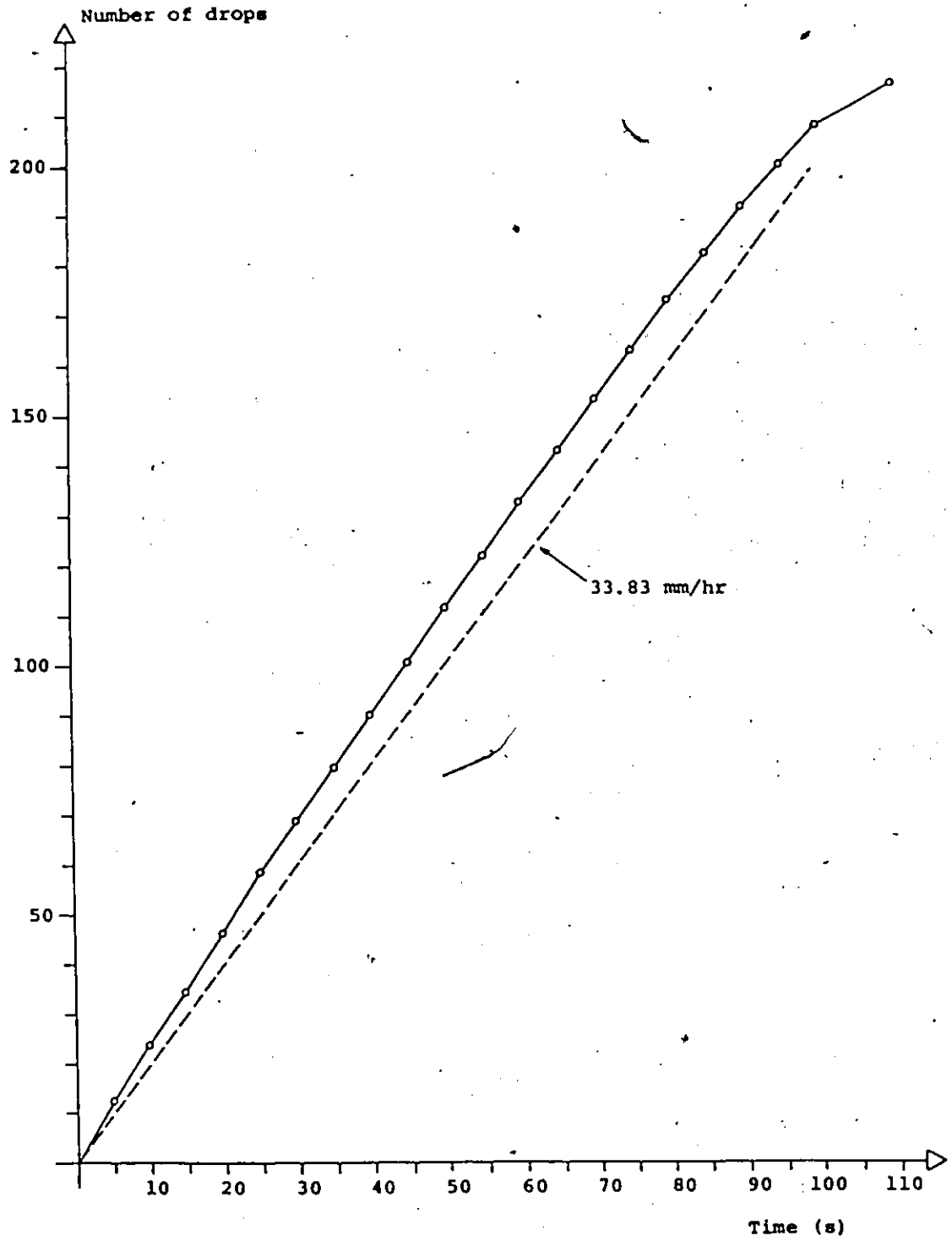


Figure A.4 Simulated rainfall intensity test results.

100 drops in 50 seconds

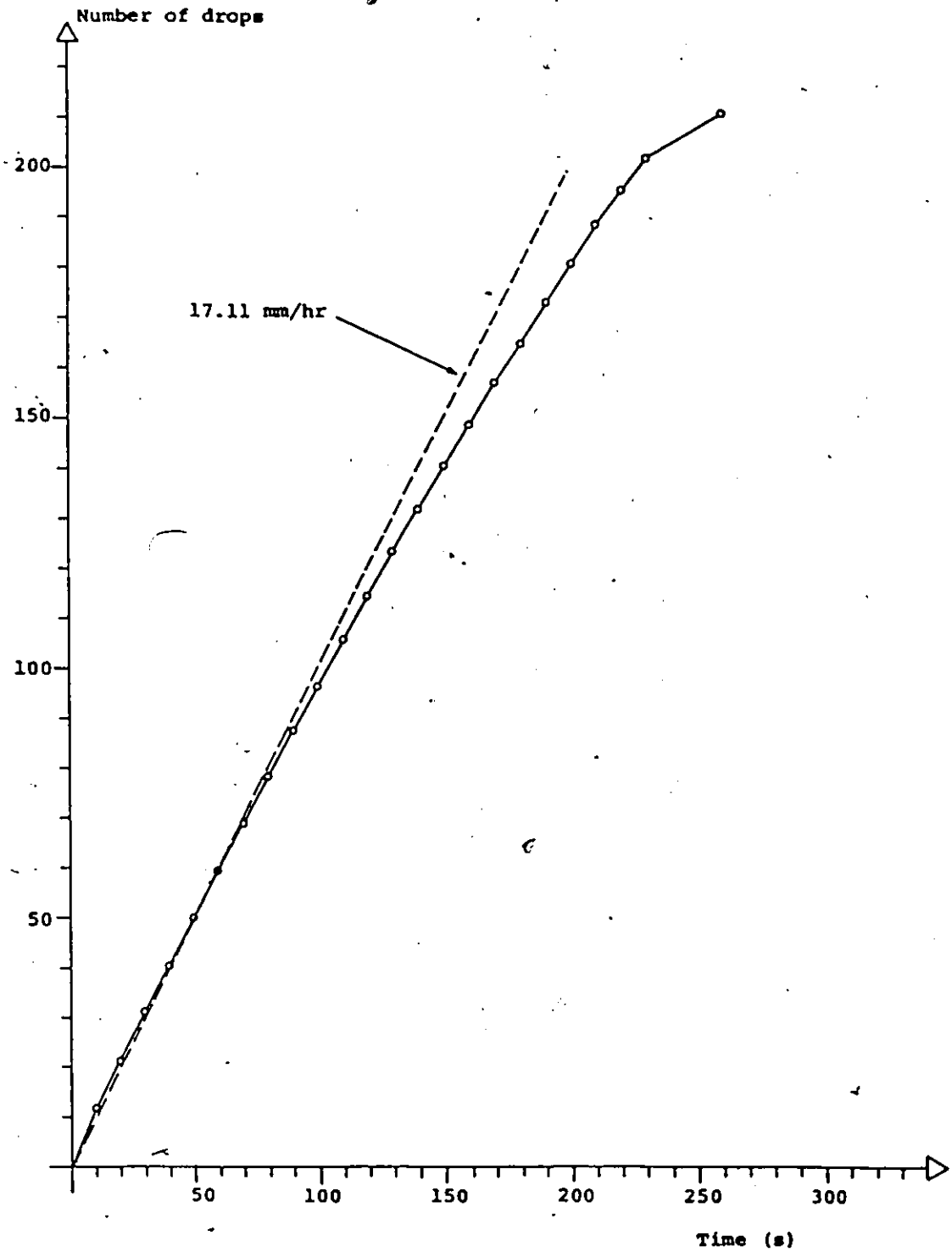


Figure A.5 Simulated rainfall intensity test results.

100 drops in 100 seconds

Table A.1 Summary of calibration test results.
Sensors marked with (*) include nozzles with 1.6 mm
inside diameter

SENSOR	AVERAGE (drops/mm)	S. D. (drops/mm)	SLOPE (hr-drops/mm ²)	Y-INTERCEPT (drops/mm)
001 *	262.4	27.0	0.3426	241.8
002 *	267.2	21.4	0.2734	250.8
003 *	272.0	19.0	0.2316	258.1
004 *	264.0	21.0	0.2705	247.4
005 *	269.6	21.2	0.2709	253.4
006 *	261.1	26.0	0.3318	241.2
007	213.4	2.8	0.0533	209.4
008 *	266.0	8.7	0.1114	259.4
009 *	262.2	4.4	0.0334	260.2
010	209.5	4.3	0.0810	203.3
011 *	262.7	12.2	0.1547	253.4
012 *	266.6	26.6	0.3388	246.3
013 *	266.6	23.1	0.2934	248.9
014 *	263.8	27.2	0.3450	243.1
015	210.3	5.1	0.0915	203.2
016	210.9	5.4	0.0999	203.2
017	212.0	7.1	0.1359	201.6

018	209.0	6.1	0.1174	199.9
019	209.7	6.4	0.1254	199.9
020	208.8	5.0	0.0974	201.2
021	213.8	6.5	0.1113	205.4
022	206.5	5.6	0.1092	198.0
023	208.5	4.2	0.0772	202.5
024	207.9	5.2	0.1026	199.9
025	216.5	2.8	0.0438	213.2
026	215.2	2.7	0.0171	213.9
027	207.0	5.5	0.1074	198.7
028	205.8	8.2	0.1598	193.4
029	204.0	5.9	0.1135	195.0
030	206.1	6.0	0.1075	197.9
031	207.7	4.5	0.0778	201.9
032	204.8	5.4	0.0960	197.5
033	206.4	5.7	0.0973	199.0
034	205.7	5.7	0.1006	198.2
035	209.4	6.0	0.0778	203.6
036	206.4	5.3	0.0968	199.1
037	208.4	4.4	0.0777	202.5
038 *	270.9	31.9	0.4076	246.4
039 *	270.8	31.9	0.4084	246.3

APPENDIX B
DATA ACQUISITION SYSTEM PROGRAM

The microcomputer program is divided into one main routine and five auxiliary subroutines. A listing of the program is presented at the end of this Appendix.

The main routine is executed at the end of the integration time and decides if data is to be stored in memory. The decision is based on the drop counter and time mark data. Figure B.1 shows a flowchart of this routine.

Two eight bit counters, named DCH and DCL for high and low order respectively, are used to count up to 64K drops. The main routine reads the data from the drop counter (DCH and DCL) and divides the number of drops by two or four. The division result (N) is expected to be smaller than 255 and therefore is stored in one memory location (see Figure 6.4). The drop counter is initialized with the remainder of the division at the beginning of a new integration time. If N is different from zero or the time mark is equal to 240, then the data is stored in memory. The time mark counter is incremented whenever data is acquired. When the reserved memory space (40 bytes) is full, the program calls subroutine "MANAGER" to dump the block of information onto tape.

The FSK modulation is achieved by subroutines "MANAGER", "RECORD" and "UPDATE". Subroutine "MANAGER" works as an overall manager; it coordinates the activities of the other subroutines and controls the recorder power supply. A flowchart of this subroutine is shown in Figure B.2.

Subroutine "RECORD" generates the control bits (start, stop and parity) and sets the modulation counters depending on the digit to be recorded. Figure B.3 shows a flowchart of this routine. There are two modulation counters: a level counter which indicates the number of levels ("1" and "0") one modulated bit contains, and a cycle counter which indicates the number of instruction cycles required for each level.

The recording is done at 300 bits per second with carriers of 1.8 kHz for logical "0" and 2.7 kHz for logical "1". The values for the modulation counters are:

	Logical "0"	Logical "1"
Level counter	12	18
Cycle counter	66	44

Using these values and an instruction cycle of 4.1905 microseconds, the information is recorded at 301.31 bits per second, that is, a deviation of 0.436 % of the desired rate. A timing diagram of the modulated signal is given in Figure B.4.

Subroutine "UPDATE" updates the modulation and serial output pins depending on the values of the modulation counters, as shown in Figure B.5.

Depressing the reset button initiates the execution of subroutine "RESET" which initializes the system. A flowchart is given in Figure B.6. This subroutine initializes the output ports, the time mark counter ($T_m=1$) and the drop counter ($DC=0$). Every time this subroutine is executed, the block of information in memory, still incomplete, is completed with zeros and dumped onto tape.

There are two time delay subroutines: "TIME LOOP 1", which lasts for the same time period as the time required to record a block of information (3.3 seconds) and is executed every time data is not recorded; "TIME LOOP 2", which determines the rainfall integration time and can be easily modified to satisfy specific requirements. It last for 56.7 seconds for an integration time of 1 minute. The two time delays are implemented using three-register loops.

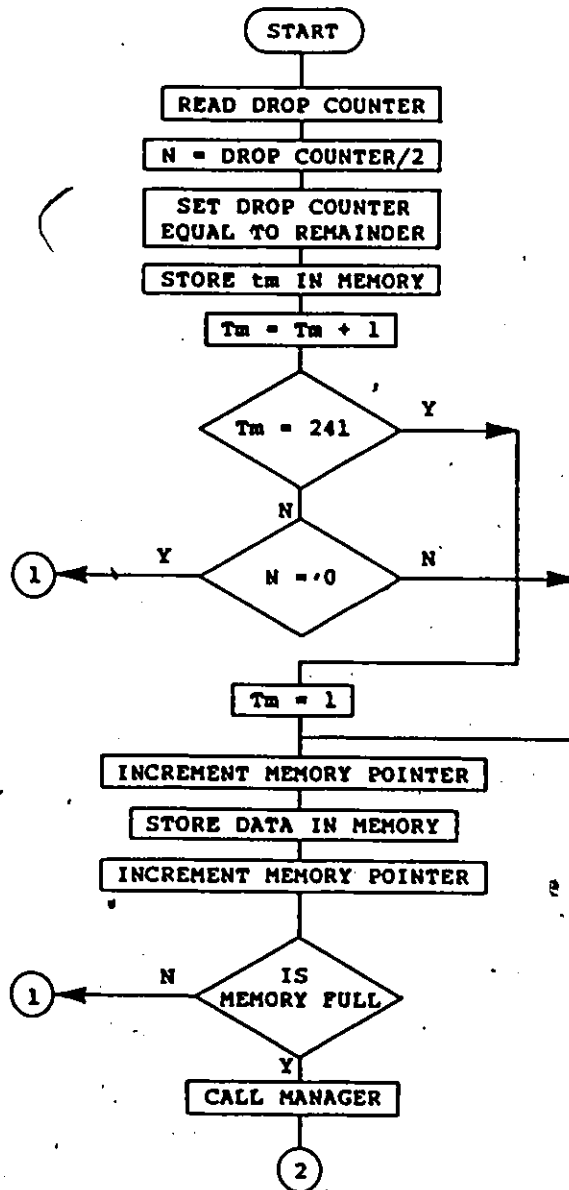


Figure B.1 MAIN ROUTINE flowchart.

1 and 2 refer to the time loops

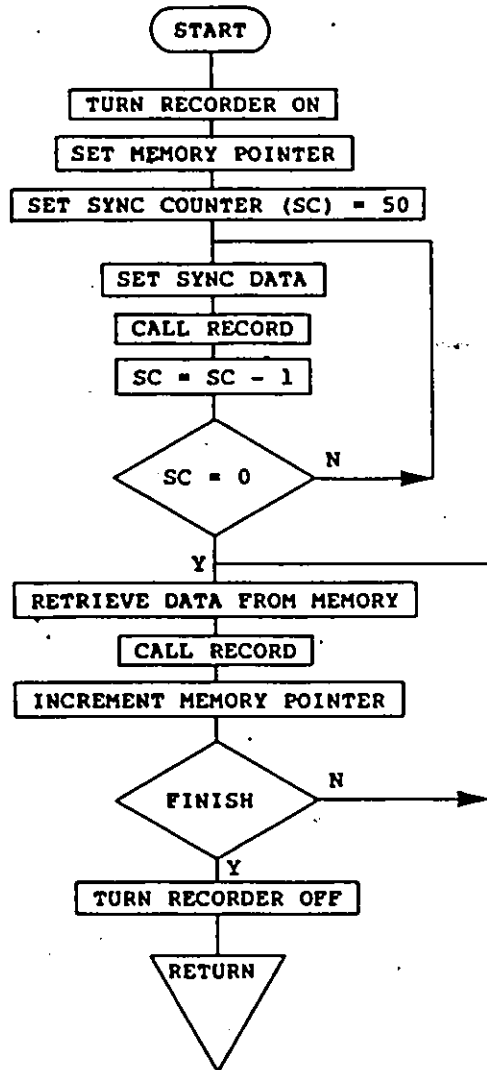


Figure B.2 Subroutine MANAGER flowchart

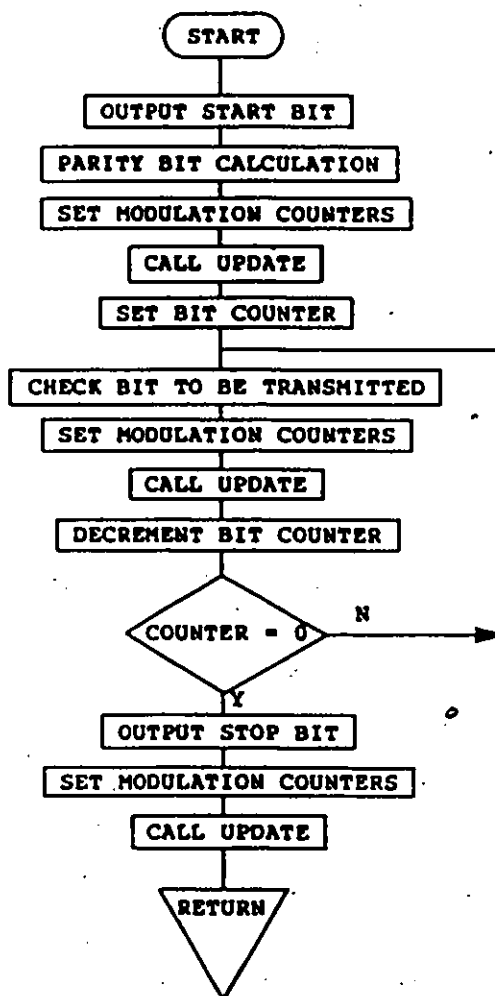
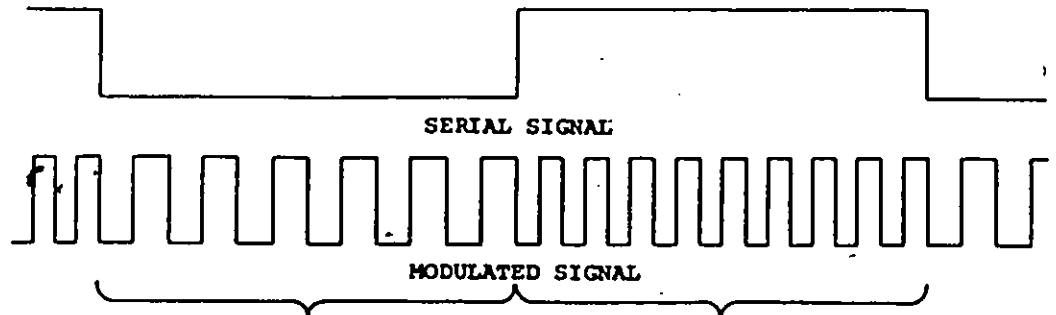


Figure B.3 Subroutine RECORD flowchart



NUMBER OF LEVELS	12	18
CYCLES/LEVEL	66	44
TIME (microseconds)	3318.8	3318.8
CARRIER FREQUENCY (Hz)	1807.8	2711.7

Figure B.4 Modulated signal timing diagram

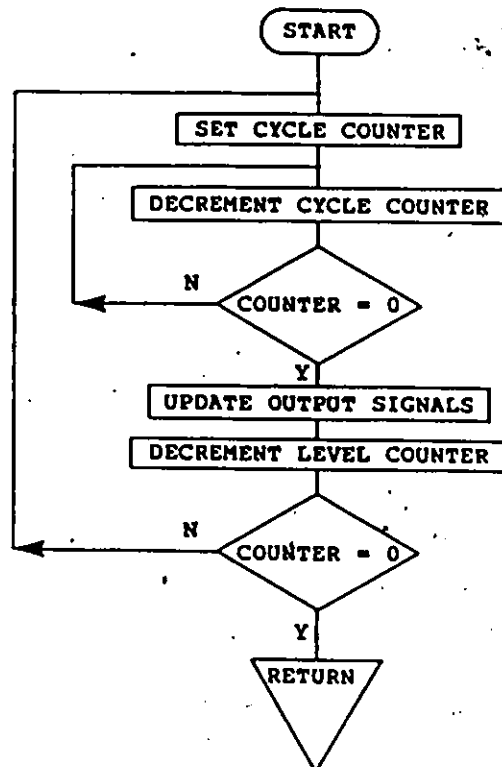


Figure B.5 Subroutine UPDATE flowchart

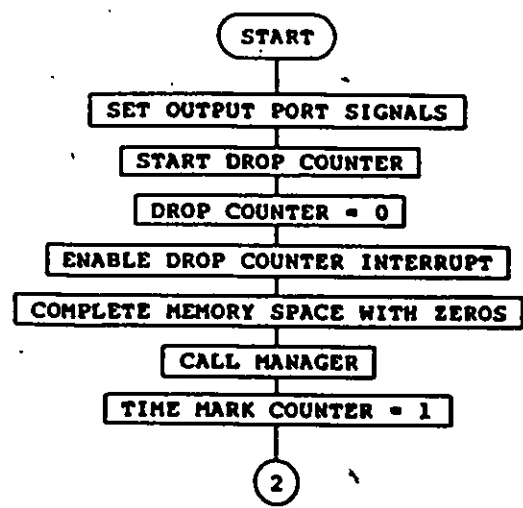


Figure B.6 Subroutine RESET flowchart

ASH48 :F1:DAS3.SRC

ISIS-II MCS-48/UPI-41 MACRO ASSEMBLER, V4.0

PAGE 1

LOC	OBJ	LINE	SOURCE STATEMENT
		1	;*****
		2	;
		3	;
		4	DATA ACQUISITION SYSTEM
		5	PROGRAM NUMBER 3
		6	;
		7	----
		8	;
		9	THIS PROGRAM IS USED BY THE MICROCOMPUTER
		10	IN THE DATA ACQUISITION SYSTEM STANDARD
		11	VERSION AND THE DROP COUNTER PRECIPITATION
		12	SENSOR.
		13	;
		14	NOVEMBER 4, 1983
		15	PTO EQU P2
0009		16	ORG 00H
0000		17	START: MOV A,#06H ;SET MODULATION OUTPUT PIN = 0
0000 2306		18	OUTL PTO,A ;SERIAL OUTPUT PIN = 1
0002 3A		19	JMP LC1 ;RECORDER OFF
0003 040A		20	NOP
0005 00		21	NOP
0006 00		22	;
		23	INTS: INC R3 ;INCREMENT DCH
0007 18		24	RETR ;
0008 93		25	NOP
0009 00		26	LC1: STRT CNT ;START DROP COUNTER
000A 45		27	CLR A ;CLEAR DCL
000B 27		28	MOV T,A
000C 62		29	EN TCNTI ;ENABLE COUNTER INTERRUPT
000D 25		30	LC2: CLR A ;CLEAR MEMORY FROM CURRENT
000E 27		31	MOV BR0,A ;POSITION
000F A0		32	INC R0
0010 18		33	MOV A,R0
0011 FB		34	ADD A,#0C0H
0012 03C0		35	JNC LC2
0014 E60E		36	CALL SB1 ;CALL "MANAGER"
0016 3400		37	MOV R1,#01H ;SET TIME MARK COUNTER
0018 B901		38	JMP SB32 ;JUMP TO TIME LOOP 2
001A 045B		39	NOP
001C 00		40	NOP
001D 00		41	NOP
001E 00		42	NOP
001F 00		43	;*****
		44	;
		45	MAIN ROUTINE
		46	THIS PART OF THE PROGRAM READS DATA FROM
		47	THE DROP COUNTER AND TIME MARK COUNTER. IF
		48	THE DATA IS DIFFERENT FROM ZERO OR THE TIME
		49	MARK IS EQUAL TO 240 THEN, THE DATA IS STORED
		50	INTO MEMORY.
		51	;
		52	REGISTERS: R0 = MEMORY POINTER
		53	R1 = TIME MARK COUNTER
		54	R2 = TEMPORARY REGISTER

ISIS-II MCS-48/UPI-41 MACRO ASSEMBLER, V4.0

PAGE 2

LOC	OBJ	LINE	SOURCE STATEMENT
		55	; R3 = MS BYTE OF DROP COUNTER
		56	; T = LS BYTE OF DROP COUNTER
		57	; R7 = DELAY
		58	;
		59	;*****
		60	;DIVIDE NUMBER OF DROPS BY TWO
0020	FB	61	LC3: MOV A,R3 ;RETRIEVE DCH DATA
0021	67	62	RRC A ;DIVIDE BY TWO
0022	42	63	MOV A,T ;READ DCL DATA
0023	67	64	RRC A ;DIVIDE DCL BY TWO
0024	AA	65	MOV R2,A ;STORE COUNT IN R2
0025	27	66	CLR A ;CLEAR ACCUMULATOR
0026	F7	67	RLC A ;ADD REMAINDER
0027	62	68	MOV T,A ;INITIALIZE COUNTER
0028	00	69	NOP ;TIMING
0029	BB00	70	MOV R3,#00H ;CLEAR DCH
002B	F9	71	MOV A,R1 ;STORE TIME MARK
002C	A0	72	MOV BR0,A
002D	19	73	INC R1 ;INCREMENT TIME MARK COUNTER
002E	0310	74	ADD A,#10H ;CHECK IF TIME MARK IS 241
0030	F63B	75	JC LC4 ;JUMP IF TIME MARK IS 241
0032	FA	76	MOV A,R2- ;CHECK IF DATA EQUAL ZERO
0033	963E	77	JNZ LC5 ;JUMP IF DATA IS NOT ZERO
0035	BF04	78	MOV R7,#04H ;TIME LOOP
0037	EF37	79	LC6: DJNZ R7,LC6
0039	044E	80	JMP SB3 ;JUMP TO TIME LOOP 1
003B	B901	81	LC4: MOV R1,#01H ;DO TIME MARK EQUAL TO 1
003D	FA	82	MOV A,R2 ;RETRIEVE DATA
003E	18	83	LC5: INC R0 ;INCREMENT MEMORY POINTER
003F	A0	84	MOV BR0,A ;STORE DATA
0040	18	85	INC R0 ;INCREMENT MEMORY POINTER
0041	F8	86	MOV A,R0 ;CHECK IF MEMORY IS FULL
0042	03C0	87	ADD A,#0C0H
0044	F64A	88	JC LC7 ;JUMP IF MEMORY IS FULL
0046	00	89	NOP ;TIMING
0047	00	90	NOP
004B	044E	91	JMP SB3 ;JUMP IF MEMORY IS NOT FULL
004A	3400	92	LC7: CALL SB1 ;CALL "MANAGER"
004C	045B	93	JMP SB32 ;JUMP TO TIME LOOP 2
		94	;*****
		95	;
		96	;TIME DELAYS
		97	;THESE SUBROUTINES PERFORM THE TIME DELAY TO
		98	;COMPLETE THE RAIN INTEGRATION TIME (1 MINUTE)
		99	;
		100	;REGISTERS: R5 = DELAY
		101	; R6 = DELAY
		102	; R7 = DELAY
		103	;
		104	;*****
004E	BF11	105	SB3: MOV R7,#11H ;TIME LOOP 1
0050	BEFD	106	MOV R6,#0FDH
0052	BD06	107	MOV R5,#06H
0054	EF54	108	SB31: DJNZ R7,SB31
0056	EE54	109	DJNZ R6,SB31

```

LOC OBJ          LINE      SOURCE STATEMENT
0058 ED54        110          DJNZ     R5,SB31
005A 00          111          NOP
005B BF67        112 SB32:     MOV      R7,#67H;TIME LOOP 2
005D BED4        113          MOV      R6,#0D4H
005F BD67        114          MOV      R5,#67H
0061 EF61        115 SB33:     DJNZ     R7,SB33
0063 EE61        116          DJNZ     R6,SB33
0065 ED61        117          DJNZ     R5,SB33
0067 00          118          NOP
0068 2300        119          MOV      A,#00H ;PRODUCE AN OUTPUT MARK
006A 02          120          OUTL    BUS,A
006B 23FF        121          MOV      A,#0FFH
006D 02          122          OUTL    BUS,A
006E 0420        123          JMP      LC3 ;JUMP TO THE MAIN ROUTINE
                124          ;
00FE            125          ORG     OFEH
00FE 0400        126          JMP     START ;JUMP TO START IF ERROR
127 ;*****
128 ;
129 ;SUBROUTINE "MANAGER"
130 ;THIS SUBROUTINE CONTROLS THE CASSETTE RECORDER
131 ;POWER SUPPLY AND TRANSMITS THE INFORMATION TO
132 ;BE RECORDED.
133 ;
134 ;I/O PINS:                P20 = MODULATED DATA
135 ;                          P21 = SERIAL DATA
136 ;                          P22 = VOLTAGE RECORDER
137 ;                          CONTROL SIGNAL
138 ;
139 ;REGISTERS:                R4 = SYNC COUNTER
140 ;                          R3 = AUXILIARY COUNTER
141 ;
142 ;*****
143 ;
0100            144          ORG     100H
0100 2302        145 SB1:     MOV      A,#02H ;SET MODULATION OUTPUT PIN = 0
0102 3A          146          OUTL    PTO,A ;SERIAL OUTPUT PIN = 1
                147          ;RECORDER ON
0103 AA          148          MOV      R2,A ;STORE PORT STATUS
0104 BB18        149          MOV      R0,#18H ;SET MEMORY POINTER
                150          ;SEND 50 BYTES OF SYNC
0106 BC32        151          MOV      R4,#32H ;SET SYNC COUNTER
0108 00          152          NOP
0109 00          153          NOP
010A 27          154 SB11:   CLR      A ;SET SYNC DATA
010B 3426        155          CALL    SB13 ;CALL "RECORD"
010D 00          156          NOP
010E 00          157          NOP
010F 00          158          NOP
0110 00          159          NOP
0111 E0A        160          DJNZ     R4,SB11
0113 F0          161 SB12:   MOV      A,#00 ;RETRIEVE DATA FROM MEMORY
0114 3426        162          CALL    SB13 ;CALL "RECORD"
0116 18          163          INC     R0 ;INCREMENT MEMORY POINTER
0117 F0          164          MOV      A,R0 ;CHECK IF FINISHED

```

LOC	OBJ	LINE	SOURCE STATEMENT
0118	03C0	165	ADD A,#0C0H
011A	E613	166	JNC SB12 ;JUMP IF NOT FINISHED
011C	BB18	167	MOV R0,#18H ;SET MEMORY POINTER
011E	BD00	168	MOV R3,#00H ;CLEAR AUXILIARY COUNTER
0120	00	169	NOP
0121	00	170	NOP
0122	2306	171	MOV A,#06H ;SET OUTPUT PORT DATA
0124	3A	172	OUTL PTO,A
0125	93	173	RETR
		174	};*****
		175	};
		176	};SUBROUTINE RECORD
		177	};THIS SUBROUTINE GENERATES THE CONTROL BITS
		178	};AND SETS THE MODULATION COUNTERS
		179	};
		180	};AT INPUT: A = DATA TO BE SEND
		181	};
		182	};REGISTERS: R5 = CYCLE COUNTER
		183	}; R6 = LEVEL COUNTER
		184	}; R7 = BIT COUNTER
		185	};
		186	};*****
0126	2A	187	SB13: XCH A,R2 ;UPDATE MODULATION OUTPUT PINS
0127	67	188	RRC A
0128	A7	189	CPL C
0129	F7	190	RLC A
012A	53FD	191	ANL A,#0FDH ;OUTPUT OF START BIT
012C	3A	192	OUTL PTO,A
012D	2A	193	XCH A,R2
012E	97	194	CLR C ;PARITY BIT CALCULATION
012F	1233	195	JBO H1 ;TEST BIT 0
0131	2435	196	JMP H2
0133	00	197	H1: NOP
0134	A7	198	CPL C
0135	3239	199	H2: JB1 H3 ;TEST BIT 1
0137	243B	200	JMP H4
0139	00	201	H3: NOP
013A	A7	202	CPL C
013B	523A	203	H4: JB2 H5 ;TEST BIT 2
013D	2441	204	JMP H6
013F	00	205	H5: NOP
0140	A7	206	CPL C
0141	7245	207	H6: JB3 H7 ;TEST BIT 3
0143	2447	208	JMP HB
0145	00	209	H7: NOP
0146	A7	210	CPL C
0147	924B	211	H8: JB4 H9 ;TEST BIT 4
0149	244D	212	JMP H10
014B	00	213	H9: NOP
014C	A7	214	CPL C
014D	B251	215	H10: JB5 H11 ;TEST BIT 5
014F	2453	216	JMP H12
0151	00	217	H11: NOP
0152	A7	218	CPL C
0153	D257	219	H12: JB6 H13 ;TEST BIT 6

LOC	OBJ	LINE	SOURCE STATEMENT
0155	2459	220	JMP H14
0157	00	221 H13:	NOP
0158	A7	222	CPL C
0159	F25D	223 H14:	JB7 H15 ;TEST BIT 7
0158	245F	224	JMP H16
015D	00	225 H15:	NOP
015E	A7	226	CPL C
015F	BF09	227 H16:	MOV R7,#09H ;SET BIT COUNTER
0161	BE0C	228	MOV R6,#0CH ;SET MODULATION LEVEL COUNTER
0163	BD0F	229	MOV R5,#0FH ;SET MODULATION CYCLE COUNTER
0165	EB08	230	MOV R3,#08H ;TIME LOOP
0167	EB67	231 SB14:	DJNZ R3,SB14
0169	34A6	232	CALL SB21 ;CALL "UPDATE"
0168	00	233	NOP
016C	00	234	NOP
016D	00	235 SB15:	NOP
016E	AB	236	MOV R3,A
		237	;CHECK BIT TO BE SENT
016F	127B	238	JBO SB16 ;JUMP IF BIT TO BE SENT IS "1"
		239	;IF BIT TO BE SENT EQUALS "0"
0171	BE0C	240	MOV R6,#0CH ;SET MODULATION LEVEL COUNTER
0173	BD0F	241	MOV R5,#0FH ;SET MODULATION CYCLE COUNTER
0175	FA	242	MOV A,R2 ;RETRIEVE PORT STATUS
0176	53FD	243	ANL A,#0FDH ;SET SERIAL OUTPUT PIN = 0
0178	AA	244	MOV R2,A ;STORE PORT STATUS
0179	2485	245	JMP SB17
		246	;IF BIT TO BE SENT EQUALS "1"
017B	BE12	247 SB16:	MOV R6,#12H ;SET MODULATION LEVEL COUNTER
017D	BD04	248	MOV R5,#04H ;SET MODULATION CYCLE COUNTER
017F	FA	249	MOV A,R2 ;RETRIEVE PORT STATUS
0180	4302	250	ORL A,#02H ;SET SERIAL OUTPUT PIN = 1
0182	AA	251	MOV R2,A ;STORE PORT STATUS
0183	00	252	NOP
0184	00	253	NOP
0185	FB	254 SB17:	MOV A,R3 ;RETRIEVE DATA
0186	67	255	RRC A ;SHIFT RIGHT DATA
0187	34A0	256	CALL SB20 ;CALL "UPDATE"
0189	EF6D	257	DJNZ R7,SB15 ;JUMP IF NOT FINISHED
		258	;SEND STOP BIT
018B	BE11	259	MOV R6,#11H ;SET MODULATION LEVEL COUNTER
018D	BD04	260	MOV R5,#04H ;SET MODULATION CYCLE COUNTER
018F	FA	261	MOV A,R2 ;RETRIEVE DATA
0190	4302	262	ORL A,#02H ;SET SERIAL OUTPUT PIN = 1
0192	AA	263	MOV R2,A ;STORE PORT STATUS
0193	B803	264	MOV R3,#03H ;TIME LOOP
0195	EB95	265 SB18:	DJNZ R3,SB18
0197	34A0	266	CALL SB20 ;CALL "UPDATE"
0199	BD08	267	MOV R3,#08H ;TIME LOOP
019B	EB9B	268 SB19:	DJNZ R3,SB19
019D	00	269	NOP
019E	93	270	RETR
019F	00	271	NOP
		272	;*****
		273	;
		274	;SUBROUTINE UPDATE

LOC	OBJ	LINE	SOURCE STATEMENT
		275);THIS SUBROUTINE UPDATES THE VALUE OF THE
		276);MODULATED SIGNAL ACCORDING TO THE LEVEL
		277);AND CYCLE COUNTERS
		278);
		279);*****
01A0	2D	280 SB20:	XCH A,R5 ;SET CYCLE COUNTER
01A1	AD	281	MOV R3,A
01A2	2D	282	XCH A,R5
01A3	00	283	NOP
01A4	EBA4	284 SB24:	DJNZ R3,SB24
01A6	2A	285 SB21:	XCH A,R2 ;UPDATE DATA PORT
01A7	67	286	RRC A ;MODULATION
01A8	A7	287	CPL C
01A9	F7	288	RLC A
01AA	3A	289	OUTL PTO,A ;OUTPUT DATA
01AB	2A	290	XCH A,R2
01AC	00	291	NOP
01AD	EEB0	292	DJNZ R6,SB22
01AF	93	293	RETR
01B0	DB09	294 SB22:	MOV R3,#09H ;TIME LOOP
01B2	EDB2	295 SB23:	DJNZ R3,SB23
01B4	24A0	296	JMP SB20
		297);
01FE		298	ORG 1FEH
01FE	0400	299	JMP START ;JUMP TO START IF ERROR
02FE		300	ORG 2FEH
02FE	0400	301	JMP START ;JUMP TO START IF ERROR
03FE		302	ORG 3FEH
03FE	0400	303	JMP START ;JUMP TO START IF ERROR
		304	END

USER SYMBOLS

H1	0133	H10	014D	H11	0151	H12	0153	H13	0157	H14	01
H2	0135	H3	0139	H4	013B	H5	013F	H6	0141	H7	01
INTS	0007	LC1	000A	LC2	000E	LC3	0020	LC4	003B	LC5	00
PTO	0009	SB1	0100	SB11	010A	SB12	0113	SB13	0126	SB14	01
SB17	0185	SD18	0195	SB19	019B	SB20	01A0	SB21	01A6	SB22	01
SB3	004E	SB31	0054	SB32	005B	SB33	0061	START	0000		

ASSEMBLY COMPLETE, NO ERRORS

APPENDIX C

DATA DECODER PROGRAM

This Appendix presents a description of the program used by the microcomputer in the data decoder. The program is divided into two routines and five auxiliary subroutines. A list of the program is included at the end of the Appendix.

The "SERIAL RECEPTION ROUTINE" retrieves the information from tape and stores it into data memory. Figure C.1 shows a flowchart of this routine. It is required to read at least 5 synchronization characters before any character different from zero is considered data. After the first data character has been read, the subsequent 39 characters are considered data and stored in memory.

Subroutine "READ DATA" reads one character from the input signal; the algorithm used is shown in Figure C.2. The basic intent of this algorithm is to minimize the effects of pulse-to-pulse jitter and frequency shifts by sampling each data bit as close to its center as possible. Subroutine "DELAY RECEPTION" is called by "READ DATA" to generate a time delay of one bit time and read the status of the input signal.

After a character has been received, the program veri-

ifies the validity of the data; if an error is detected the program jumps to subroutine "ERROR" to inform the user. The program detects two types of errors: (a) the parity bit received does not match with the parity bit calculated by the decoder; and (b) the stop bit is not detected at the end of a character received. Figure C.3 shows a flowchart of the algorithm used for parity calculation. It starts by clearing the carry flag and setting a loop counter to 8. During execution of the loop, the least significant bit of the data is tested and then rotated. If the bit tested is equal to zero, the carry flag is complemented. After the loop has been completed the carry flag will be set if an odd number of ones is encountered and reset otherwise.

The "SERIAL TRANSMISSION ROUTINE" retrieves the data stored in memory, converts it into ASCII code and transmits it to the central computer for data processing.

To convert from straight binary to ASCII code, the data is first converted to BCD. The algorithm used to convert from binary to BCD is shown in Figure C.4. BIN is the binary number to be converted and BCD is a BCD string used to accumulate the result. The algorithm works as follows: each pass through the loop, BIN is multiplied by two resulting in a carry if the MSB of BIN is set. If a carry is produced, it will be added to the result of two times the BCD string. The result is scaled by performing a Decimal Adjust Accumulator instruction. The process is repeated for each

bit of BIN.

The conversion from BCD to ASCII is carried out using a straightforward algorithm. The nibbles of the BCD number are separated and logically OR'ed with the number 30H. No parity bit is used in the ASCII code.

Once the information has been converted into ASCII code, it is transmitted asynchronously to the central computer. Serial transmission is far simpler than serial reception since no synchronization is required. All that is required is to generate time loops at the desired bit rate and present the character to be transmitted serially at an I/O pin. The algorithm used is presented in Figure C.5. The information is transmitted at 1200 bits per second via a RS-232C compatible line driver. Subroutine "DELAY TRANSMISSION" generates a time delay of one bit time.

The end of the transmission is indicated to the central computer by the special character "CNTRL-Z". Depressing push-button S1 causes the execution of subroutine "INTERRUPT" which transmits the special character.

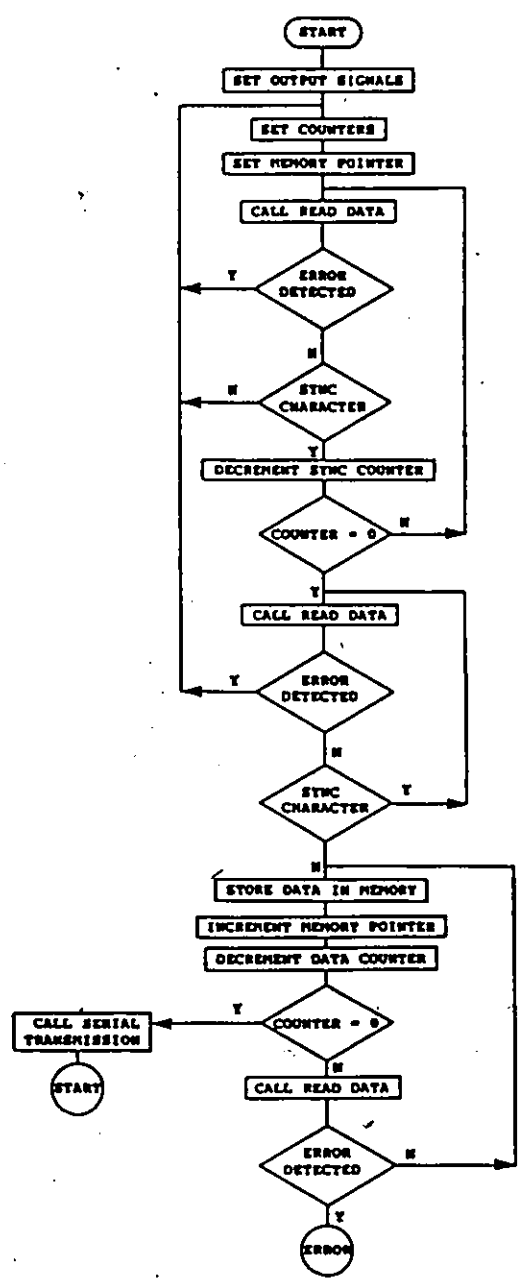


Figure C.1 SERIAL RECEPTION ROUTINE flowchart

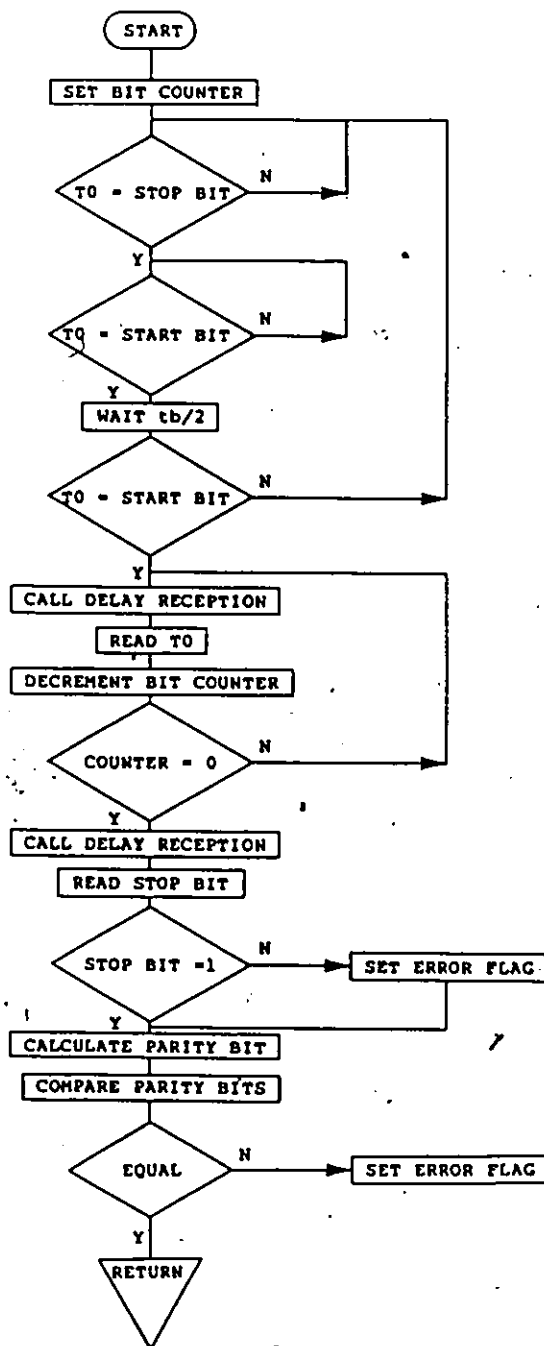


Figure C.2 Subroutine READ DATA flowchart.

Time t_b is equal to one bit time

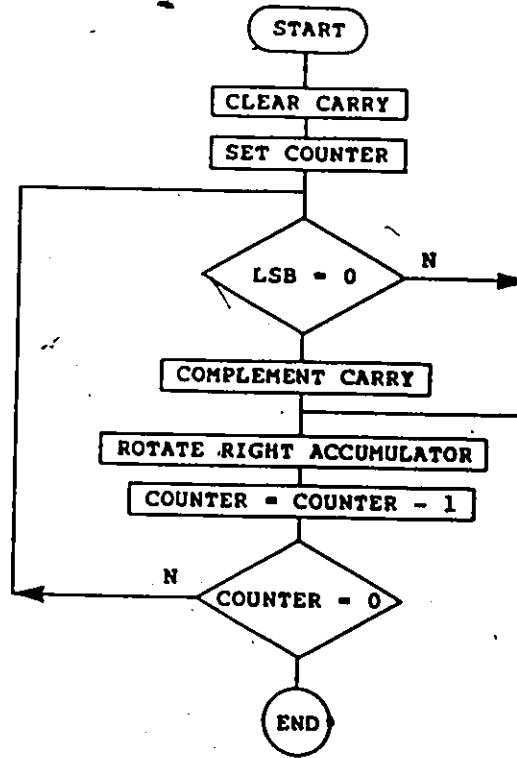


Figure C.3 Algorithm for parity calculation

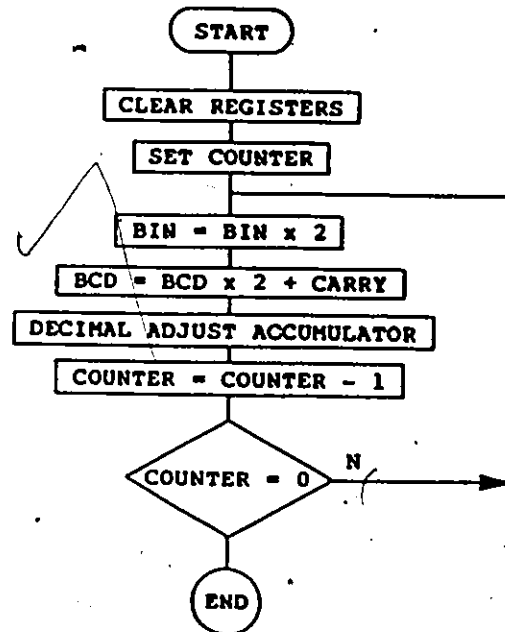


Figure C.4 Binary to BCD conversion algorithm

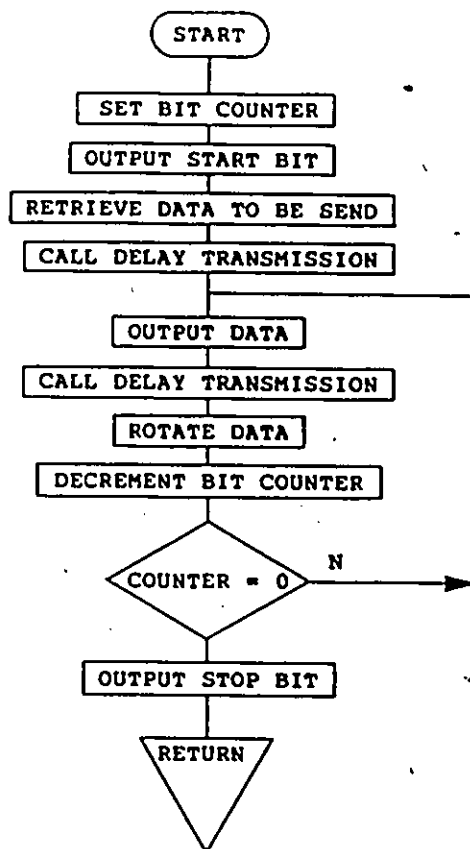


Figure C.5 SERIAL TRANSMISSION ROUTINE flowchart

ASM4B :F1:DEC1.SRC

ISIS-II MCS-4B/UPI-41 MACRO ASSEMBLER, V4.0

PAGE 1

LOC	OBJ	LINE	SOURCE STATEMENT
		1	;*****
		2	;
		3	;
		4	;
		5	;
		6	;
		7	;
		8	;
		9	;
		10	;
		11	;
		12	;
		13	;
0000		14	ORG 00H
0000 05		15	EN I
0001 0410		16	JMP START
		17	;
		18	;
0003		18	ORG 03H ;SUBROUTINE INTERRUPT
0003 BFFF		19	INT: MOV R7,#0FFH ;SEND "CNTRL-Z"
0005 B03F		20	MOV R0,#3FH ;SET KEY DEBOUNCE COUNTER
0007 BA01		21	MOV R2,#01H ;SET MEMORY POINTER
0009 EF03		22	DJNZ R7,INT ;SET DATA COUNTER
000B 8603		23	JNI INT ;JUMP IF INT=0
000D BF1A		24	MOV R7,#1AH ;MOVE DATA (CTRL-Z)
000F 1441		25	CALL SB40
		26	;
		27	;
		28	;
		29	;
		30	;
		31	;
		32	;
		33	;
		34	;
		35	;
		36	;
		37	;
		38	;
		39	;
		40	;
0010		41	ORG 10H
0010 2301		42	START: MOV A,#01 ;SET TxD OUTPUT PIN = 1
0012 3A		43	OUTL P2,A
0013 8928		44	MOV R1,#28H ;SET DATA COUNTER
0015 B818		45	MOV R0,#18H ;SET MEMORY POINTER
0017 BC05		46	LOC2: MOV R4,#05H ;SET SYNC COUNTER
		47	;
0019 1463		48	LOC3: CALL SB1 ;RECEIVE 5 SYNC BYTES
001B FB		49	MOV A,R3 ;CALL "READ DATA"
001C 9617		50	JNZ LOC2 ;TEST IF ERROR
001E FA		51	MOV A,R2 ;JUMP IF ERROR DETECTED
001F 9617		52	JNZ LOC2 ;RETRIEVE DATA
0021 EC19		53	DJNZ R4,LOC3 ;JUMP IF NOT SYNC BYTE
0023 1463		54	LOC4: CALL SB1 ;CALL "READ DATA"

ISIS-II MCS-40/UP-41 MACRO ASSEMBLER, V4.0

PAGE 2

LOC	OBJ	LINE	SOURCE STATEMENT
0025	FB	55	MOV A,R3 ;TEST IF ERROR*
0026	9617	56	JNZ LOC2 ;JUMP IF ERROR DETECTED
0028	FA	57	MOV A,R2 ;RETRIEVE DATA
0029	C623	58	JZ LOC4 ;JUMP IF SYNC BYTE
002B	0433	59	JMP LOC5 ;JUMP IF NOT SYNC BYTE
		60	;
002D	1463	61	LOC6: CALL SB1 ;CALL READ DATA
002F	FD	62	MOV A,R3 ;TEST IF ERROR
0030	96E5	63	JNZ SB7 ;JUMP IF ERROR IN DATA
0032	FA	64	MOV A,R2 ;RETRIEVE DATA
0033	A0	65	LOC5: MOV R0,A ;STORE DATA IN MEMORY
0034	18	66	INC R0 ;INCREMENT MEMORY POINTER
0035	E92D	67	DJNZ R1,LOC6 ;CHECK IF FINISHED
0037	143B	68	CALL SB4 ;CALL "SERIAL TRANSMISSION"
0039	0410	69	JMP START
		70	;
		71	;XX
		72	;
		73	;SERIAL TRANSMISSION ROUTINE
		74	;TRANSMITS TO THE CENTRAL COMPUTER THE
		75	;THE INFORMATION STORED IN MEMORY.
		76	;
		77	;REGISTERS: R0 = MEMORY POINTER
		78	; R1 = MEMORY POINTER
		79	; R2 = BYTE COUNTER
		80	; R3 = BIT COUNTER
		81	;
		82	;XX
		83	;
003B	B818	84	SB4: MOV R0,#18H ;SET MEMORY POINTER
003D	14B0	85	SB41: CALL SB5 ;CALL "BINARY-TO-ASCII"
003F	BA03	86	MOV R2,#03H ;SET BYTE COUNTER
0041	B907	87	SB40: MOV R1,#07H ;SET DATA POINTER
0043	B80B	88	SB42: MOV R3,#08H ;SET BIT COUNTER
0045	27	89	CLR A
0046	3A	90	OUTL P2,A ;OUTPUT START BIT
0047	14E0	91	CALL SB6 ;CALL "DELAY TRANSMISSION"
0049	F1	92	MOV A,R1 ;RETRIEVE DATA FROM MEMORY
004A	00	93	NOP ;TIMING
004B	00	94	NOP
004C	00	95	SB43: NOP
004D	00	96	NOP
004E	3A	97	OUTL P2,A ;UPDATE OUTPUT DATA
004F	14E0	98	CALL SB6 ;CALL DELAY TRANSMISSION
0051	77	99	RR A
0052	ED4C	100	DJNZ R3,SB43
0054	2301	101	MOV A,#01
0056	3A	102	OUTL P2,A ;OUTPUT STOP BIT
0057	14E0	103	CALL SB6 ;CALL DELAY TRANSMISSION
0059	C9	104	DEC R1 ;DECREMENT MEMORY POINTER
005A	EA43	105	DJNZ R2,SB42 ;CHECK IF FINISHED
005C	18	106	INC R0 ;UPDATE MEMORY POINTER
005D	F8	107	MOV A,R0 ;GET NEW DATA
005E	03C0	108	ADD A,#0C0H
0060	E63D	109	JNC SB41

LOC	OBJ	LINE	SOURCE STATEMENT
	0062	93	110 RETR
		111	;*****
		112	;
		113	;SUBROUTINE "READ DATA"
		114	;THIS SUBROUTINE READS THE INCOMING SERIAL
		115	;DATA; CONVERTS IT INTO PARALLEL FORMAT AND
		116	;CHECKS THE VALIDITY OF THE DATA
		117	;
		118	;AT EXIT: R2 = DATA
		119	; R3 (b7) = 1 IF PARITY ERROR
		120	; R3 (b0) = 1 IF STOP BIT ERROR
		121	;
		122	;REGISTERS; R2 = DATA REGISTER
		123	; R3 = BIT COUNTER
		124	; ERROR FLAGS
		125	; R7 = DELAY
		126	;
		127	;*****
		128	;
0063	8A00	129	SB1: MOV R2,#00H ;CLEAR DATA REGISTER
0065	8B09	130	MOV R3,#09H ;SET BIT COUNTER
0067	2667	131	SB11: JNTO SB11 ;JUMP IF INPUT SIGNAL (TO)=0
0069	3669	132	SB12: JTO SB12 ;JUMP IF TO=1
006B	BFDD	133	MOV R7,#0DDH;SET COUNTER FOR HALF-BIT DELAY
006D	00	134	SB13: NOP
006E	EF6D	135	DJNZ R7,SB13
0070	3667	136	JTO SB11 ;CHECK MIDDLE OF START BIT
0072	BF03	137	MOV R7,#03H ;SET COUNTER TIME DELAY
0074	EF74	138	SB14: DJNZ R7,SB14
0076	BF02	139	SB15: MOV R7,#02 ;SET COUNTER TIME DELAY
0078	EF78	140	SB16: DJNZ R7,SB16
007A	14A3	141	CALL SB3 ;CALL "DELAY RECEPTION"
007C	FA	142	MOV A,R2 ;READ INPUT DATA
007D	67	143	RRC A
007E	AA	144	MOV R2,A
007F	ED76	145	DJNZ R3,SB15
0081	F7	146	RLC A
0082	AA	147	MOV R2,A ;R2=DATA AND CARRY=PARITY BIT
0083	85	148	CLR F0 ;FLAG (F0)=PARITY BIT
0084	E6B7	149	JNC SB17 ;JUMP IF PARITY BIT = 0
0086	95	150	CPL F0 ;IF PARITY BIT = 1 THEN F0 = 1
0087	14A3	151	SB17: CALL SB3 ;READ STOP BIT
0089	F68D	152	JC SB18
008E	BB01	153	MOV R3,#01H ;IF THERE IS NO STOP BIT,
		154	;MAKE R3 = 01H
008D	97	155	SB18: CLR C ;PARITY CALCULATION
008E	BF08	156	MOV R7,#08H
0090	1293	157	SB19: JBO SB20
0092	A7	158	CPL C
0093	77	159	SB20: RR A
0094	EF90	160	DJNZ R7,SB19 ;CARRY = CALCULATED PARITY
0096	B67C	161	JFO SB21 ;CHECK PARITY
0098	E6A2	162	JNC SB22
009A	049E	163	JMP SB23
009C	F6A2	164	SB21: JC SB22

ISIS-II MCS-4B/UP1-41 MACRO ASSEMBLER, V4.0

PAGE 4

LOC	OBJ	LINE	SOURCE STATEMENT
009E	2380	165	SB23: MOV A,#80H ;R3 = 80H IF PARITY ERROR
00A0	4B	166	ORL A,R3
00A1	AB	167	MOV R3,A
00A2	83	168	SB22: RET
		169	;*****
		170	;
		171	;SUBROUTINE "DELAY RECEPTION"
		172	;THIS SUBROUTINE WAITS ONE BIT TIME AND READS
		173	;ONE DATA BIT FROM INPUT PIN TO
		174	;
		175	;AT EXIT: CARRY (C) = DATA ON TO
		176	;
		177	;REGISTERS: R6, R7 = DELAYS
		178	;
		179	;*****
		180	;
00A3	BF8C	181	SB3: MOV R7,#8CH ;SET TIME DELAY
00A5	BE03	182	MOV R6,#03H
00A7	EFA7	183	SB31: DJNZ R7,SB31
00A9	EEA7	184	DJNZ R6,SB31
00AB	97	185	CLR C ;CLEAR CARRY
00AC	26AF	186	JNZ SB32 ;JUMP IF TO = 0
00AE	A7	187	CPL C ;COMPLEMENT CARRY
00AF	83	188	SB32: RET
		189	;
		190	;*****
		191	;
		192	;SUBROUTINE "BINARY-TO-ASCII"
		193	;THIS SUBROUTINE PERFORMS THE BINARY TO
		194	;ASCII CONVERSION
		195	;
		196	;AT INPUT: R0 = POINTING DATA LOCATION
		197	;
		198	;AT EXIT: R7 = ASCII MS DIGIT
		199	; R6 = ASCII
		200	; R5 = ASCII LS DIGIT
		201	;
		202	;REGISTERS: R0 = MEMORY POINTER
		203	; R1 = MEMORY POINTER
		204	; R2, R3 = COUNTER
		205	; R5, R6, R7 = DATA REGISTERS
		206	;
		207	;*****
		208	;
00B0	B705	209	SB5: MOV R1,#05H ;SET COUNTER
00B2	BA03	210	MOV R2,#03H ;CLEAR MEMORY
00B4	B100	211	SD51: MOV @R1,#00H
00B6	19	212	INC R1
00B7	EAB4	213	DJNZ R2,SB51
00B9	BA08	214	MOV R2,#08H ;BINARY TO BCD CONVERSION
00BB	97	215	SD52: CLR C
00BC	F0	216	MOV A,@R0 ;RETRIEVE BIN NUMBER
00BD	F7	217	RLC A ;MULTIPLY BY TWO
00BE	B905	218	MOV R1,#05H ;SET MEMORY POINTER
00C0	B802	219	MOV R3,#02H ;SET COUNTER

```

LOC  OBJ          LINE      SOURCE STATEMENT
00C2  A0          220      MOV     R0,A      ;STORE DATA
00C3  F1          221  SB53:  MOV     -A,R1     ;RETRIEVE BCD NUMBER
00C4  71          222      ADDC   A,R1     ;CARRY PLUS TWO TIMES BCD
00C5  57          223      DA     A        ;DECIMAL ADJUST
00C6  A1          224      MOV     R1,A     ;STORE BCD NUMBER
00C7  19          225      INC    R1
00C8  EHC3       226      DJNZ   R3,SB53
00CA  EAB8       227      DJNZ   R2,SB52
00CC  B905       229      MOV     R1,#05H  ;BCD TO ASCII CONVERSION
00CE  F1          230      MOV     A,R1     ;RETRIEVE DATA
00CF  530F       231      ANL    A,#0FH   ;MASK DATA (4 LSB's)
00D1  4330       232      ORL    A,#30H   ;ADD 4 MSB's
00D3  21          233      XCH    A,R1
00D4  19          234      INC    R1       ;REPEAT WITH MS-NIBBLE
00D5  47          235      SHAP   A
00D6  530F       236      ANL    A,#0FH   ;
00D8  4330       237      ORL    A,#30H   ;
00DA  21          238      XCH    A,R1
00DB  19          239      INC    R1       ;REPEAT WITH NEXT BYTE
00DC  4330       240      ORL    A,#30H   ;
00DE  A1          241      MOV     R1,A
00DF  83          242      RET
243  ;*****
244
245      ;SUBROUTINE "DELAY TRANSMISSION",
246      ;THIS SUBROUTINE PROVIDES A DELAY OF ONE BIT
247      ;TIME FOR DATA TRANSMISSION AT 1200 BAUDS
248
249      ;REGISTERS:      R4 = DELAY
250
251  ;*****
252
253  SB6:  MOV     R4,#0A0H;SET COUNTER
254  SB61: DJNZ   R4,SB61
255      RET
256  ;*****
257
258      ;SUBROUTINE "ERROR"
259      ;THIS SUBROUTINE FILLS THE REMAINING MEMORY
260      ;SPACE WITH THE NUMBER 0FFH (255)
261      ;WHEN AN ERROR IS DETECTED
262
263      ;REGISTERS:      R0 = MEMORY POINTER
264      ;                  R1 = DATA COUNTER
265
266  ;*****
267
268  SB7:  MOV     A,#0FFH ;SET DATA TO BE SENT
269  SB71: MOV     R0,A     ;STORE DATA IN MEMORY
270      INC    R0
271      DJNZ   R1,SB71
272      CALL   SB4      ;CALL SERIAL TRANSMISSION
273      JMP    START
274      END

```